# INVESTIGATION OF ALGAE DISTRIBUTION IN EYMIR LAKE USING SITE MEASUREMENTS AND REMOTELY SENSED DATA

A THESIS SUBMITTED TO
THE GRADUATE SCHOOL OF NATURAL AND APPLIED SCIENCES
OF
MIDDLE EAST TECHNICAL UNIVERSITY

BY

TAREK ELAHDAB

IN PARTIAL FULFILLMENT OF THE REQUIREMENTS
FOR
THE DEGREE OF MASTER OF SCIENCE
IN
ENVIRONMENTAL ENGINEERING

SEPTEMBER 2006

Approval of the Graduate School of Natural and Applies Sciences

Prof.Dr. Canan Özger
Director

I certify that this thesis satisfies all the requirements as a thesis for the degree of Master of Science.

Prof. Dr. Filiz B.Dilek
Head of Department

This is to certify that we have read this thesis and that in our opinion it is fully adequate, in scope and quality, as a thesis for the degree of Master of Science

Assist. Prof. Dr. Ayşegül Aksoy
Supervisor

**Examining Committee Members**

Prof. Dr. Kahraman Ünlü (METU,ENVE) _____

Assist. Prof. Dr. Ayşegül Aksoy (METU,ENVE) _____

Prof. Dr. Filiz B.Dilek (METU,GGIT) _____

Prof. Dr. Gürdal Tüncel (METU,ENVE) _____

Assist. Prof. Dr. Zuhal Akyürek (METU,ENVE) _____

**I hereby declare that all information in this document has been obtained and presented in accordance with academic rules and ethical conduct. I also declare that, as required by these rules and conduct, I have fully cited and referenced all material and results that are not original to this work.**

Name, Last name: Tarek ELAHDAB

Signature :

## *ABSTRACT*

## *INVESTIGATION OF ALGAE DISTRIBUTION IN EYMIR LAKE USING SITE MEASUREMENTS AND REMOTELY SENSED DATA*

*Tarek Elahdab*

*M.Sc, Department of Environmental Engineering*

*Supervisor: Assist.Prof.Dr.Ayşegül Aksoy*

*September 2006, 110 pages.*

The aim of this study is to determine the distribution of Chla in Eymir Lake using remotely sensed data and in-situ data. The study was carried out in three phases; the first phase was taking ground real data from the lake for a 6-month period, secondly the remotely sensed satellite image was taken and analyzed, thirdly a correlation was obtained between the ground data and satellite image, and lastly mapping of the Chla in the lake was made. During the study also the change of the lake during the 6-month period was monitored. The results showed a great variation in the concentration of Chla in the period measured from spring till early fall, from very low almost undetectable concentrations to noticeably very high values especially during summer. The secchi disc depth values ranged from about 3 meters in early spring, to as low as 15 centimeters in late summer; this made it very much related to Chla values. Chla concentrations had a high relationship with the following parameters: DO, TSS, Depth and secchi disc. As for the remotely sensed data also an acceptable level of correlation was obtained between them and Chla data both from laboratory results and in-situ probe.



Keywords: Eymir Lake, Remote Sensing, Chlorophyll-a, Eutrophication.

# *ÖZ*

## *EYMİR GÖLÜNDEKİ ALG DAĞILIMININ SAHA ÖLÇÜMLERİ VE UZAKTAN ALGILAMA DATASI İLE İNCELENMESİ*

*Tarek Elahdab*

*M.Sc, Çevre Mühendisliği Bölümü*

*Danışman: Yard.Doç.Dr.Ayşegül Aksoy*

Eylül 2006, 110 sayfa

Bu çalışmanın hedefi Eymir gölündeki klorofil-a konsantrasyonu uzaktan algılanan veri ve saha içi yöntemleri kullanarak belirlemektir. Bu çalışma üç fazdan oluşuyordu; birinci fazda yaklaşık altı ay boyunca sahadan veri toplandı, ikinci fazda gölün uydu görüntüsü alındı, ve üçüncü fazda sahadan toplanan verinin ile uydu görüntünün arasındaki korelasyın belirlendi, ve son olarak göldeki klorofil-a haritaları çizildi. Ayrıca, çalışma boyunca göldeki klorofilin değişimide gözetlendi. Klorofil sonuçları çalışma peryodunde ilk bahardan son bahara kadar büyük değişim gösterdi. Bu değişim ilk baharda çok küçük konsantrasyonlarda başlıyarak yazın çok yüksek değerlere ulaştı. Sekki disk değerleri aralığı ilk baharda üç metreden başlayıp yazın onbeş santimetreye kadar düştüö bu sebepten dolya sekki disk klorofıl-a'ya bağlı olduğu düşünülüyor. Ayrıca, klorofil-a'yla çözülmüş oksijen, toplam askıda katı madde, derinlik ,ve sekki disk derinliği yüksek bağlantı gösterdi. Uzaktan algılama yöntemine ilişkin olarak, hem sahadan hem labaratuvardan bulunan kolorfil konsantarsyonları uydu görüntüsüyle kabul edilebilecek seviyede yüksek kerelasyon belirlendi.

Anahtarsözcük: Eymir gölü, uzaktan algılama, klorofil-a, ütrüfikasyon.

*To my Beloved Wife*

## *ACKNOWLEDGMENTS*

The author wishes to express his gratitude to everyone who contributed to accomplishing this study. He must single out his supervisor Assistant Professor Dr. Ayşegül Aksoy, who gave support, guidance and encouragements for the study and supported it during the months it took to bring it to fruition.

The author also would like to thank the examining committee members Prof.Dr Filiz B.Dilek, Prof Dr. Kahraman Ünlü, Prof Dr.Gürdal Tüncel and Assist Prof Dr. Zuhal Akyürek for their comments.

The author would like also to express his thanks to Mr. Muhittin Aslan and Mrs. Gamze Güngör Demirci for their great help and contributions in field work, laboratory experiments and supplying data.

Lastly, the author would like to acknowledge and express his deepest appreciation to his wife Mrs. Benan Rifaioğlu Elahdab for her endless support in all times.

# *TABLE OF CONTENTS*

# *LIST OF TABLES*

# *LIST OF FIGURES*

# *CHAPTER 1*

# *INTRODUCTION*

Eutrophication, characterized by the overgrowth of algae, has become a real concern for several lakes in the world. Eutrophication is considered as one of the main factors for the severe deterioration of water quality and aquatic life, and eventually results in the death of the lake. Although it is a natural phenomenon, human activity has decreased the duration of the overall process to decades and even several years, compared to hundreds to thousands of years. Point sources, current land use practices and increased agricultural activities have given rise to nutrient loads to lakes, and therefore, enhanced the conditions for algal growth (Horne & Goldman, 1994).

The concentration of algae is impacted by several parameters in the water. Nutrient concentrations, such as nitrogen (N) and phosphorus (P) compounds, light penetration, temperature of water are among them. Increased algae concentrations, on the other hand, impact mainly the dissolved oxygen concentrations and turbidity. Therefore, monitoring of such parameters is required to control the water quality in a lake.

To observe the state of the water quality or protect any lake, a monitoring and management program is needed. However, this needs a lot of time, effort and finance. Traditional monitoring techniques involve sampling and laboratory analysis. These methods may be cumbersome and costly, requiring several personnel, proper sampling, and a well established laboratory. In most cases, researchers would be interested in determining the most representative locations for sampling in order to decrease the number of samples taken due to limited laboratory capacity, issues regarding the hauling of samples, and costs of analysis. However, current advances in technology are working in favor of easing the difficulties associated with traditional monitoring and analysis methods. Development of multi-parameter, ion-sensitive probes are promising in order to observe higher number of sampling points in the lake. With these systems, analysis is done in-situ without taking the samples to a laboratory. Nonetheless, these systems are in the development phase and it is possible to observe a limited number of water quality parameters with high accuracy (EPA, 2005). Moreover, as in the traditional sampling methods, the researcher is still limited with the number of points he/she can monitor.

In the last decades, remote sensing has emerged as a technology for water quality monitoring. With remote sensing, satellite images are used to gather information about the water body. Providing there is enough ground truth data for calibration of the image to the real parameter quantities in the lake, this technology may enable us to apply monitoring

programs without even being on site. Moreover, a continuous distribution of certain parameters can be obtained which may decrease the risk of missing critical and problematic areas in the lake. The analysis can be done frequently, in a very short time and with lower costs compared to conventional methods. In addition, monitoring using the remote sensing technology would be advantageous for locations hard to reach. Nelson et al. (2003) mentioned that remote sensing approach is very useful for huge lakes, or where there are a lot of lakes in a location as in Michigan USA. For such places, remote sensing may be a feasible alternative for regional assessments.

In this study, algae concentrations in Lake Eymir are observed using satellite images, in-situ measurements, and traditional laboratory analysis. Lake Eymir is a eutrophic lake. It has been used for water supply, sports, fishing, etc. Unfortunately, the water quality in the lake has deteriorated in the last 15 to 20 years. However, this lake is still one of the few natural recreational areas in the vicinity of Ankara. Therefore, its conservation and quality monitoring is important.

This study focuses on determining the temporal and spatial distribution of Chl-a in the lake. In addition, the relationship between Chl-a and turbidity is investigated. To obtain these goals, three different sources of data were utilized. Firstly, data were collected on-site using a multiparameter sonde. Secondly, samples were collected and analyzed in the laboratory. And finally, satellite images were acquired. Data were collected on several dates starting from early spring and extending to early fall. To assess the factors enhancing Chl-a (algae) presence, few other

parameters were also measured such as pH, temperature, dissolved oxygen (DO), and secchi depths (SD). Therefore the objectives of this study can be summarized as follows:

- To monitor the temporal and spatial Chl-a distribution in the lake
- To analyze the impact of Chl-a on clarity of the water

# *CHAPTER 2*

# *BACKGROUND*

## 2.1 Trophic state of lakes

Eutrophication as described by Harper & David, 1992 is the term used to describe the biological effects of the increase in concentration of plant nutrients, usually N and P, on aquatic ecosystems (Horne & Goldman, 1994). In other words, Eutrophication is the enrichment of an aquatic ecosystem with nutrients. It is usually a slow natural process which happens almost in all lakes and this process may take several thousands of years. On the other hand, there is the artificial Eutrophication, which came into play after the industrial revolution more then a century ago. Artificial Eutrophication is a very fast process that may take only few years to happen, but often follows the same stages as the natural one.

As industries developed, the waste disposed into the environment increased dramatically. A great deal of those wastes has been disposed to surface waters like lakes, rivers, etc. Together with the industrial sources,

erosion of soil, discharge of wastewaters, and usage of chemical fertilizers in agriculture resulted in the enhanced transport of nutrients to the aquatic systems. In return, these inputs gave increase to Eutrophication problem.

A lake passes through three trophic states which indicate the stage of Eutrophication. These are mainly the Oligotrophic, mesotrophic and eutrophic states. Oligotrophic lakes, as described by (Horne & Goldman, 1994), are generally deep with steep sides and have relatively small drainage area. As they are deep and have relatively low concentrations of nutrients (N & P), they are unproductive, or have very low productivity. As a result, they possess low algae concentrations. The lake is clear with high SDs. Oligotrophic lakes have also abundant amounts of DO, mainly supersaturated around the year. But, due to low productivity, the range of aquatic live and biodiversity are limited.

Mesotrophic state happens when the discharge of wastes from non-point (runoff) and point sources, or both, increase and nutrients are supplied to the lake. Mesotrophic as defined by Webster Dictionary is having a moderate amount of dissolved nutrients. One of the characteristics is to have a SD of 2 to 8 meters (Horne & Goldman, 1994). Since they are considered as productive lakes, they have higher mass of algal blooms than the Oligotrophic lakes. Of course, this means that they contain more diverse aquatic life.

Eutrophic stage happens when the amount of nutrients accumulated in the lake becomes very high. As a result of high productivity, sediment depth increases and the depth of the lake is

reduced. If precautions are not taken to slow down the process, the lake eventually becomes a marsh or a swamp. In eutrophic lakes, high algae production close to the surface can be expected if the light required for photosynthesis is abundant. For the oxygen concentrations, they vary from supersaturated near the surface during the day to very low values at the bottom or during the night. The transparency of the lake diminishes and the SDs drop below 1 m (even to few centimeters) in a eutrophic lake (Horne &Goldman, 1994). As the lake becomes highly productive, algae are reproduced extensively and high Chl-a concentrations are observed.

The algae content of a lake can be used as one of the indicators of the trophic state of a lake. Typical ranges of Chl-a concentrations for different trophic states are summarized in Table 1.1.

Table 2.1: Typical ranges of Chl-a concentrations for different trophic states

| Trophic state | Chl-a ($mg/m^3$)[1] | Annual mean Chl-a ($mg/m^3$)[2] | Annual max. Chl-a ($mg/m^3$)[3] |
|---|---|---|---|
| Ultra-Oligotrophic | 0.001-0.5 | ≤ 1.0 | ≤ 2.5 |
| Oligotrophic | 0.3-3 | ≤ 2.5 | ≤ 8.0 |
| Mesotrophic | 2-15 | 2.5-8.0 | 8-25 |
| Eutrophic | 10-500 | 8-25 | 25-75 |
| Hypereutrophic | | ≥ 25 | ≥ 75 |

As algae growth increases intensively, it causes bad odor and taste of water. The consumption of oxygen increases which may create anoxic

[1] Wetzel, 1975

[2] Vollenweider and Kerekes, 1980 (OECD criteria)

[3] Vollenweider and Kerekes, 1980 (OECD criteria)

condition (condition when oxygen levels are very low) especially in the sediment level. Anoxic conditions lead to a series of chemical and microbial processes that otherwise would not take place such as nitrate ($NO_3$) amonification, denitrification, and desulfurication (Lampert & Sommer, 1997). Also because of photosynthesis, an increase in the pH occurs, which in turn creates a shift from ammonium to toxic ammonia. In addition, aquatic organisms may die due to damage of gills or great depletion DO concentrations, especially in the late summer (Tang & Kawamura, 2005).

**2.2 Lake Eymir**

Lake Eymir is located 20 km south of Ankara and was announced as an environmentally protected area in 1990. Eymir is hydrologically connected to Lake Mogan via concrete lined channel which is located in the southwest of Eymir and with an underground link as well. Lake Mogan, Kıslakcı Stream (a perennial stream at the northern end), and groundwater sources feed the lake. The excess water of the lake drains into İmrahor Creek at the north (Altınbilek et al., 1995).

Lake Eymir, with its average depth of about 3 m, is classified as a shallow lake. The lake area changes between 1.05-1.25 $km^2$ depending on the depth of water. The catchment area is 971 $km^2$ with 13 km of shoreline (Tan and Beklioglu, 2005).

Many sources of pollution affected the state of the lake to date.

Those sources were mainly originated from discharge of wastewaters of Gölbaşı district, the wastewaters coming from the sewage treatment plant of TEİAŞ (Turkish Electricity Transmission Company), and the Kışlakçı Creek. In addition, there are a number of restaurants on the shores of the lake which might have contributed to the pollution. In order to improve the water quality of the lake some actions had been taken. In 1994, the slaughterhouse that was discharging to an area close to the lake was shut down. The TEİAŞ residency was connected to the Gölbaşı sewerage system. In addition, in 1995, a 25833 m of bypass line was put in service by ASKİ (Ankara Water and Sewage Directorate) in order to avoid the wastewaters of the Gölbaşı district from entering the lake. However, since the pumps were not operated adequately, Lake Eymir continued to be a receiving body for the Gölbaşı wastewaters (Altınbilek et al,. 1995).

Many studies regarding the lake have been conducted through the years especially after 1990, as the pollution in the lake became of concern. One of the most important and comprehensive studies was conducted by ASKİ in coordination with the Middle East Technical University (Altınbilek et al., 1995). The study included water quality surveys for a period of about 1 year in 1994-1995. This study revealed the eutrophic characteristics of the lake with high concentrations of total phosphorus (TP), Chl-a, and total suspended solids (TSS) (727 ± 433 μg/l, 27 ± 22μg/l, 38 ± 18 mg/l, respectively), and low SDs (56 ± 19 cm). In that study, phytoplankton were determined as the primary producers. The macrophytes were deemed as insignificant. In 1997-August 1998 period, TP, Chl-a, and secchi disk depths were measured as 324 ± 31 μg/l, 19 ± 3 μg/l, 101 ± 43 cm, respectively (Beklioglu et al., 2003). The bypass line was

in service (at least intermittently) during this period. In August 1998-1999 a biomanipulation project was started in the lake which resulted in the removal of 55% of benthi-planktivorous fish. The reported TP, Chl-a, SS, and secchi depths during that study were 381 ± 21 μg/l, 9.4 ± 6 μg/l, 11.4 ± 2.6 mg/l, and 262 ± 145 cm, respectively (Beklioglu et al., 2003). In 2001, Lake Eymir experienced extreme drought resulting in up to 1 m decrease in the depth of water. During this period, the coverage of submerged macrophytes increased to 90%. In 2002, the water level was restored and the coverage of macrophytes decreased to 63%. Chl-a concentration was 21 ± 37 μg/l (Beklioğlu et al., 2003).

**2.3 Remote sensing of algae**

Remote sensing, as defined by the Canadian center of remote sensing is "the science (and to some extent, art) of acquiring information about the Earth's surface without actually being in contact with it. This is done by sensing and recording the reflected or emitted energy, and processing, analyzing, and applying that information."

The process of remote sensing involves many steps and has several important elements. First of all, there should be an energy source, which is in most cases the sun. This energy will travel through atmosphere until it gets in contact with the target object. The energy (or a portion of the energy) then will be reflected by the object, and picked up or sensed by the remote sensor, which is a plane or a satellite. Information is recorded electronically, and then transmitted to a ground station where it is

transformed into an image. Then the image is processed analyzed, interpreted, and information is acquired about the target object.

Commercial remote sensing is only a couple of decades old, and it is developing very fast. It is expected that in future, with the developing technology, satellite images would be cheaper and provide more detailed and higher spatial resolution images that can be used in many fields. Glasgow & Burkholder (2004) mentioned that lately governments and large industries showed interest in remote sensing and investing into the development of the technology. It is perceptible that use of this technology as a real-time monitoring system or as a part of early warning systems for potential environmental problems and risks is a matter of time (EPA, 2005).

Every matter in the environment has a different absorbance and reflectance of energy at certain wavelength of the light spectrum (Vahtmae & Kutser, 2006). This makes it easier to detect and distinct them from each other. For this reason remote sensing has become a very important method for research of many environmental issues. Examples of environmental remote sensing applications include the detection of trophic state of surface waters, weather analysis, soil state and erosion analysis, landuse determinations, etc. (Barrett and Curtis, 1992). Besides determining the Chl-a concentrations, remote sensing have been applied to determine TSS (Sipelgas & Raudsepp, 2006; Miller & Mckee, 2004; Hu & Chen,2004), SD, water flow pattern (H.French & Miller, 2005), turbidity (K.Vincent & Qin, 2003) and other parameters. The method can be applied to make both qualitative and quantitative observations.

Chl-a as defined by Webster Dictionary[4] "is the green photosynthetic pigment found chiefly in the chloroplasts of plants". Chl-a concentration is used as an indicator for the algal biomass. It is a photoreceptor and plays an important role in the photosynthesis. It has peak absorbance of energy at certain parts of the light spectrum (peak at 680 nm in clear water) (Shevyrnogov & Sidko, 1998). In Figure 2.1 the reflectance characteristics of clear and algae laden waters is presented. The absorption areas of the reflectance curve are caused by the absorption of blue and red light by chlorophyll as it uses the light to produce energy. The reflectance peak in the green area wavelength is due to the partial reflectance, which causes algae to be perceived as green (Han, 1997).

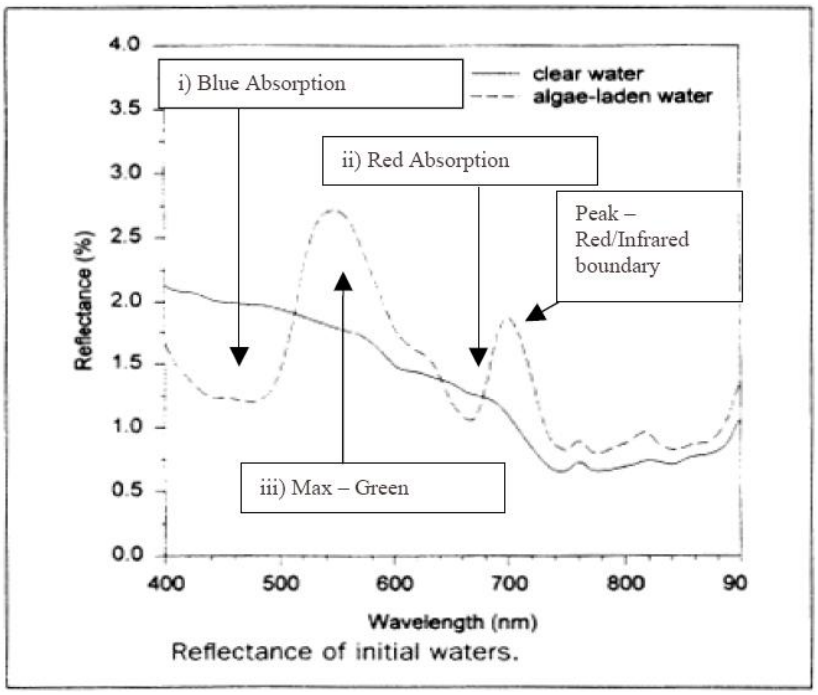


Figure 2.1: Reflectance Characteristics of clear and algal water (Han, 1997)

[4] www.webster.com , November 2005.

There are several studies in the literature that focus on deriving models to describe the Chl-a concentrations in water bodies. The models are not universal and specific to each study site. This is due to the different conditions and constituents present in different water bodies. Therefore different optical properties of the water columns for different sites require the development of site-specific empirical equations (Sipelgas & Raudsepp, 2006). Although, there are several studies for application of remote sensing in determination of Chl-a content in seas and oceans example studies summarized below will focus on fresh surface waters.

One of the important studies made regarding the topic is a study carried out by Wolter & Johnston (2005). The imagery of the satellite QuickBird was used in the research in order to classify the submergent aquatic vegetation (SAV). The average accuracy of the classification was around 80%. Concerns were raised about the shading that could have affected the accuracy of the investigation. The author stated the usefulness of using QuickBird imagery in environmental applications, but at the same time questioned the feasibility of using it because of the high costs of acquiring data.

Giardino & Pepe (2001) used the Landsat TM (Thematic Mapper) images acquired in 1997 to model the Chl-a concentrations in a lake in Italy. Samples were taken from the lake at the same time when the image was acquired to measure Chl-a, SD and temperature. Then the satellite image was processed and corrected atmospherically to eliminate the effects of cloud or haze in the image. Then, a statistical approach was used to determine the relationship between ground truth data and remotely

sensed data. The following equation was proposed to define the Chl-a concentrations:

$$\text{Chl-a } (mg/m^3) = 11.18d_{TM1} - 8.96d_{TM2} - 3.28 \quad [1]$$

Where, $d_{TM1}$ and $d_{TM2}$ are the readings from the first and the second bands of the satellite, respectively. For 4 sampling points, the correlation coefficient ($R^2$) between the model (equation 1) and the remotely sensed data was 0.999.

In a study by Thiemann & Kaufman (2000), the Indian remote sensing satellite (IRS) image was used to model the Chl-a concentrations in a lake in Germany. Four images were acquired on different dates in order to investigate the temporal change. However, in the regression analysis they used only two sampling points. The $R^2$ was 0.28 for the green band and 0.51 for the infrared band. The poor results were due to cloud presence in the summer images and low concentrations in autumn. Besides using satellite images, field spectra were used. In this method, the reflectance was measured in-situ. Therefore, adverse impacts of illumination, cloud or haze were eliminated. For the field spectra, $R^2$ values reached up to 0.89.

In another study (Ostlund & Flink, 2001), several regression models were tested for Chl-a in Lake Erken in Sweden. $R^2$ ranged from 0.76 to 0.93 for a limited number of sampling points.

Hamilton & Davis (1993) showed that remote sensing is also useful in detecting low concentrations of Chl-a (as low as 0.16 mg/$m^3$) in the lakes. The study was carried out in Lake Tahoe, California. The images from AVIRIS satellite were used to predict the bathymetry of the lake and the Chl-a concentration. They indicated that the results were very sensitive to other parameters at low Chl-a concentrations.

Buttner & Korandi (1987) performed Chl-a analysis at Lake Balaton using the images of Landsat MSS. The data were collected within 4-5 hours of the satellite overpass. $R^2$ between the measured Chl-a and remotely sensed images ranged from 0.71 to 0.90. But, the results of regression for TSS were poorer. Mapping of Chl-a was also carried out for spatial assessment.

In a study conducted by George (1997) in the English Lake District, airborne remote sensing was used instead of a space satellite in the English Lake District. A sensor was mounted on an airplane and the image was taken. Ground truth data were also collected at the same time the image was obtained. $R^2$ for the relationship between the measured and remotely sensed data were in the range of 0.71 and 0.98 for several lakes of different trophic states.

Zimba & Gidelson (2006) stated that ground truth data must be collected in a very "optimal" way such that, the number of samples should be sufficient and covering the area of interest as much as possible, sampling and measurement should be done carefully so that results would be accurate, and finally the time of measurement must be very close to the

time of capturing the satellite image. In their study, data were collected about a month after the image was captured. The resulting $R^2$ for the relationship between the measured and remotely sensed data was around 0.3 to 0.4. In contradiction, Nelson et al. (2003) showed in their study that as long as the system is the same, using datasets of different dates collected on different dates will not affect the result of the analysis. These two studies seem to be in contradiction with each other, but actually they show that the situation may differ from one system to another.

# *CHAPTER 3*

# *METHODOLOGY*

## 3.1 Field Study

In order to determine the Chl-a concentrations in Lake Eymir, field work was employed. For this purpose, 17 sampling points were selected in the lake as depicted in Figure 3.1. These points cover the extents of the lake. The locations of the sampling points were determined using a Magellan Sportrak GPS receiver. However, since it is practically not possible to get samples from the same exact coordinate at different sampling dates, sampling coordinates were recorded for each sampling activity. However, care was given to take samples in the vicinity of the selected sampling points.


Figure 3.1: Locations of sampling points, the red arrows indicate the discharge to and exit of water from the lake.

Data from Eymir Lake were collected starting from April 2005 and ending with the end of October 2005. The attempts to conduct the study before April and after October were unsuccessful due to logistic issues. The lake surface was frozen or icy until late March, which made the sampling study impossible mainly due weather conditions and the unavailability of the boat used for sampling. Similarly, the boat was unavailable after October.

Measurements were taken at 17 sampling points using a multiparameter water quality sonde. In this study, YSI 6600 EDS (Figure 3.2) was used as the multiparameter water quality sonde. This instrument can measure the following parameters; DO, turbidity, temperature, depth, Chl-a, oxidation-reduction potential, and pH. It works under -5 and + 45

degrees C[5]. This probe automatically records data in user specified time intervals. The time interval was set to two seconds, and the probe was suspended into water very slowly and data were recorded until it hit to the bottom of the lake. Then, the data were transferred to a regular PC or a laptop. Since measurements were obtained in a very short time compared to laboratory analysis, it was possible to get in-situ measurements at all sampling points in a sampling study. It took about 5-10 minutes to obtain in-situ data at each sampling point after the sonde was released.


Figure 3.2: YSI 6600 EDS[6]

[5] **YSI Incorporated** http://www.ysi.com 9th of October 2005
[6] **YSI Incorporated** http://www.ysi.com 9th of October 2005

In addition to the listed water quality parameters above, SDs were measured as well at 17 sampling points to check the transparency of the water. For this purpose a standard 20 cm weighted disk of alternating black-and-white secchi disk was used. The disk was lowered in the water until the black-and-white quadrants were no longer distinguishable (Figure 3.3). At that point, the depth was recorded using the graduated line connected to the secchi disk.

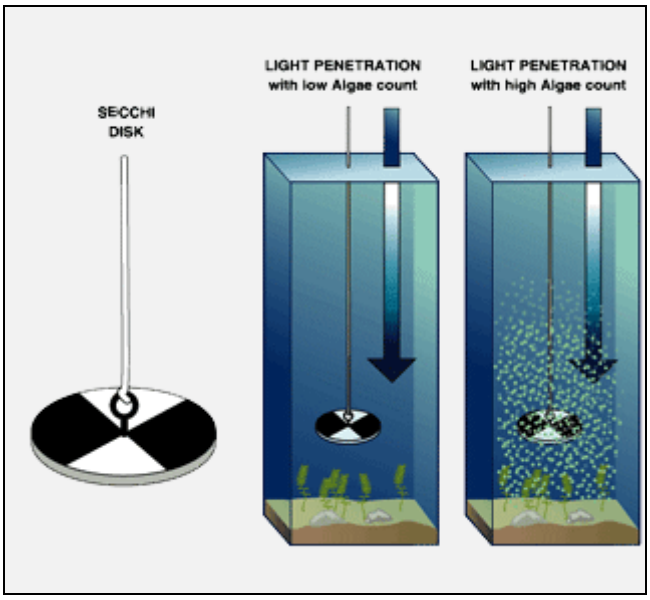


Figure 3.3: SD measurement[7]

In addition to in-situ measurements with the sonde, traditional sampling and laboratory analysis were performed for Chl-a. Due to time restrictions and the high number of samples for analysis, only 4 sampling points were employed. These points are depicted in Figure 3.4. The

[7] **The Heritage Council** http://www.heritagecouncil.ie/waterways/images/secchi.gif 12th of October 2005

distribution of sampling points for laboratory analysis was adopted from a previous study performed in Lake Eymir (Altınbilek et al., 1995). As a result, more or less similar points were checked. From west to east, these points correspond to the sampling point numbers of 4, 9, 12 and 16 within the 17 sampling points selected for in-situ measurements.


Figure 3.4: Sampling points for laboratory analysis

Samples were taken from the lake using a Van Dorn water sampling apparatus (Figure 3.5). Samples were obtained from the surface, mid-depth and bottom sections at each sampling point. The apparatus was setup and lowered to the specified depth. Then, its messenger was dropped to close the caps of the cylindrical container, resulting in the entrapment of about 3 lt of lake water. Then it was pulled out of water, and the sample was emptied into PVC containers. These containers were

immediately put in a cooler and kept away from direct sun. In the laboratory, sample containers were transferred into another large capacity cooler.

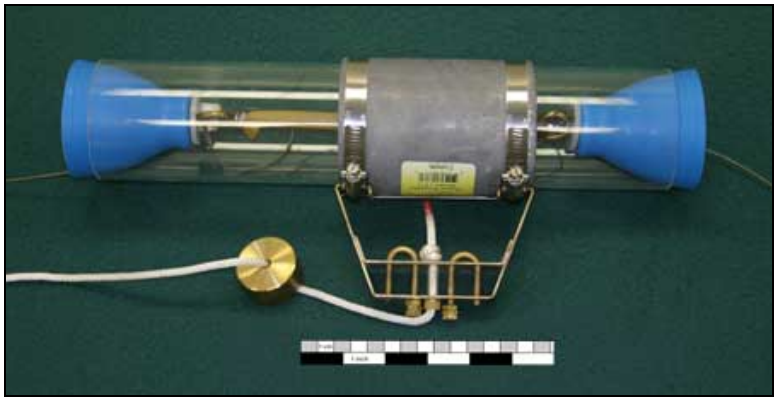

Figure 3.5: Van Dorn Water Sampling apparatus[8]

The Field work was always done in the early morning. In-situ measurements and sampling operations lasted for about 3-5 hours on the average. In most cases, field work was completed before noon. A boat supplied by the Middle East Technical University was used for the sampling activities in the lake. Transportation was supplied by the University and the Environmental Engineering Department. Figure 3.6 shows the sampling schedule. In all sampling dates, data were acquired using the sonde. However, on dates shown by the green lines, no laboratory measurements were conducted due to logistical issues.

[8] **Santa Barbara City College Biological Sciences,** http://www.biosbcc.net/ocean/marinesci/01intro/toindex.htm 12th of October 2005

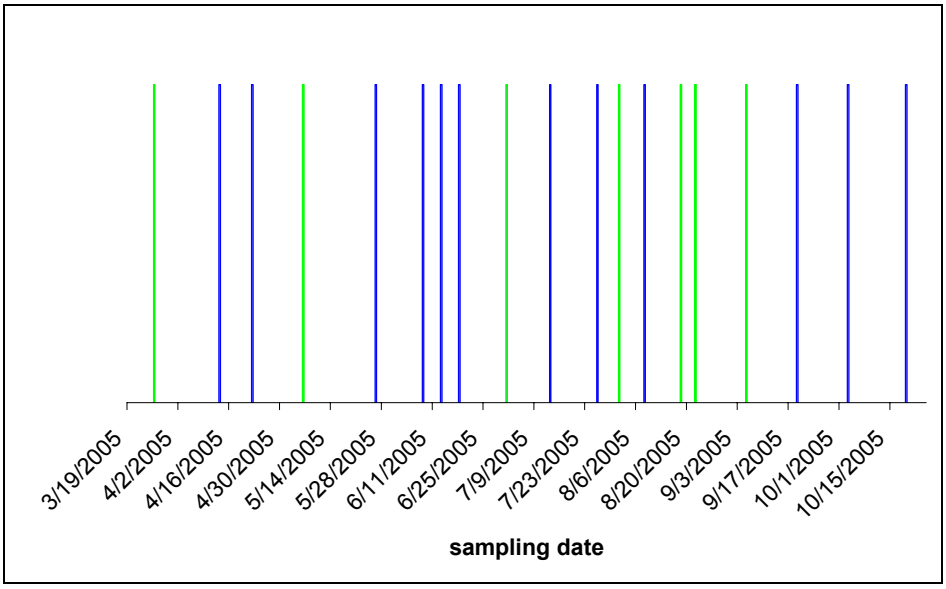


Figure 3.6: Sampling schedule (green lines – on dates shown by green lines, no laboratory measurements were conducted)

## 3.2 Laboratory Analysis

Samples were analyzed for Chl-a and TSS in the laboratory. In most cases, laboratory work was conducted immediately after coming from the field. In the worst case, experiments were finalized within a couple of days.

### 3.2.1 Analysis of Chl-a

Chl-a concentrations were measured using the improved ethanol extraction method (ISO: 10260, 1992 standard) by Papista et al. (2002). Ethanol extraction was preferred over the standard acetone extraction since it was shown to be superior compared to standard acetone extraction

method (Papista et al., 2002).

The procedure applied is summarized below:

1- 250 ml of sample was filtered using a glass wool filter (Figure 3.7).
2- The filter paper was put into a covered glass container.
3- 20 ml of 90% pure ethanol was poured over the filter paper into the container (Figure 3.8).
4- The container was closed and put into a warm water bath at 75 $^{o}$C for 15 minutes.
5- After removing the container from the bath, it was left to cool down to room temperature (30 min to 1 hr). The filter paper was shaken off and removed from the container. Then the container was put into a cooler and kept in there for about a day.
6- Absorbed light by the processed sample was measured using the HACH 2400 Spectrophotometer at 665 nm wavelength against an ethanol blank.
7- Step 6 was repeated at 750 nm
8- Then about 0.01-0.02 ml hydrochloric acid (HCl) was added into the cuvette containing the sample and mixed occasionally in an interval of about 30 minutes (Initial testing indicated that absorption readings were stabilized after mixing for 30 minutes).
9- Steps 6 and 7 were repeated.

The Chl-a concentrations were determined using the below equation;

$$\text{Chl-a } (\mu g/lt) = (A-A_a)*29.6*V_e/ (V_n*L) \quad (3.1)$$

$V_e$: extract volume, ml

$V_n$: sample volume, l

L: light path length, mm

$A=A_{665}-A_{750}$=absorbance difference before acid addition

$A_a=A_{665acid}-A_{750acid}$=absorbance difference after acid addition


Figure 3.7: Vacuum filtration apparatus used for Chl-a and TSS experiments

Figure 3.8: Filter papers immersed in %90 pure ethanol solution (notice the green color due to Chl-a extracted into the ethanol)

### 3.2.2 Analysis of TSS

This experiment was performed using a gravimetric method according to Standard Methods (2540 D; APHA, 1997). Procedure is as follows:

1- 5.5 cm diameter Whatmann glass wool filter papers were dried in an oven at 105$^{o}$C for about one hour.
2- Filter papers were cooled down to room temperature in a dessicator and weights are recorded using a sensitive weight (Sartorius BA21S)
3- 50 ml sample was filtered through a filter paper using vacuum

filtration.

4- Filter paper with the filtrate was dried again at 105°C for about one hour cooled down to room temperature in a dessicator and weighed again.

TSS amounts were calculated using the below expression:

$$TSS\ (mg/l) = (W_f - W_u)/(1000\ V_s)$$

Where,

$W_f$ = weight of filter paper after filtration (gr)

$W_u$ = weight of filter paper before filtration (gr)

$V_s$ = volume of sample filtered (l)

### 3.3 Chl-a determination using remotely sensed data

Due to the relatively small area of Lake Eymir, images of high spatial resolution were preferred. In literature, algae or Chl-a studies were conducted using the images obtained primarily from Landsat, SeaWiFS, and EOS. However, since the lake area is relatively small, images of higher spatial resolutions are required. With other satellites of lower spatial resolution, the data available for analysis would be limited due to the area of the lake. As a result, QuickBird images were used. In literature, very few studies found that applied QuickBird images for algae or Chl-a investigation.

QuickBird has a spatial resolution of 61 cm for panchromatic sharpened and 2.44 m for multispectral images. QuickBird was launched on October 18th, 2001. It is currently one of the few commercial satellites proving the data with the highest spatial resolution. QuickBird collects an industry-leading 16.5 km swath of imagery (DIGITALGLOBE, 2005**)**. In table 3.1, the bands utilized by QuickBird are presented. Each band represents a specific range in the light spectrum at which the sensor of the satellite can acquire images.

Table 3.1: Band information for the QuickBird Satellite (Digital globe, 2005)

| | Bandwidth | Spatial Resolution |
|---|---|---|
| Band1 | 0.45 - 0.52μm (blue) | 2.44 - 2.88 meters |
| Band2 | 0.52 - 0.60μm (green) | 2.44 - 2.88 meters |
| Band3 | 0.63 - 0.69μm (red) | 2.44 - 2.88 meters |
| Band4 | 0.76 - 0.90μm (near infrared - NIR) | 2.44 - 2.88 meters |

Two images were ordered from the QuickBird Satellite. The first image (Figure 3.9) was taken on June 26th, 2005, and the other on August 6th, 2005. Previous orders were unsuccessful due to cloudiness. Therefore, only summer conditions were analyzed using the remotely sensed data.

In an ideal situation, the ground truth data (in-situ data or laboratory analyzed samples) should have been gathered on the same day the image was taken. However, unfortunately, it was not possible to learn the exact satellite processing date beforehand. Only potential time of

imaging was supplied which spanned a period of 2 weeks. Although several field works were performed in the potential dates, it was not possible to obtain the ground truth data on the dates the images were taken. In addition, the recreational activities in summer also limited the sampling work. As a result, calibration of the images and concentration comparisons were employed for the closest field study dates. For the first image (taken on 26$^{th}$ of June), the closest field works were on June 18$^{th}$ (laboratory analysis) and July 1$^{st}$ (in-situ measurements). For the second image (taken on 6$^{th}$ of August), the data of the field work employed on 8$^{th}$ of August was used as the reference. Unfortunately, it was possible to order only two images due to the scarcity of funds to purchase images.

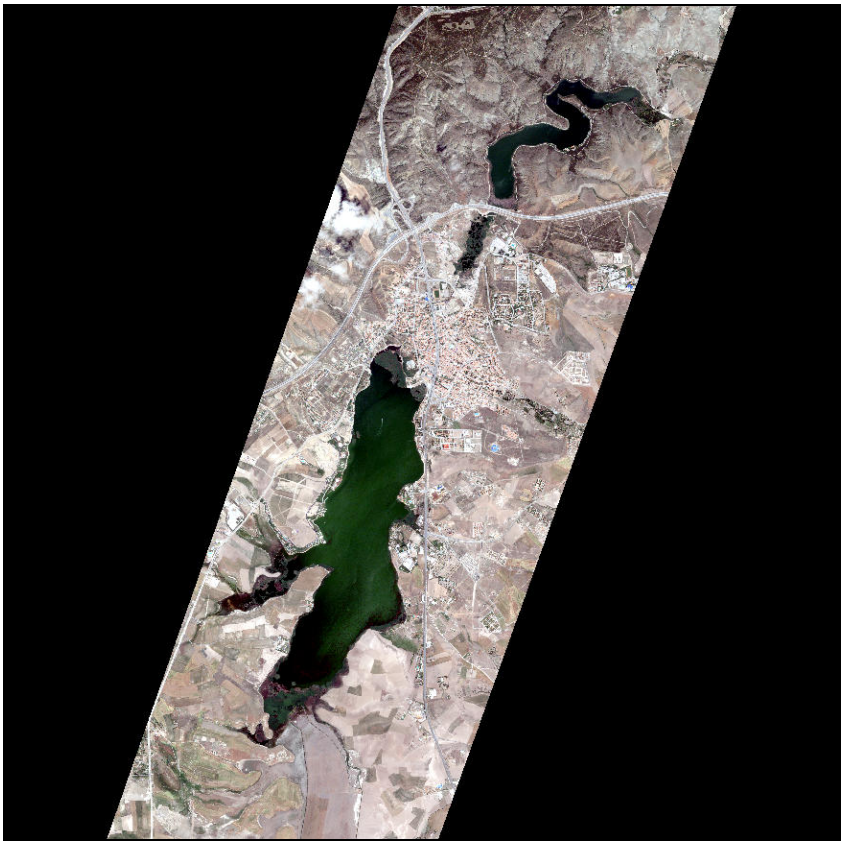

Figure 3.9: QuickBird image taken on 26th of June (Lake Eymir is at the top above Lake Mogan)

The QuickBird images were analyzed using the image processing software ERDAS IMAGINE version 8.7 by Leica Geosystems. In order to remove the interferences that may result at the border of water and land, the land sections were excluded from the image and only the water body of Lake Eymir was examined. The software was used to acquire reflectance (Figure 3.10) and the corresponding digital numbers (DNs) (Figure 3.11; Figure 3.12) at each pixel of the image for each band (green, blue, red, and infrared). For the regression analysis, DNs at different bands at the sampling points were the independent parameters and the measured Chl-a values were the dependent parameters. Regression

analysis was performed using Microsoft Excel. ***ARCGIS 9.0*** by ***ESRI*** was also used to map the Chl-a concentrations in the lake for the data obtained at different times by multiparameter sonde.

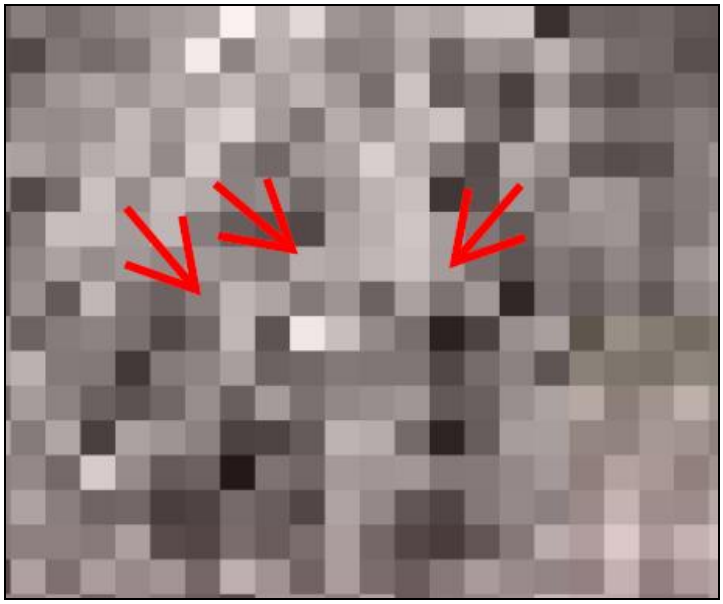

Figure 3.10: Pixels showing the reflectance

| | | | | | | | | | | | | | | | | | |
|---|---|---|---|---|---|---|---|---|---|---|---|---|---|---|---|---|---|
| 72 | 45 | 72 | 72 | 72 | 81 | 72 | 72 | 72 | 72 | 72 | 67 | 72 | 72 | 72 | 72 | 72 | 72 |
| 63 | 63 | 63 | 63 | 63 | 66 | 63 | 63 | 63 | 63 | 63 | 63 | 63 | 63 | 63 | 63 | 63 | 63 |
| 23 | 23 | 96 | 23 | 23 | 84 | 23 | 23 | 23 | 23 | 23 | 23 | 23 | 23 | 23 | 23 | 23 | 96 |
| 34 | 34 | 55 | 34 | 34 | 66 | 66 | 34 | 34 | 34 | 34 | 72 | 34 | 34 | 34 | 34 | 34 | 55 |
| 33 | 65 | 20 | 22 | 54 | 44 | 44 | 43 | 31 | 13 | 41 | 12 | 11 | 0 | 66 | 34 | 45 | 20 |
| 84 | 84 | 25 | 84 | 84 | 25 | 25 | 84 | 84 | 84 | 84 | 23 | 84 | 84 | 66 | 66 | 84 | 84 |
| 76 | 76 | 66 | 76 | 76 | 66 | 66 | 76 | 76 | 76 | 72 | 72 | 72 | 81 | 44 | 44 | 76 | 76 |
| 81 | 81 | 14 | 81 | 81 | 14 | 14 | 81 | 81 | 81 | 63 | 63 | 63 | 66 | 63 | 81 | 81 | 81 |
| 66 | 66 | 26 | 66 | 66 | 26 | 26 | 66 | 66 | 66 | 96 | 23 | 23 | 63 | 63 | 63 | 26 | 66 |
| 84 | 84 | 96 | 84 | 84 | 96 | 96 | 84 | 84 | 84 | 84 | 76 | 84 | 23 | 23 | 23 | 96 | 84 |
| 45 | 45 | 55 | 45 | 45 | 96 | 45 | 45 | 45 | 84 | 23 | 23 | 23 | 34 | 34 | 34 | 23 | 45 |
| 66 | 66 | 66 | 66 | 66 | 55 | 66 | 66 | 66 | 45 | 34 | 34 | 34 | 34 | 34 | 72 | 34 | 66 |
| 44 | 44 | 44 | 44 | 72 | 20 | 34 | 34 | 55 | 34 | 34 | 45 | 34 | 34 | 34 | 63 | 0 | 44 |
| 25 | 25 | 25 | 25 | 63 | 25 | 0 | 0 | 20 | 0 | 65 | 66 | 23 | 14 | 0 | 23 | 84 | 25 |
| 66 | 66 | 66 | 84 | 23 | 66 | 84 | 84 | 25 | 84 | 84 | 44 | 84 | 84 | 84 | 34 | 76 | 66 |
| 14 | 14 | 14 | 45 | 72 | 14 | 76 | 76 | 66 | 76 | 76 | 25 | 76 | 76 | 76 | 0 | 81 | 14 |
| 26 | 26 | 26 | 66 | 63 | 26 | 81 | 81 | 14 | 81 | 81 | 66 | 34 | 55 | 34 | 26 | 26 | 26 |
| 96 | 96 | 96 | 96 | 23 | 96 | 96 | 96 | 96 | 96 | 96 | 96 | 0 | 20 | 0 | 96 | 96 | 96 |
| 55 | 55 | 55 | 55 | 55 | 55 | 55 | 55 | 55 | 55 | 55 | 55 | 84 | 25 | 84 | 55 | 55 | 55 |
| 20 | 20 | 20 | 20 | 20 | 20 | 20 | 20 | 20 | 20 | 20 | 20 | 76 | 66 | 76 | 20 | 20 | 20 |

Figure 3.11: Corresponding DNs for each pixel of the image

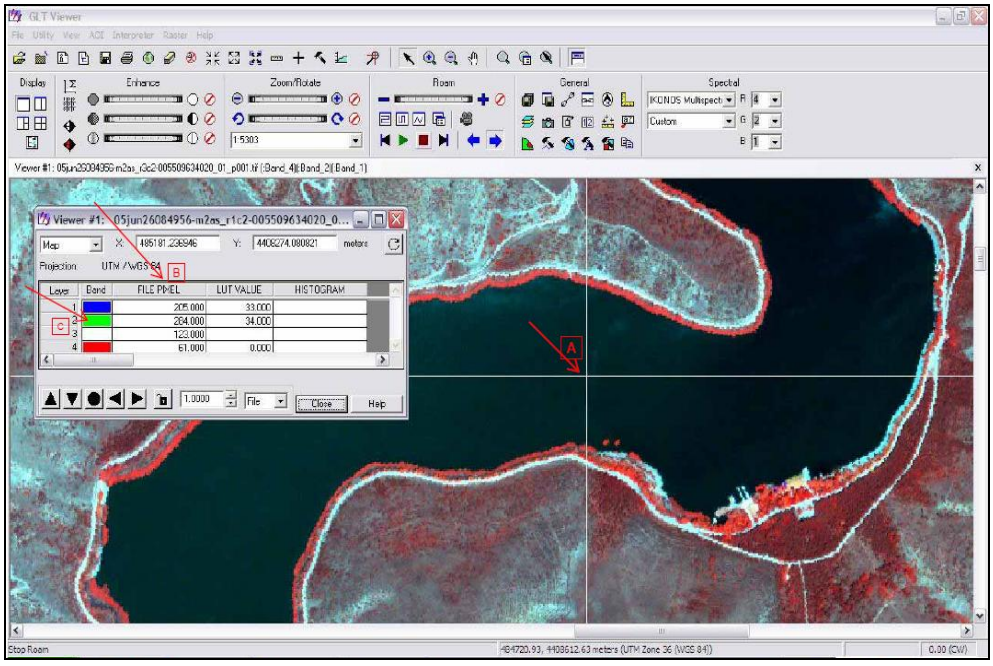


Figure 3.12: Acquiring DNs for pixels at the sampling points using ERDAS Imagine (A: Sampling point, B: Pixel values (DNs), C: Blue, green, infrared, and red bands)

# *CHAPTER 4*

# *RESULTS and DISCUSSION*

In this section the collected data by three different methods (remotely sensed data, in-situ measurement, and laboratory analysis) are presented and analyzed. It should be noted that during the study period, there has been no input from Lake Mogan to Eymir due to drought conditions. The channel between the two lakes was blocked.

## 4.1 Laboratory Measurements

The Chl-a concentrations obtained through laboratory analysis are summarized in Table 4.1. The plot of average values for different sampling dates is presented in Figure 4.1. The measurements indicate that the lake is hypereutrophic in terms of Chl-a according to the OECD criteria.

Table 4.1: Average Chl-a Concentrations obtained for four sampling points (Laboratory analysis) (standard deviations are given in parenthesis)

| Sampling Date | Avg. Chl-a (lab) (µg/l) |
|---|---|
| 13-Apr-05 | 238 (198) |
| 26-May-05 | 53 (32) |
| 8-Jun-05 | 30 (4) |
| 13-Jun-05 | 34 (23) |
| 18-Jun-05 | 32 (7) |
| 13-Jul-05 | 52 (17) |
| 25-Jul-05 | 205 (101) |
| 8-Aug-05 | 432 (124) |
| 5-Sep-05 | 102(111) |
| 19-Sep-05 | 336 (175) |
| 3-Oct-05 | 184 (71) |
| 19-Oct-05 | 160 (87) |

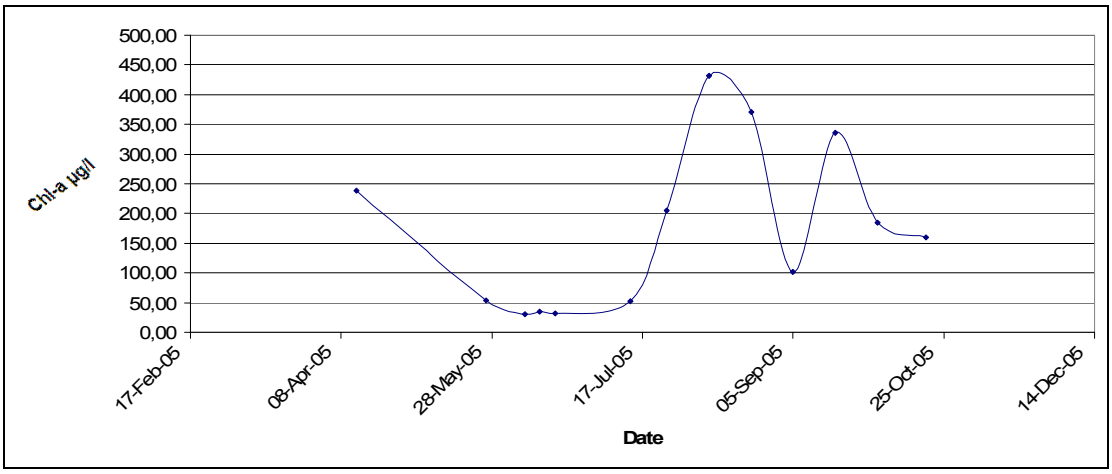


Figure 4.1: Change of average Chl-a concentrations (µg/l) with time (laboratory analysis).

The high concentrations observed in April are probably due to a turnover or due to the pollutants carried by the runoff. Figures 4.2 and 4.3 show the monthly maximum daily ambient temperatures observed and the monthly rainfall received in the area, respectively. Data are received from the Police College meteorological station close by the lake which is operated by the State Meteorological Institution. It should also be noted that although at all stations the similar temporal trend was observed in Chl-a concentrations, relatively high values were observed at sampling point 4 in April, which had a significant impact on the high average quantity for that month. As seen in Figure 4.2, by April there is a significant increase in the average monthly daily maximum temperatures and the amount of rainfall received (Figure 4.3). This may have resulted in the enhancement of algal production.

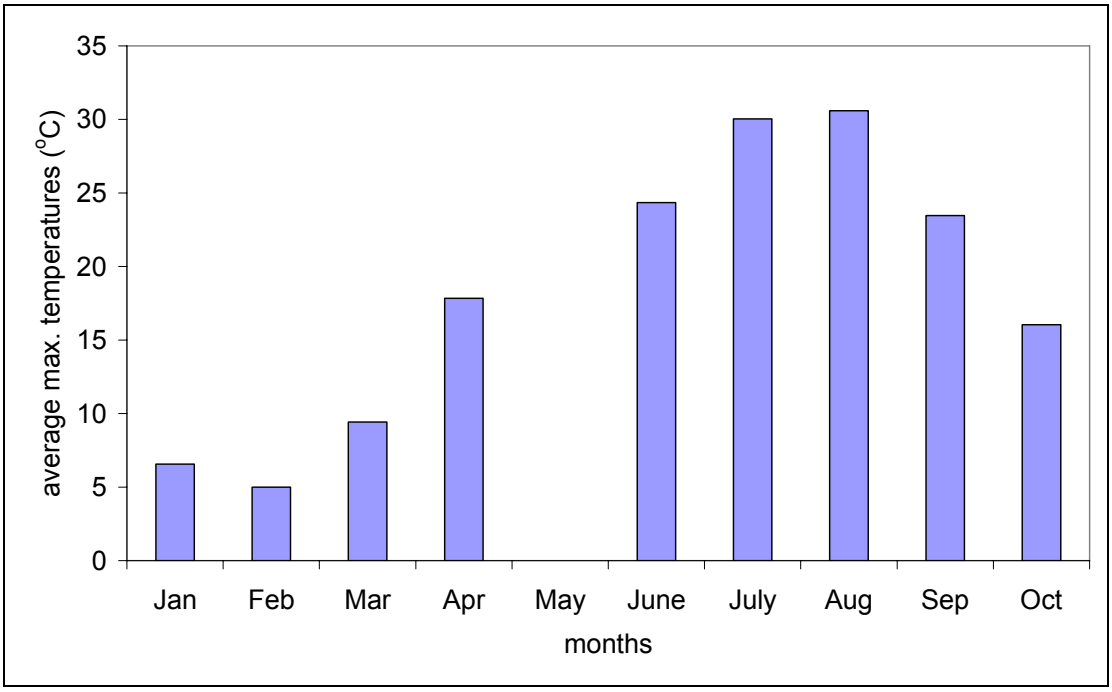


Figure 4.2: Monthly average daily maximum temperatures observed in the area

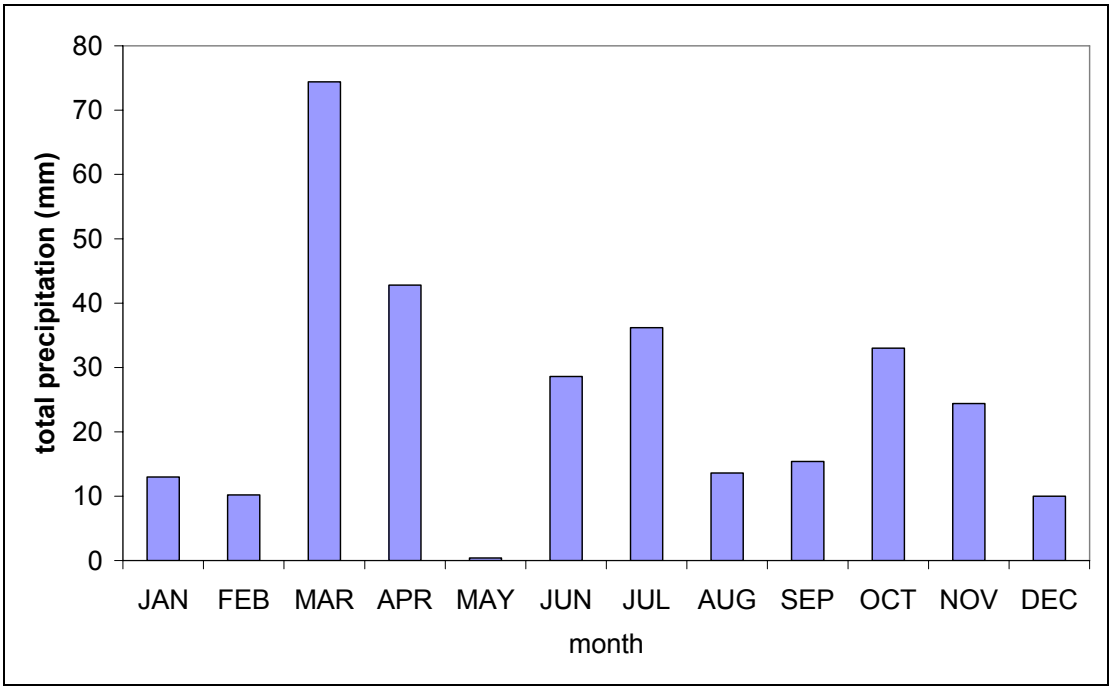


Figure 4.3: Monthly average precipitation observed in the area

The highest precipitation amount was observed in March and April 2005 (Figure 4.3). The total amount of rainfall received in these two months constitutes about 40% of the total precipitation in 2005. This increases the possibility of pollutants being carried to the lake via runoff and Kışlakçı Creek, which might have increased the algal biomass as well. However, it should be noted that because of the relatively large suspended algal particles present in the lake, the observed standard deviations in the measurements (Table 4.1) were high.

Table 4.2 presents the average TSS concentrations obtained in the laboratory analysis with the standard deviations. TSS concentrations also indicate that there was an activity in April. This may be as a result of turnover and runoff (or precipitation) reaching to the lake. The increase in TSS in summer months may be due to decreased water levels as a result of evaporation and increased Chl-a. The average TSS values are also depicted in Figure 4.4. It is clear that TSS and Chl-a concentrations follow the same trend. This may be an indication of the impact of Chl-a on the overall TSS values together with the solids brought by the runoff.

Table 4.2: Average TSS concentrations obtained for four sampling points (Laboratory analysis) (standard deviations are given in parenthesis)

| Sampling Date | Avg. TSS (lab) (mg/l) |
|---|---|
| 13-Apr-05 | 80 (50) |
| 26-May-05 | 22 (22) |
| 8-Jun-05 | 17 (39) |
| 13-Jun-05 | 8 (2) |
| 18-Jun-05 | - |
| 13-Jul-05 | 4 (1) |
| 25-Jul-05 | 24 (7) |
| 8-Aug-05 | 36 (18) |
| 5-Sep-05 | 14 (9) |
| 19-Sep-05 | 35 (21) |
| 3-Oct-05 | 29 (6) |
| 19-Oct-05 | 20 (5) |

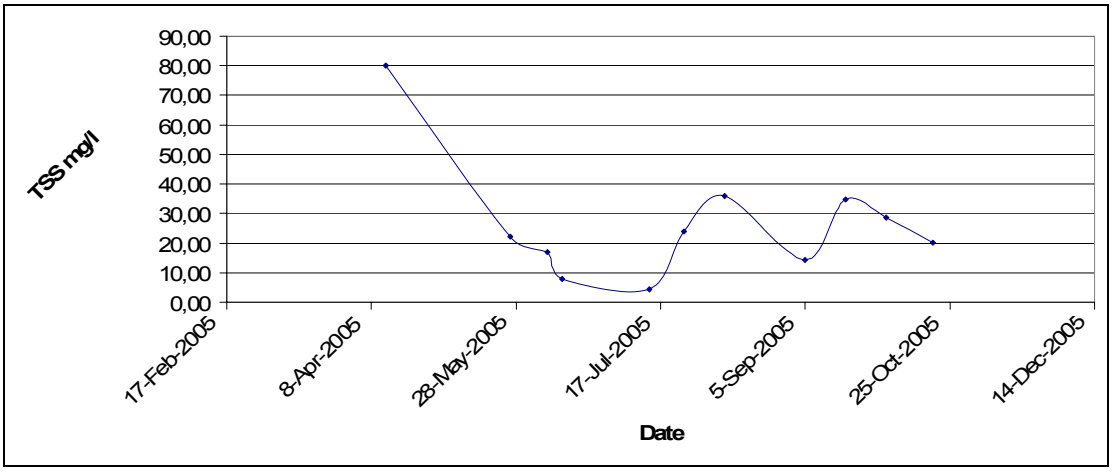


Figure 4.4: Change of average TSS concentrations (µg/l) with time (laboratory analysis).

When SD was compared to Chl-a concentrations, the relationship given in Figure 4.5 was obtained. An exponential decay was observed in SD as Chl-a concentrations increased. This exponential decrease is probably due to the concentration of algae at the upper levels of the lake and the attenuation of light with the depth. As the activity of Chl-a increases very much near the surface, it causes the water to be turbid, which in turn prevents the light from reaching higher depth, and this causes the algae to be more near surface in order to receive light for photosynthesis. As a result SDs decrease very much and the trend in Figure 4.5 will be observed.

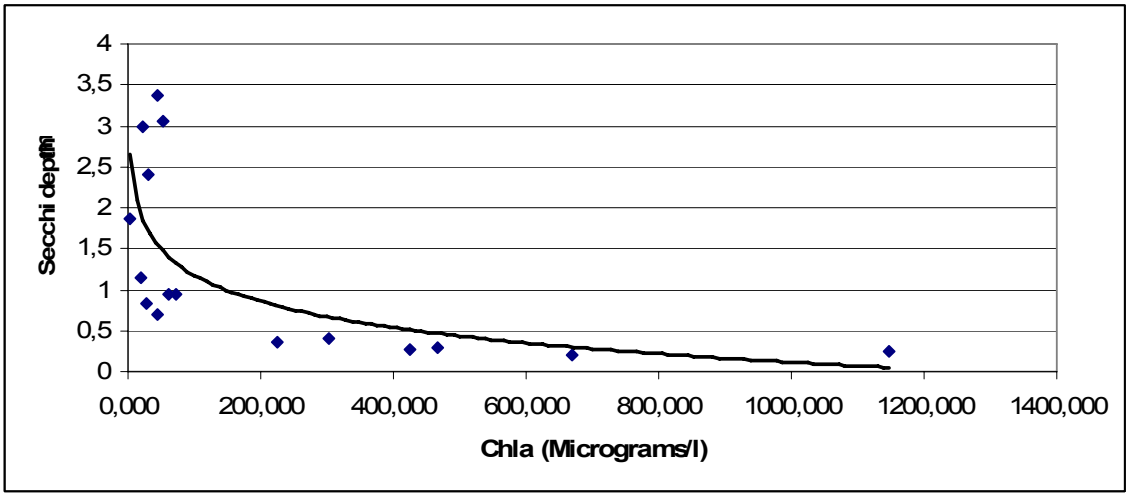


Figure 4.5: SD versus Chl-a.

Figure 4.6 shows the linear relationship between Chl-a and TSS concentrations. As can be seen $R^2$ is low due mainly to the April conditions. As discussed before, external particles reaching to the lake via runoff may impact the overall TSS. However, when this condition is

ignored (April condition is omitted), $R^2$ increases to 0.76. This is because as algal activity increase, more algae will be produced and will be suspended in water. These suspended algae will contribute to the TSS. But it should be noted here that not all the TSS is coming from algae. This can be seen in Figure 4.6. The trend line does not pass from zero, which implies the availability of other constituents in water contributing to TSS. However, it can be stated that, algal activity has a significant impact on the TSS concentrations, and therefore, on turbidity. Therefore, in order to control the turbidity, algal production should be controlled.

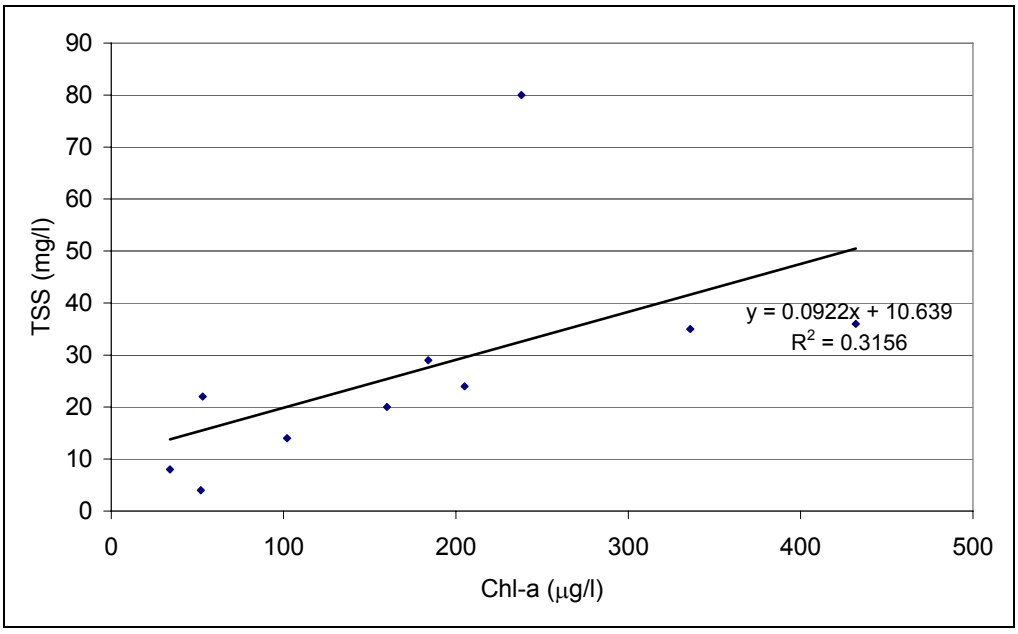


Figure 4.6: Relationship between Chl-a and TSS (laboratory measurements, P=0.001).

When a comparison is made between the typical $NO_3$ concentrations (Figure 4.7) in a eutrophic shallow lake, and average concentrations observed in Eymir (Figure 4.8), similar trend was observed. In spring and

autumn, $NO_3$ concentrations increase. In summer, $NO_3$ concentrations are minimized. As mentioned earlier, Eymir can receive the wastewaters of Gölbaşı district if the pumps operating the bypass line are not on. One of the major sources of nitrogen to lakes is the $NO_3$ in the rainfall. Even if the $NO_3$ falls into soil, it can move easily and reach the lake through runoff (J.Horne, 1994). These sources can be impacting the nitrate concentrations in Lake Eymir. In addition, nitrate from the bottom layers can be introduced to top layers by turnover as well. However, more work is required to identify the sources of $NO_3$ in Lake Eymir.

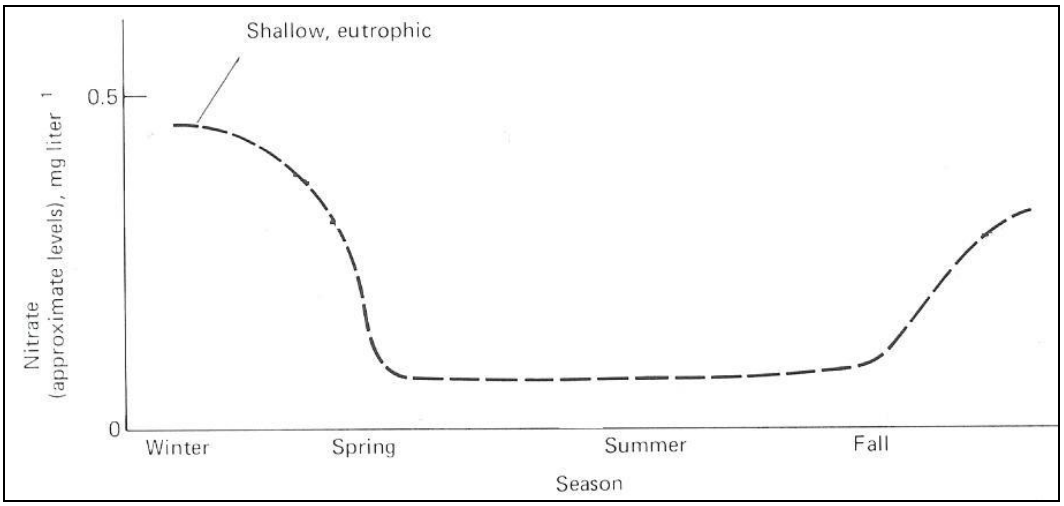


Figure 4.7: Typical seasonal $NO_3$ concentrations for shallow eutrophic lakes (J.Horne, 1994)

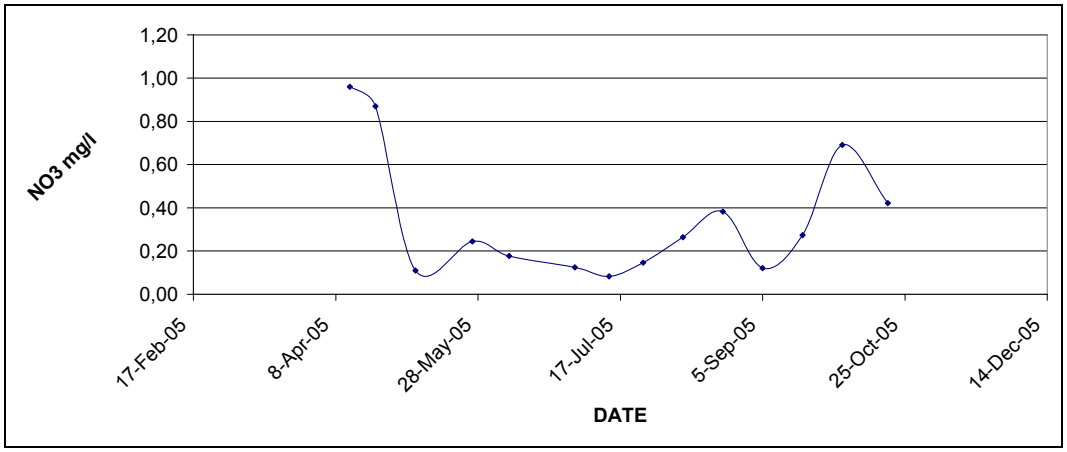


Figure 4.8: Average $NO_3$ concentrations in the lake for different sampling dates

The typical phosphate ($PO_4$) concentrations in a shallow eutrophic lake and $PO_4$ concentrations in Lake Eymir are shown in Figures 4.9 and 4.10, respectively. The reason of the increase in $PO_4$ with time in Figure 4.9 is the release from the sediment. The main factor that affects the release of $PO_4$ from sediments is the increase in pH above 8 by autumn as a result of algal activity. As pH increases, the P-binding capacity of the soil decreases. The hydroxide ions replace $PO_4$, which is soluble in water and used by the algae (Brönmark, 1999). As will be discussed in the next section pH increased above 8 in Lake Eymir. However, the $PO_4$ trend for Lake Eymir (Figure 4.10) was not similar to the typical case (Figure 4.9). This is due to excessive algal blooms in late summer and early autumn. $PO_4$ was consumed as it become available. This case was not valid for $NO_3$ (i.e. $NO_3$ followed the typical trend) since there existed blue-green algae in Lake Eymir (Beklioglu et al., 2003) which could fix nitrogen from atmosphere. As mentioned by Beklioglu (2002), the available species of algae in Lake Eymir are chlorophyta (green algae), cryptophyta, cyanobacteria (blue-green algae), bacillariophyta (gold-brown), and

dinoflagellate (red-brown). It is also seen that algae continued to grow, although $PO_4$ concentrations dropped in late summer months. Recent studies (Sullivan, 2004) show that the concentrations below which algae cannot acquire P falls to nanomolar range. Additionally, algae response to the depletion in P is not immediate and takes time. The stage at which P is depleted with no decrease in Chl-a concentrations is called zero response stage (Sullivan, 2004).

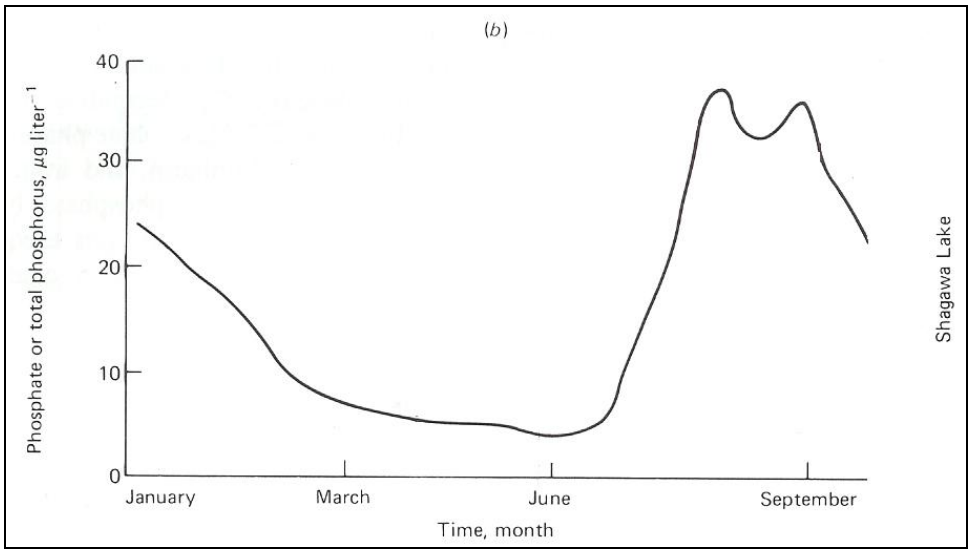


Figure 4.9: Typical Seasonal phosphate change for shallow eutrophic lakes (J.Horne, 1994)

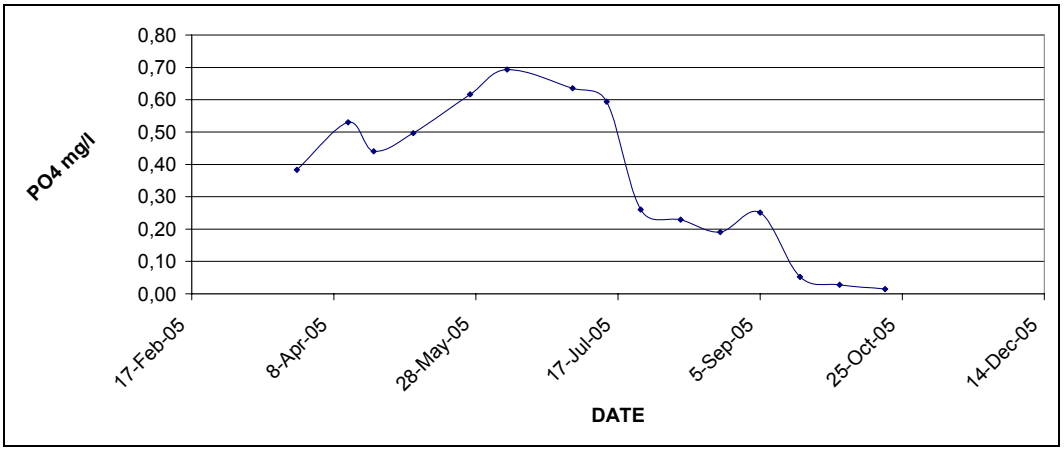


Figure 4.10: Change of phosphate in the lake with time.

## 4.2 Measurements with the sonde

The average Chl-a measurements at 17 sampling points are represented in Figure 4.11. As for the laboratory analysis, significant increase was observed in the Chl-a concentrations by summer months. This was the case for the sonde measurements. However, the behavior in April and autumn were not captured by the sonde measurements. That is, the decrease in Chl-a concentrations in autumn were not seen for the average values. It was seen that the variation in Chl-a concentrations at different sampling points increased in the summer months. The variations may be due occurrence of algal blooms.

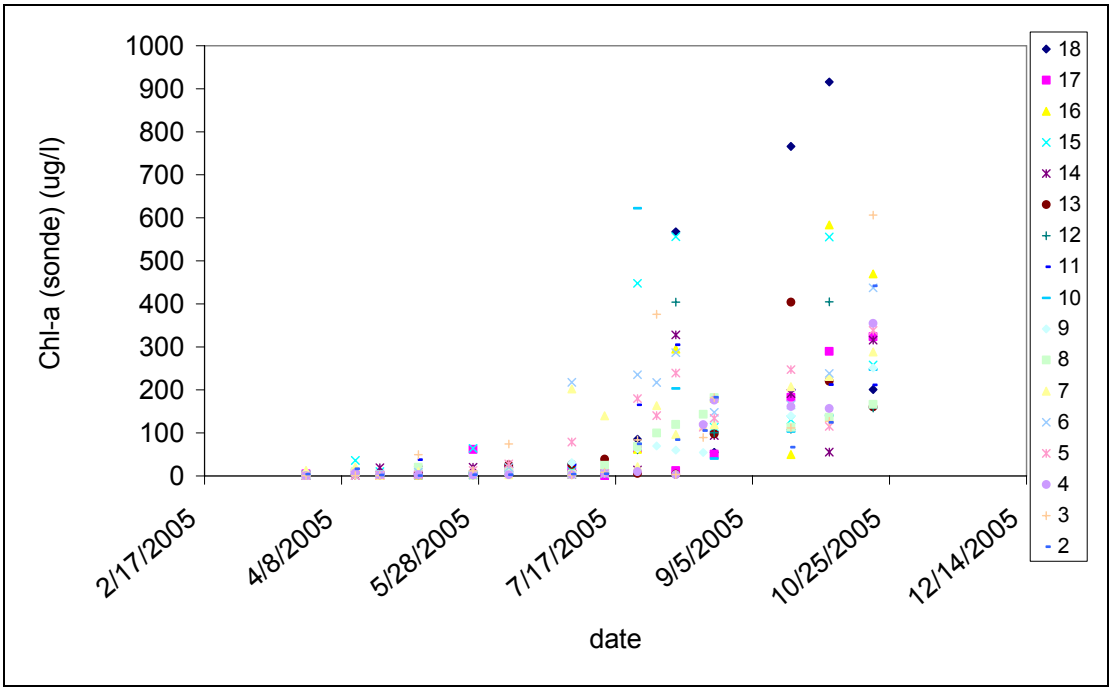


Figure 4.11: Chl-a concentrations obtained with the sonde at different sampling points (from Station 2 to Station 18).

The average Chl-a concentrations measured by the sonde were, in general, lower compared to the laboratory analysis (Figure 4.12). This may be due to the Chl-a measurement technique employed by the sonde. The Chl-a probe determines the concentrations using fluorometry in vivo, without disturbing the cell. However, due to the design of the sonde, lake water comes into contact with the probe through the side openings present on the cylindrical container that is mounted to the tip of the sonde. When the sonde is lowered, the velocity of the probe may push the large algal particles away from those openings. In addition in vivo fluorometry may be less efficient than the in-vitro method yielding less fluorescence. This may result, in overall, lower concentrations. It is also important to remember, that the results of in vivo analysis will not be as accurate as

those from the certified extractive analysis procedure. Although the sonde is certified for DO, temperature, pH measurements by EPA (2005), it has not been verified for the Chl-a measurements yet. However, it has been shown to be sensitive to changes in the concentrations. Figure 4.12 compares the average Chl-a concentrations obtained for the probe and laboratory measurements. Although average Chl-a values measured by the probe were in general lower than the laboratory results, in autumn higher concentrations were read by the probe. This may be due to a malfunction since problems were observed in the operation of the probe in those dates. In addition the first entrance of the probe into the water, getting close to the sediment, and fish can interfere with the readings. It should also be noted that laboratory measurements represent the average for 4 sampling points only. Whereas, average values given for the sonde measurements represent the average of 17 sampling points with a high number of readings for each point. Therefore, it is possible that the impact of large concentrations at the top portion at a sampling point can be phased out with several low values at the other portions.

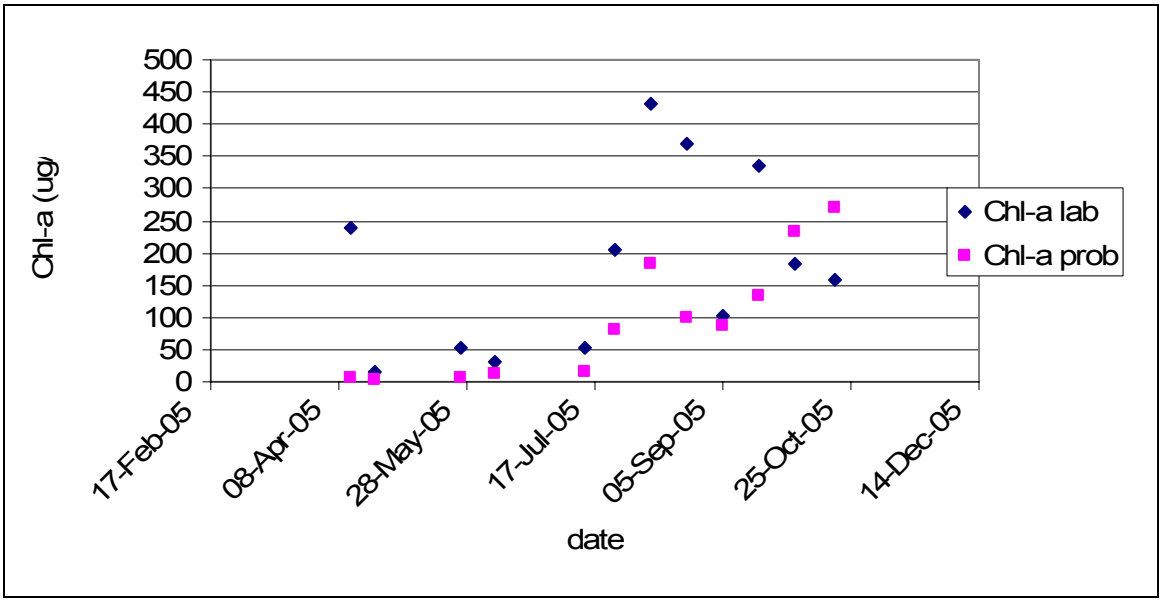


Figure 4.12: Comparison of average Chl-a quantities obtained with the Chl-a probe and the laboratory analysis.

Although the concentrations obtained using the laboratory extraction and in vivo measurements were not the same, the results indicated that in vivo measurements were sensitive to the concentration changes. Assuming that the systematic error was similar at all points in the lake; spatial distribution was studied using the probe data. Although the concentrations may not be precise, probe data can give an idea about the spatial distribution. For this purpose, example sampling dates were selected arbitrarily excluding the April and late autumn. Mapping of Chl-a was employed using ArcGIS Desktop using the Inverse Distance Weighted (IDW) method. As described by the Environmental Modeling Systems, Inc., IDW is "one of the most commonly used techniques for interpolation of scatter points. IDW is based on the assumption that the interpolating surface should be influenced most by the nearby points and

less by the more distant points. The interpolating surface is a weighted average of the scatter points and the weight assigned to each scatter point diminishes as the distance from the interpolation point to the scatter point increases"[9]. This method was used and approved to be successful by many researchers in mapping of not only environmental parameters in aquatic systems, but also for air and soil parameters. (Matejicek & Engst, 2006; Wu & Winer 2003; Robinson & Metternicht, 2006; Binder & Schimer, 2005; Wu & Zheng, 2005; Lloyd & Atkinson, 2004; Lima & Vivo, 2003). The limitation of this method is that as the sample points get sparse, the accuracy decreases. Especially, lack of concentration values at the boundary (perimeter) of the lake would be introducing error to the mapping of Chl-a. Therefore, there may be bias in the Chl-a maps that will be presented below due to the number of sampling points used. However, this method is used to have a general overview of areas with relatively high and low concentrations. Figures 4.13 to 4.17 represent the average Chl-a distributions in the lake for the sampling dates of June 8th, July 1st, July 13th, August 8th, and September 6th.

[9] **Environmental Modeling Systems, Inc** http://www.ems-i.com/ December 2005

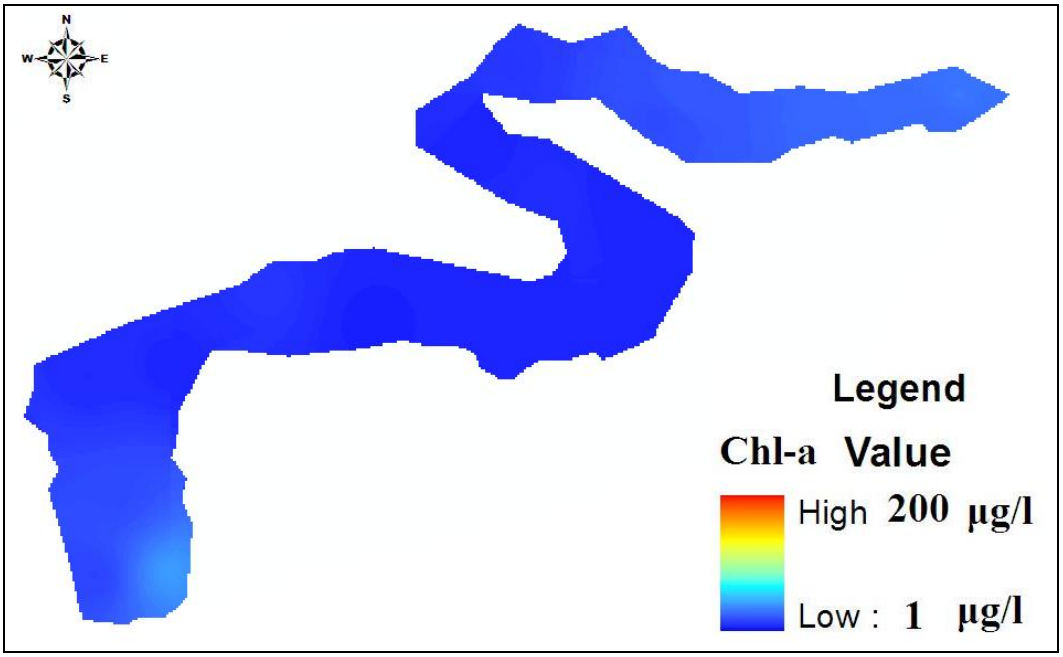


Figure 4.13: Average Chl-a concentration distribution for June 8th (probe data)

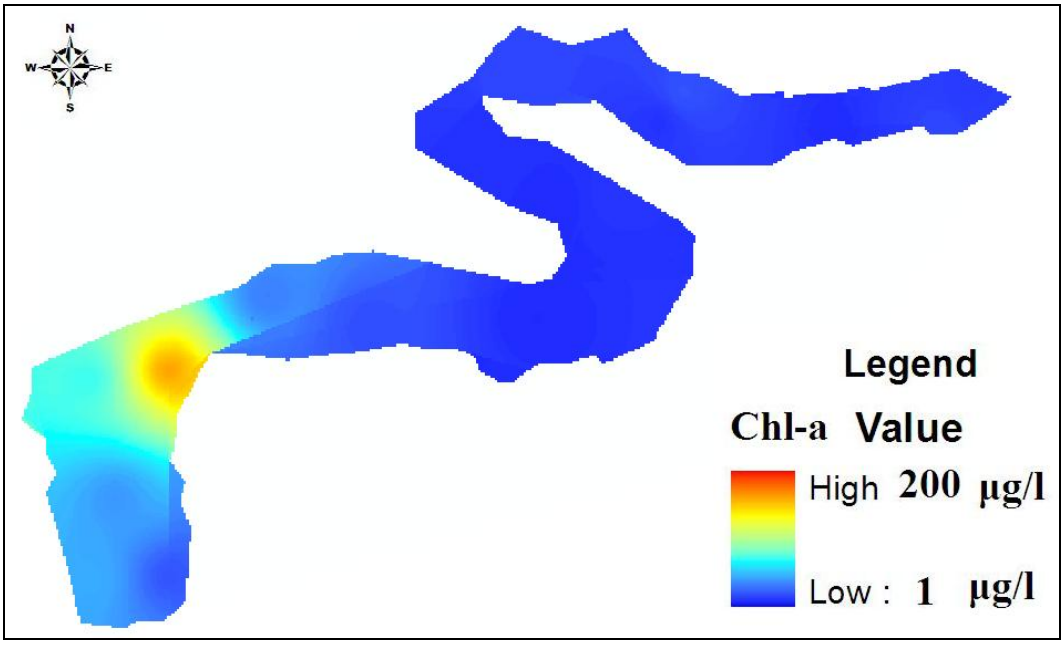


Figure 4.14: Average Chl-a concentration distribution for July 1st (probe data)

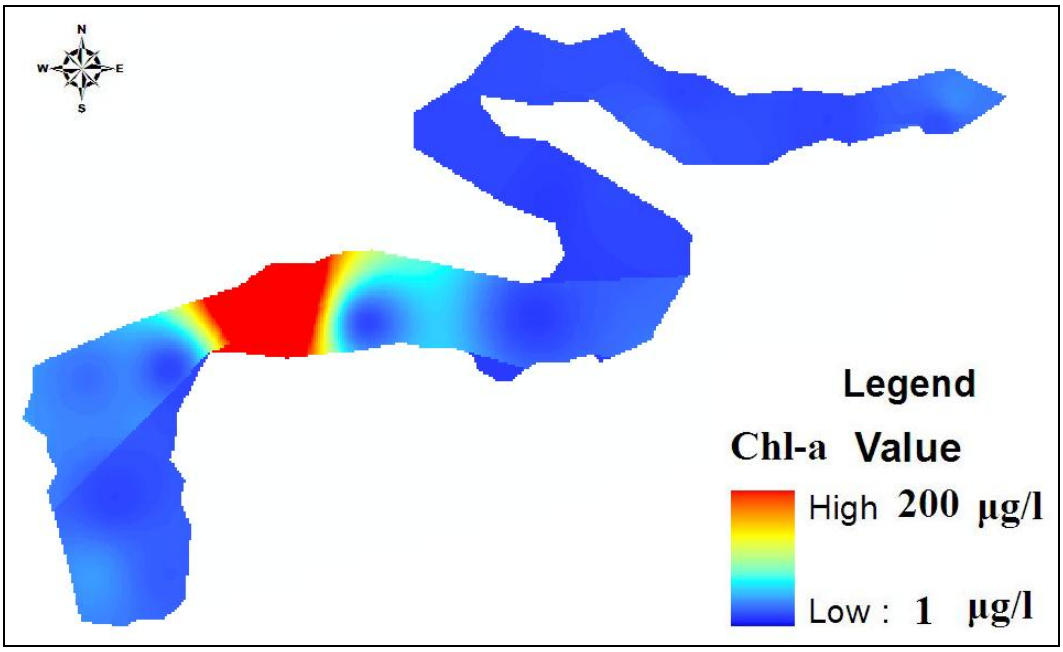


Figure 4.15: Average Chl-a concentration distribution for July 13th (probe data)

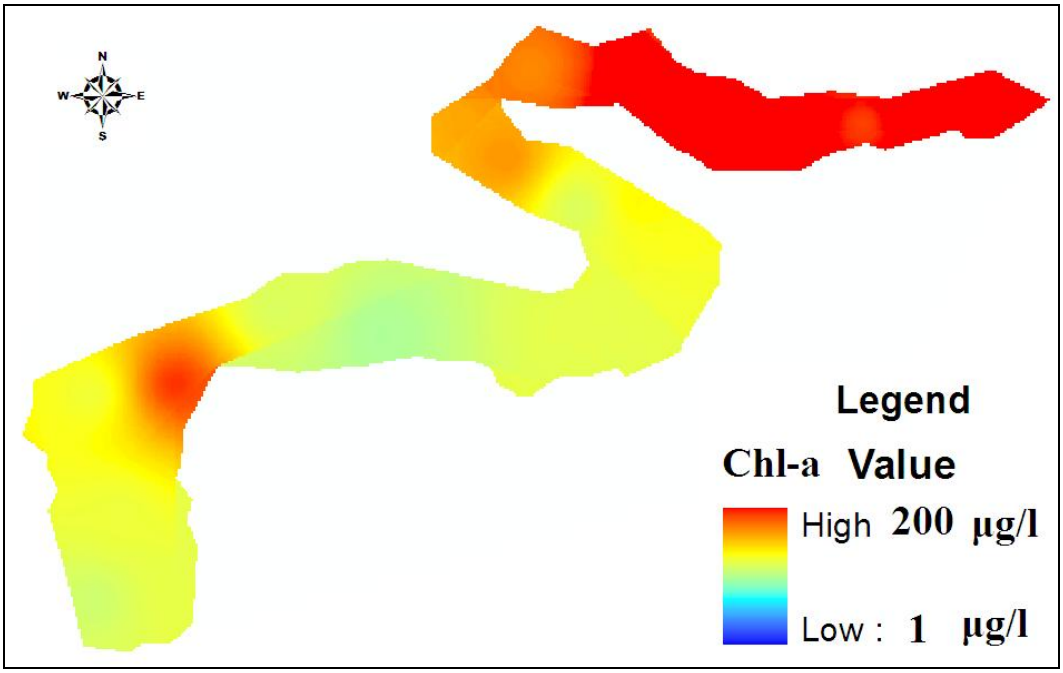


Figure 4.16: Average Chl-a concentration distribution for August 8th (probe data)

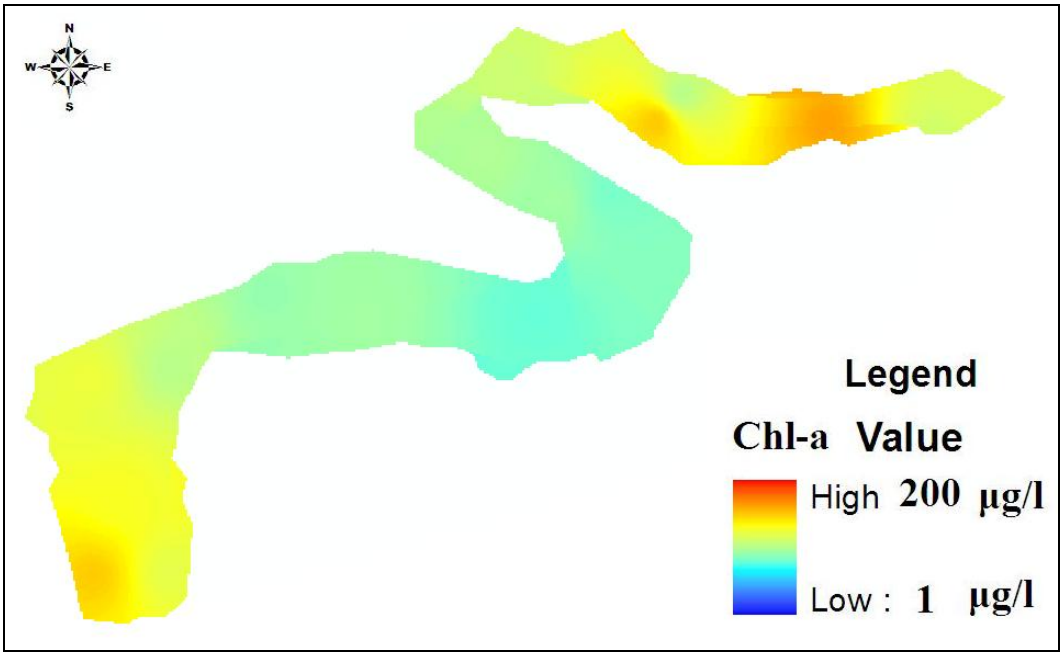


Figure 4.17: Average Chl-a concentration for September 5th (Probe)

As seen in the maps above, the distribution of Chl-a in the lake changed with time. Similar to the trend in average Chl-a concentrations observed with time in Lake Eymir, Chl-a concentrations increased with summer months, peaked in August and decreased on 5th of September. By late July and August, higher average concentrations were observed at locations closer to the inlet and outlet of the lake. These locations are relatively shallow compared to the middle section. Therefore, light penetration to the bottom layer is higher at these locations. In addition, it is expected that rooted algae growth is favored at these locations which would increase the Chl-a concentrations.

When the water surface temperature was examined, it was found that across the lake the surface temperature variation is only about 2 $^{o}$C

(Table 4.3). Therefore, the surface was considered stable throughout the lake, which is one of the factors enhancing surface algal blooms (Tang & Kawamura, 2005). On the other hand, wind may have an effect on the location of algal blooms. The wind speed was very variable throughout the study; it ranged from 1m/sec to 13 m/sec in different directions (DMI, 2005). In shallow lakes, especially in summer months when the depth of water decreased further, the algae can be carried to different places by the turbulence created by the wind action. However, as stated before, the results may have bias due to probe measurements.

Table 4.3: The range of observed surface temperatures in the lake on different sampling dates

| **Measurement Date** | **Temperature Range ($^oC$)** |
|---|---|
| 26 March | 8 – 10 |
| 26.May | 19 – 21 |
| 13 July | 25 – 27 |
| 8 August | 26 – 27 |
| 19 September | 19 – 21 |
| 19 October | 13 – 15 |

When the areas of high concentrations in the maps of Chl-a were examined many observations were recorded. In the map of 8$^{th}$ of June, the concentration ranged from 4 to 40 μg/l with an average of 15 μg/l. The area of highest concentrations was the south western end of the lake with an area covering around 4 % of the lake. Regarding the map of 1$^{st}$ of July, the

concentrations ranged from 7 to 160 μg/l with an average of 32 μg/l, and the area of high concentration was near the north western part and covering about 6 % of the surface of the lake. For the 13th of July map, he data ranged from 12 to 420 μg/l with an average of 43 μg/l, with the area of high concentration shifting about 270 meters to the eats with respect to the map of 1st of July. For the map of 8th of August the average concentration was about 175 μg/l with a maximum of around 400 μg/l, the areas with the highest concentrations of greater then 200 μg/l were around the north eastern part of the lake mostly covering about 23 % of the lake. And lastly for the map of 5th of September, the average concentration was about 112 μg/l, with a range from 100 to 162 μg/l. Although the lake was almost homogenous as the range of concentration values is small, areas with higher concentrations were observed near the south western and north eastern ends of the lake covering about 45 % of the lake surface. Starting from June the areas of higher concentrations or what can be called algal blooms, covered only about 4% of the lake with values around 40 μg/l. This blooms expanded in later months to 6%, 23% and 45 % for July, August and September respectively, with concentrations increasing to more than 400 μg/l especially in August. The blooms also shifted their places in the lake starting from near the wastewater discharge in south western part of the lake, transporting till the other end in the north eastern part, this indicates the motion of the water in the lake, which was explained before mainly as a result of the wind blowing on the surface of the lake. On the other hand the increase of the concentration of Chl-a through summer was an expected trend, as the temperature and the sunlight availability for photosynthesis increased.

The distribution of algae is important for management purposes. In Chl-a maps, it is seen that by late summer months, algal activity increases at shallow locations. Therefore, at least at these locations, algae at the surface can be removed from the lake. In addition, algal distribution can indicate problematic areas as well. Sampling programs can be modified based on the Chl-a maps. Both the number and location of sampling points can be determined using these maps.

Besides surface temperatures, the vertical temperature profile, thermal stratification, is very important for the quality of the lake. Lake turnover typically happens in spring and fall. It occurs in spring after the melting of ice cover in which it is called spring turnover. Usually it takes more time in deep lakes than in shallow lakes (Wetzel, 2001). Similar process happens in fall, when the temperature decreases and a negative input of heat starts in the lake, in which is called fall turnover. As a result of turnover, oxygen deficient bottom layers and oxygen rich top layers interchange. In addition, introduction of nutrients and other compounds from the sediments can be enhanced as a result of a turnover. In Figure 4.18, a typical thermal stratification of a lake into 3 layers, epilimnion, metalimnion and hypolimnion are shown.

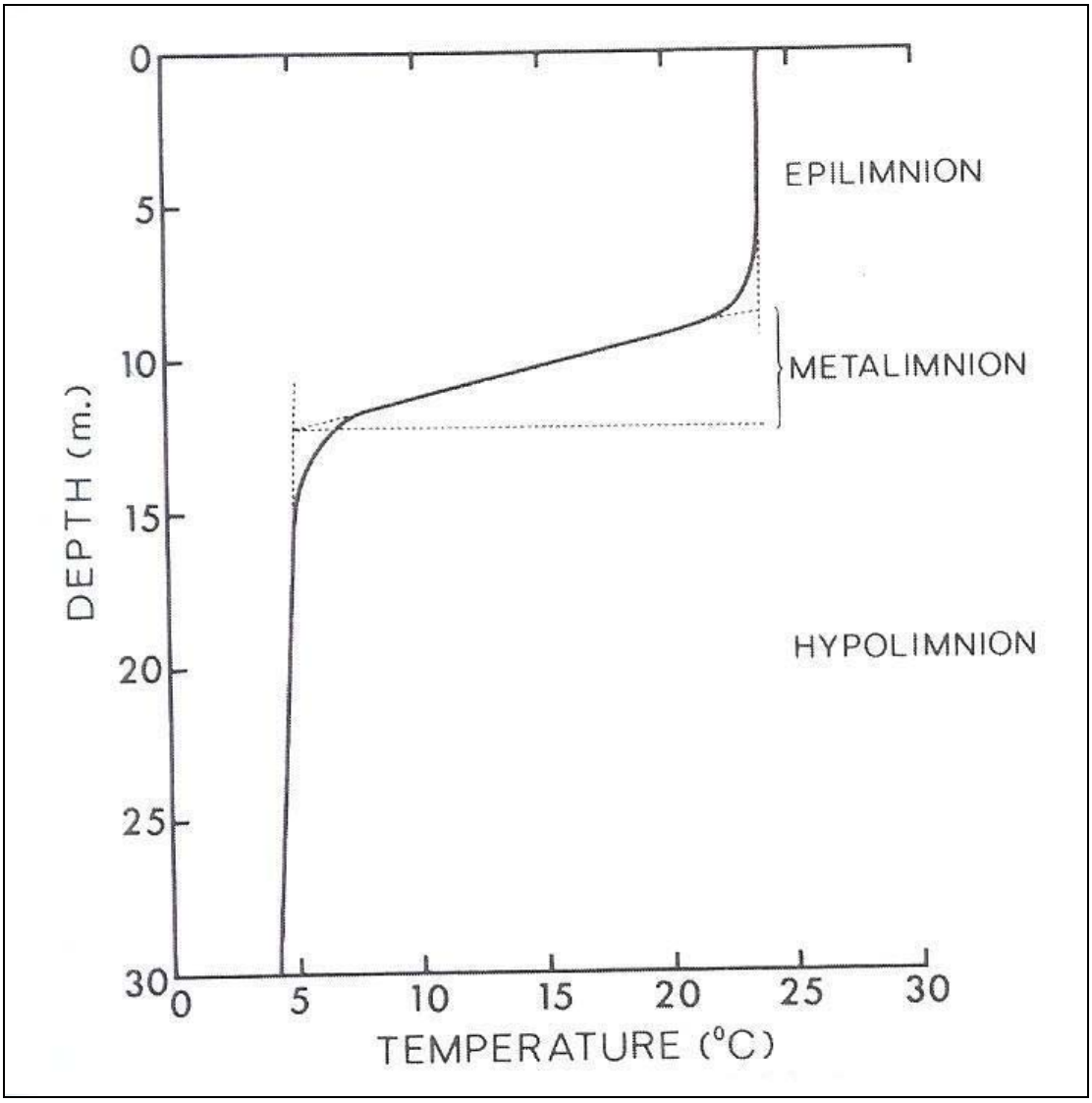


Figure 4.18: Typical thermal stratification of a lake into the epilimnetic, metalimnetic, and hypolimnetic water strata. Dashed lines indicate planes for determining the approximate boundaries of metalimnion (Wetzel, 2001).

In Figures 4.19, the temperature profiles at station number 9 are shown for several sampling dates. This station is located at the deepest part of the lake. Therefore, the maximum difference in the vertical temperature profile can be expected in the vicinity of this station.

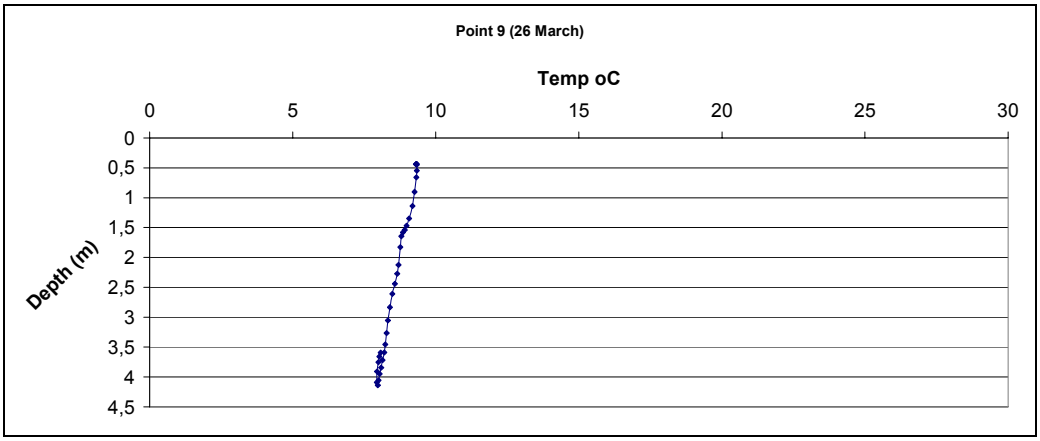


Figure 4.19.a

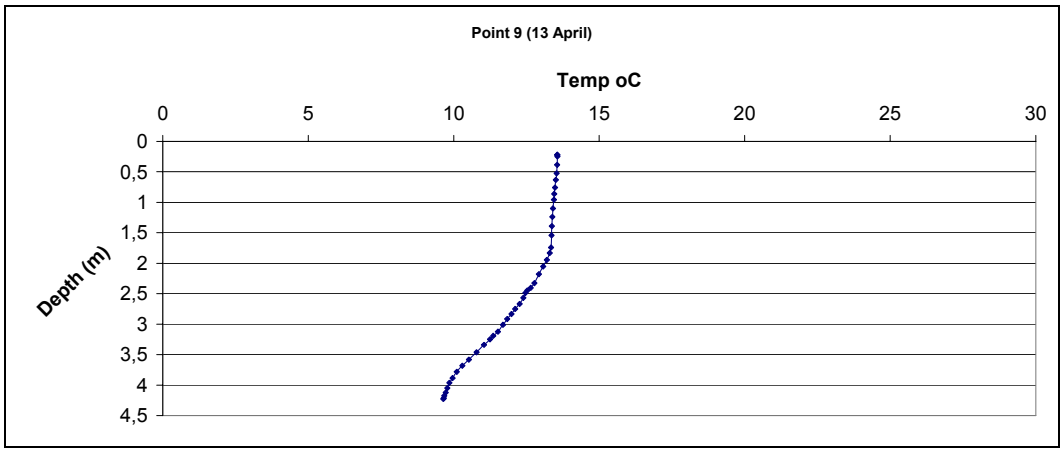


Figure 4.19.b

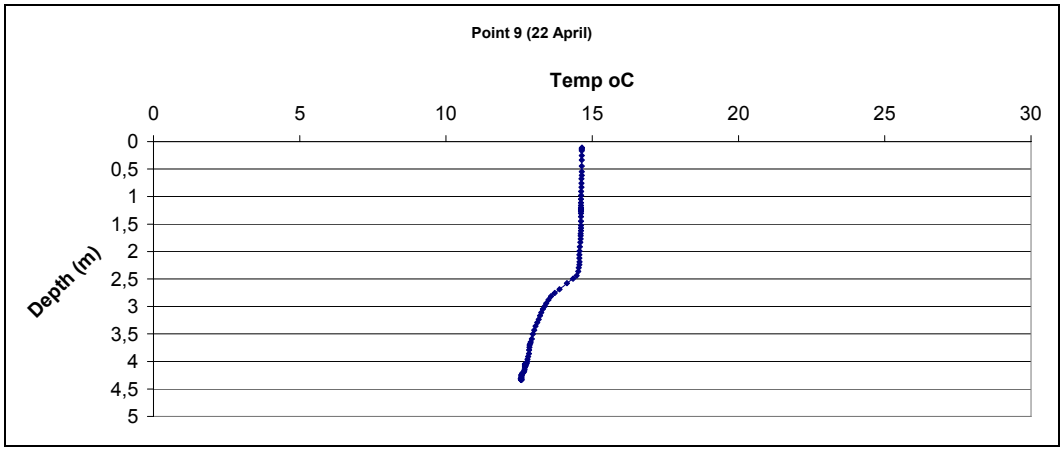


Figure 4.19.c

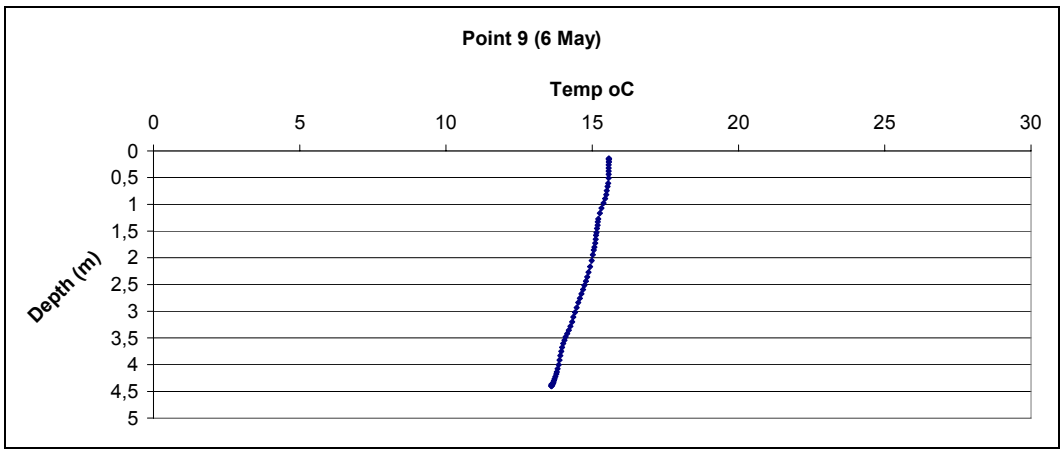


Figure 4.19.d

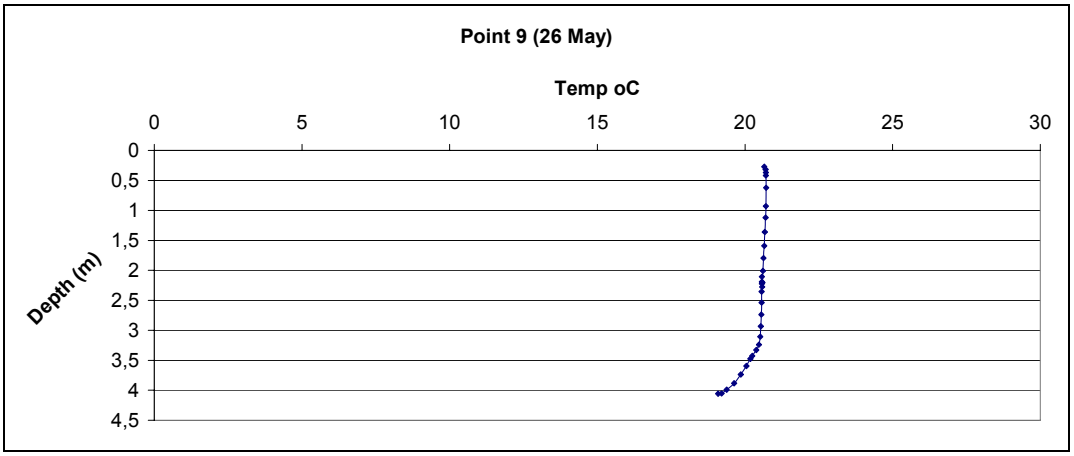


Figure 4.19.e

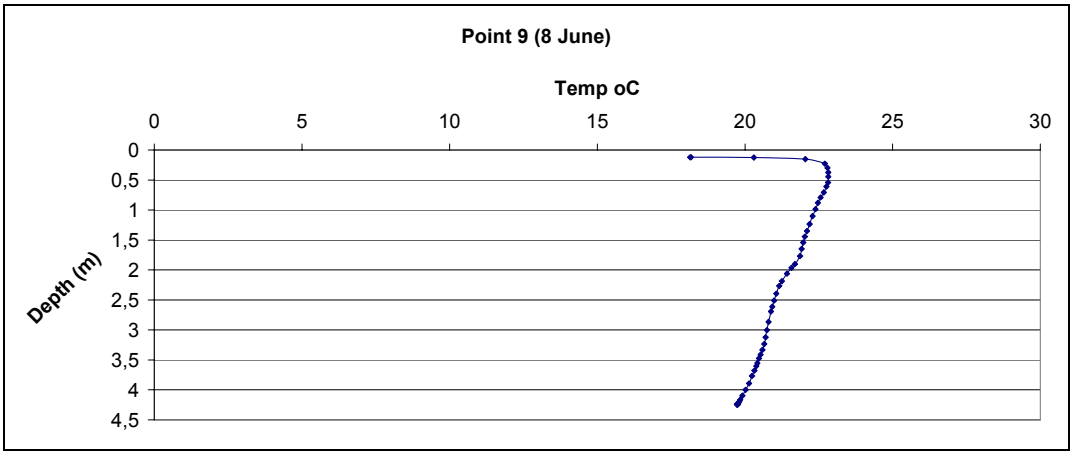


Figure 4.19.f

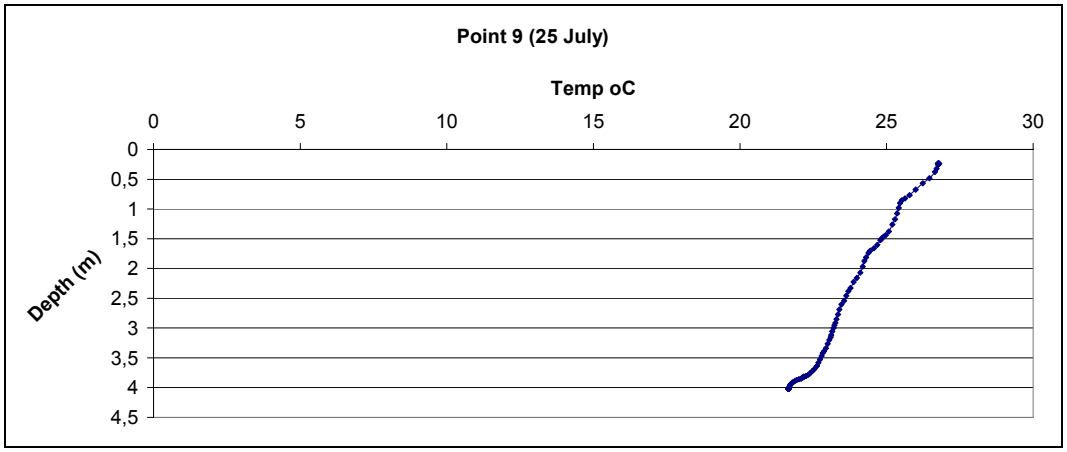


Figure 4.19.g

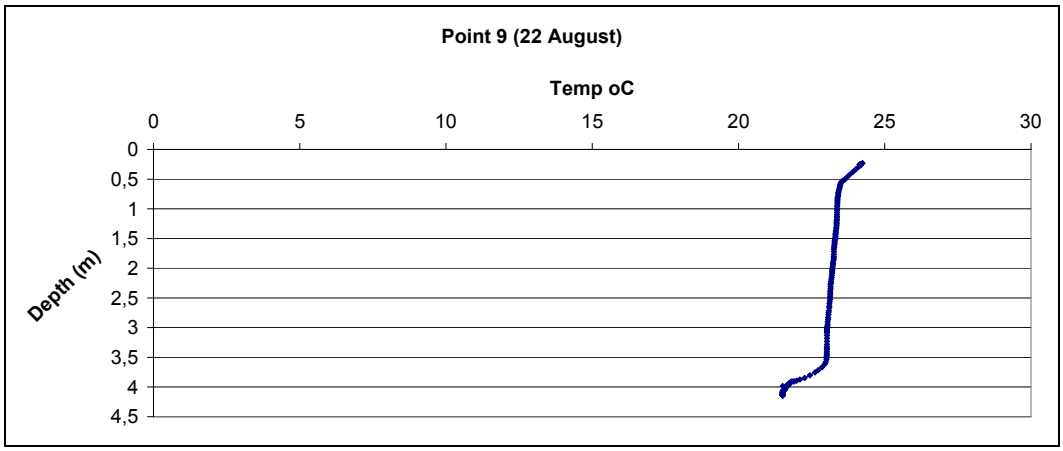


Figure 4.19.h

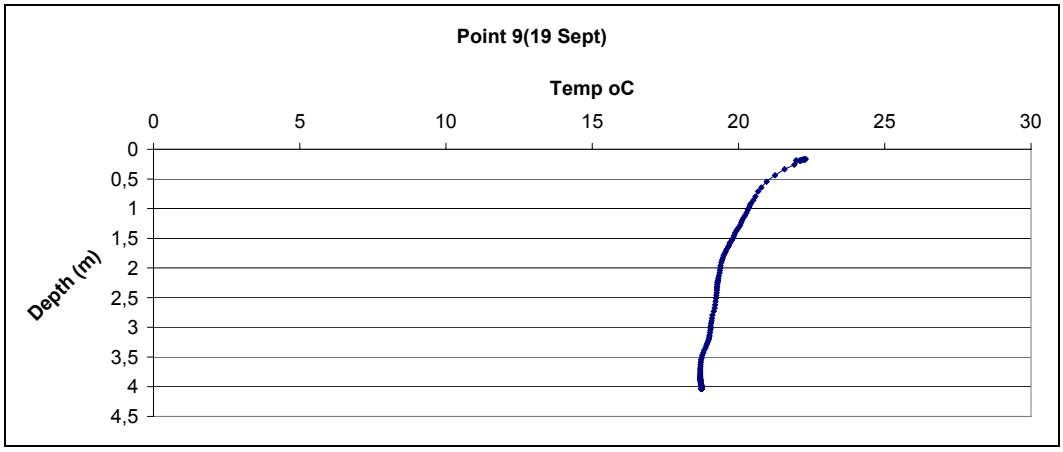


Figure 4.19.i

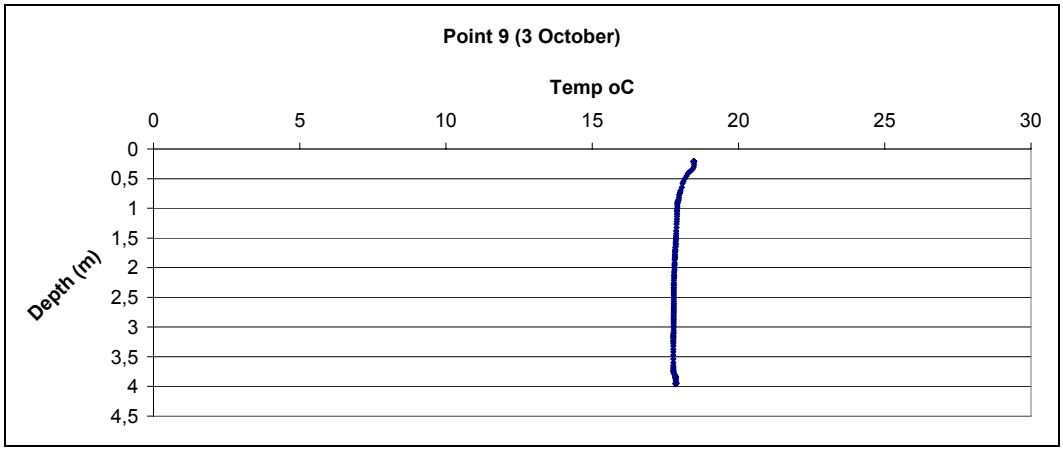


Figure 4.19.j

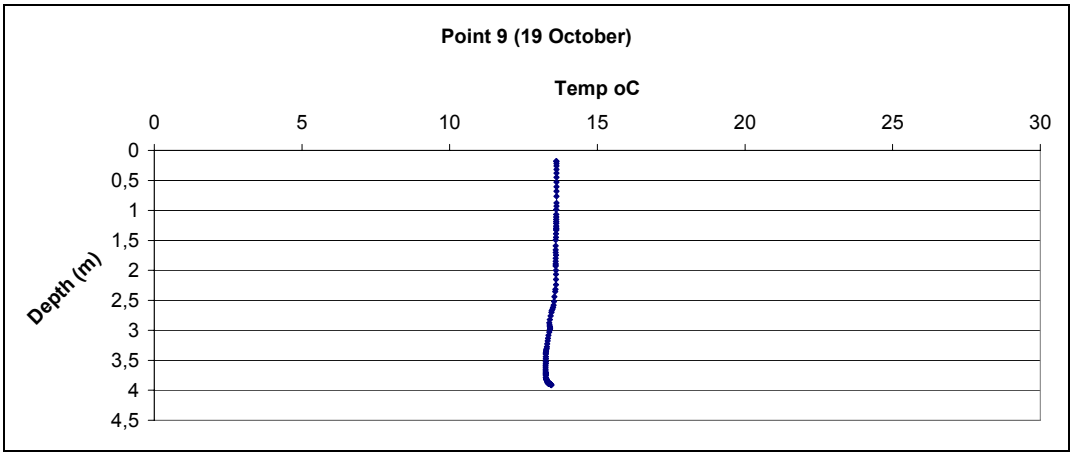


Figure 4.19.k

Figure 4.19: Temperature profiles for station 9 on different sampling dates from March (a) to October (k).

When Figure 4.19 is examined, it is seen that between April and October, the maximum temperature difference between the surface and the bottom ranges between 2.5 – 4.5 $^{o}$C. In March and October, this variation is 1.0 - 1.5 $^{o}$C. Well mixing of bottom and top layers is expected, due to wind action as well as convective mixing, when the temperature difference at the bottom and top layers are small. In fact, the impact of wind action on the turnover of shallow lakes is a well established fact when the temperature profile with depth is uniform (Thomann and Mueller, 1987; Wetzel 2001). The extent of temperature variations with respect to depth is depicted in Figure 4.19.

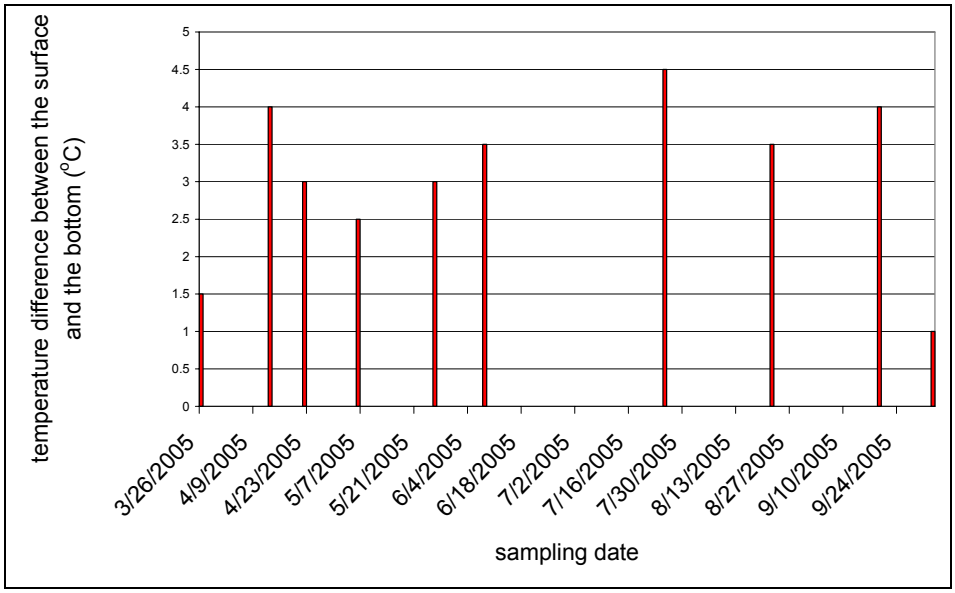


Figure 4.20: Maximum temperature variations with respect to depth at station 9

One of the main sources of DO in lakes is the photosynthetic activity as well as turbulence created by wind. A typical DO profile in eutrophic lakes can be seen in Figure 4.21 (J.Horne, 1994). The DO profiles for station 9 are depicted in Figure 4.22. DO values dropped by depth especially in summer months. Therefore, DO trend with depth was similar to that of eutrophic lakes (Figure 4.21) in these months.

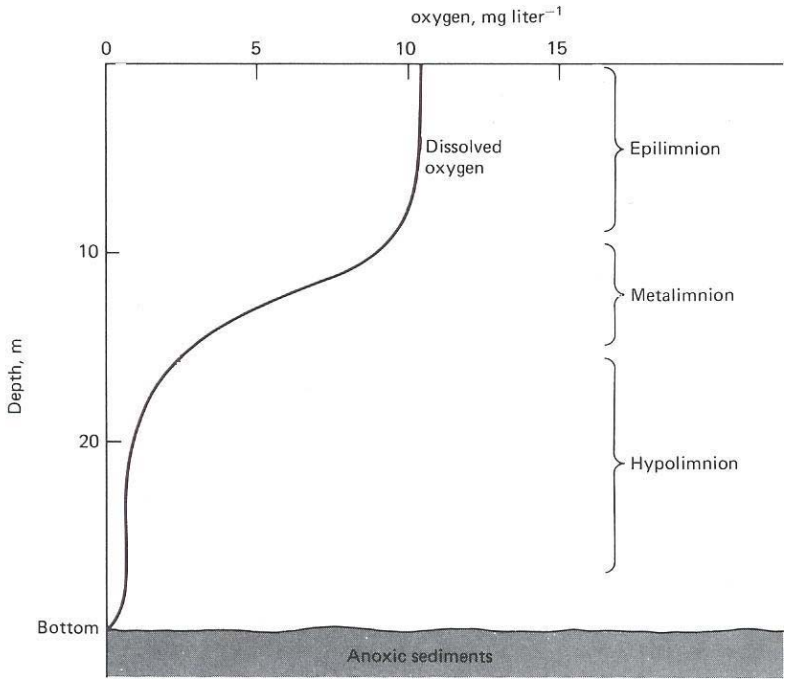


Figure 4.21: Typical DO summer profile in a eutrophic lake (J.Horne, 1994).

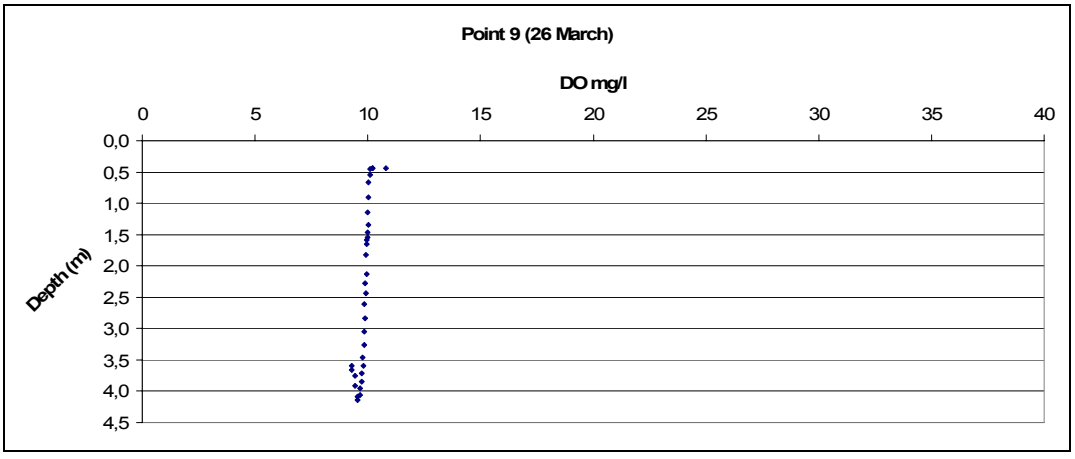


Figure 4.22.a

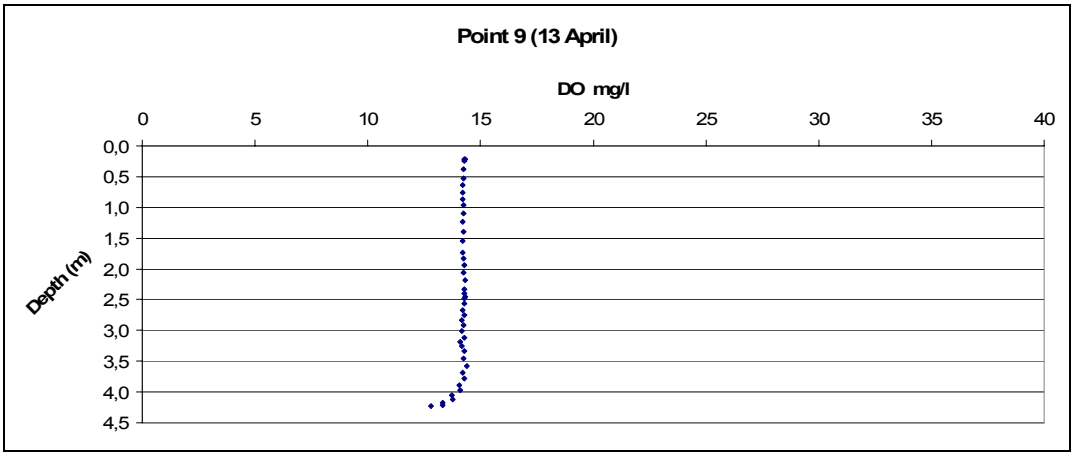


Figure 4.22.b

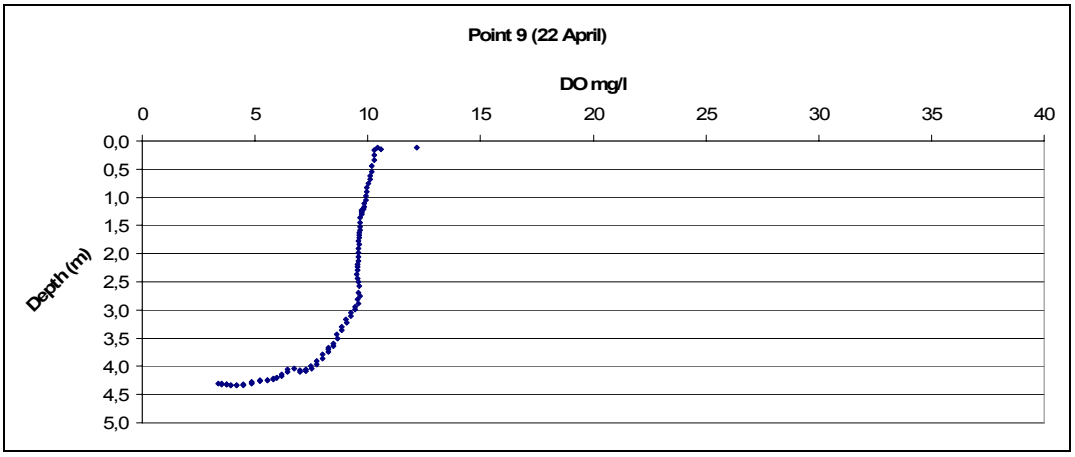


Figure 4.22.c

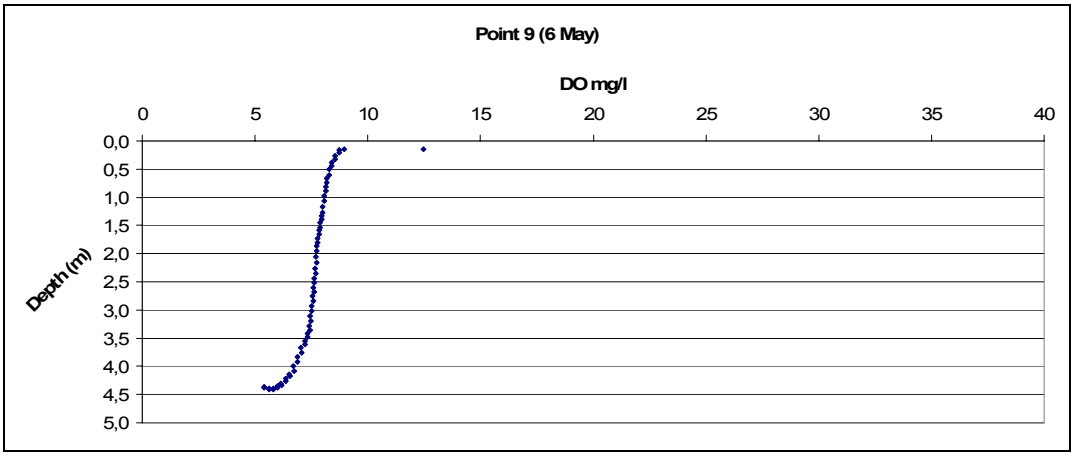


Figure 4.22.d

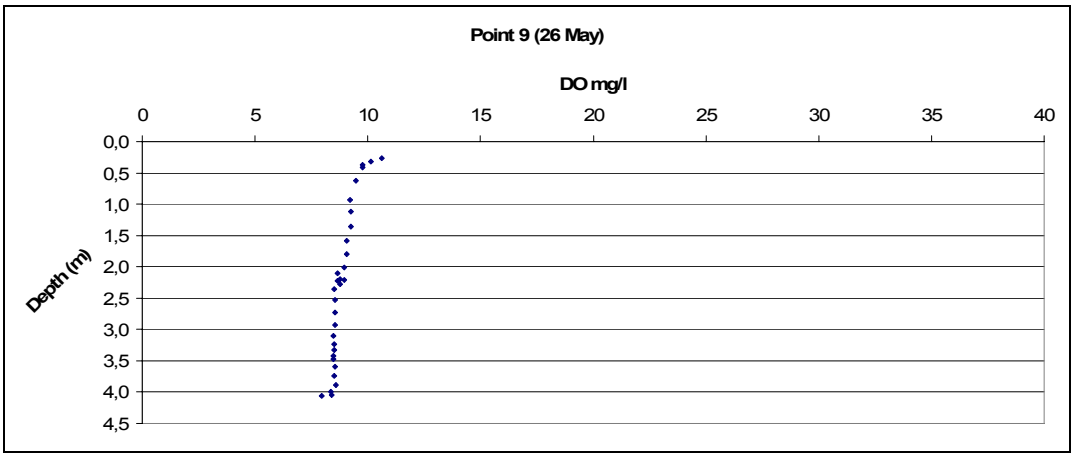


Figure 4.22.e

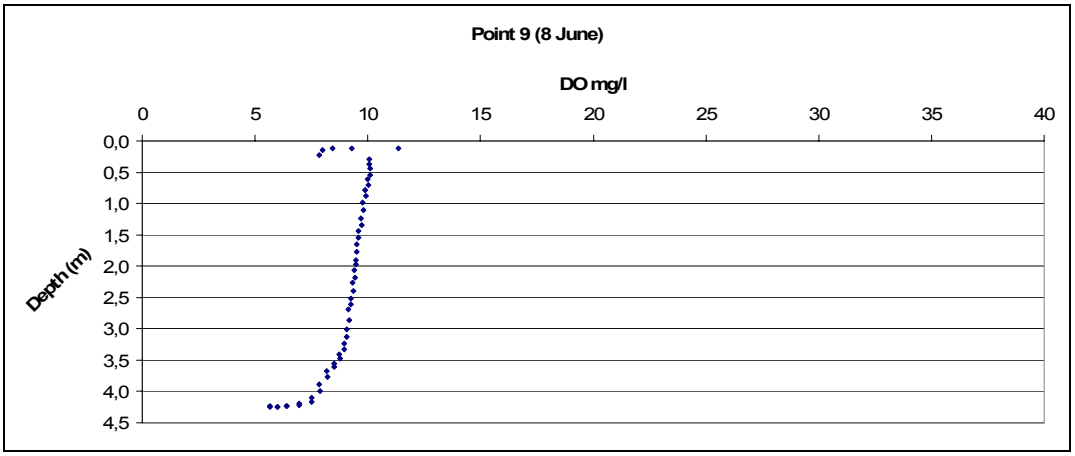


Figure 4.22.f

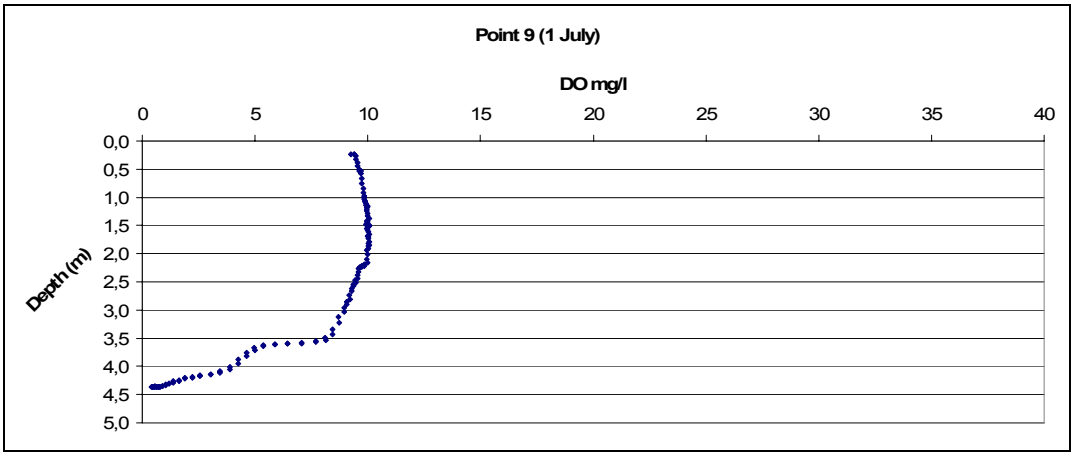


Figure 4.22.g

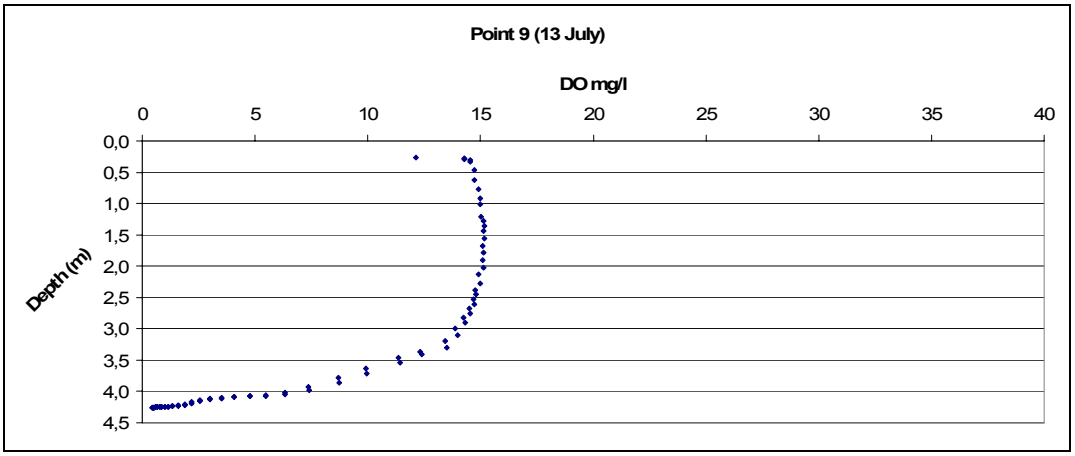


Figure 4.22.h

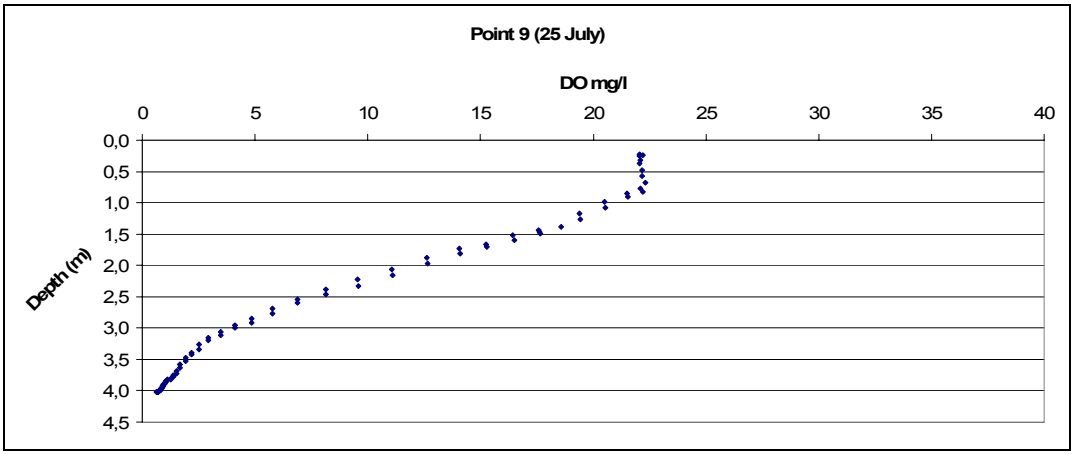


Figure 4.22.i

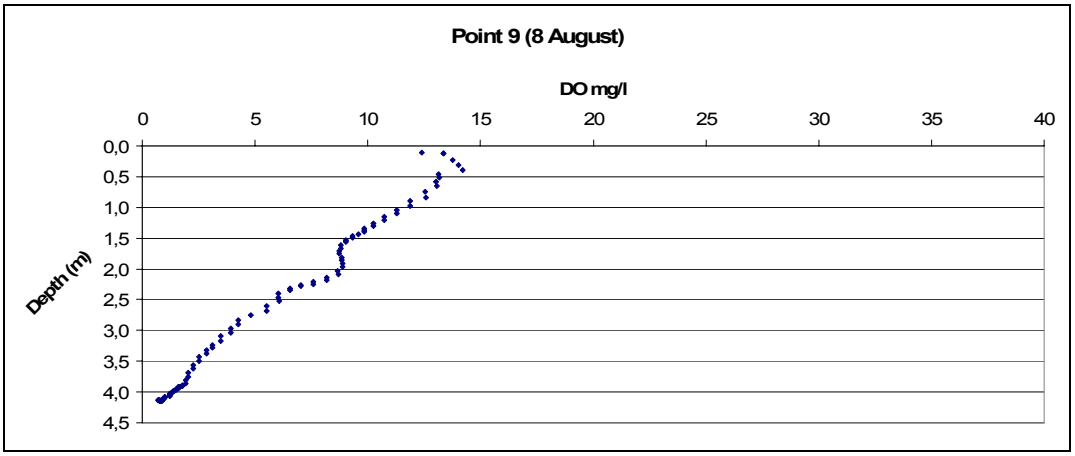


Figure 4.22.j

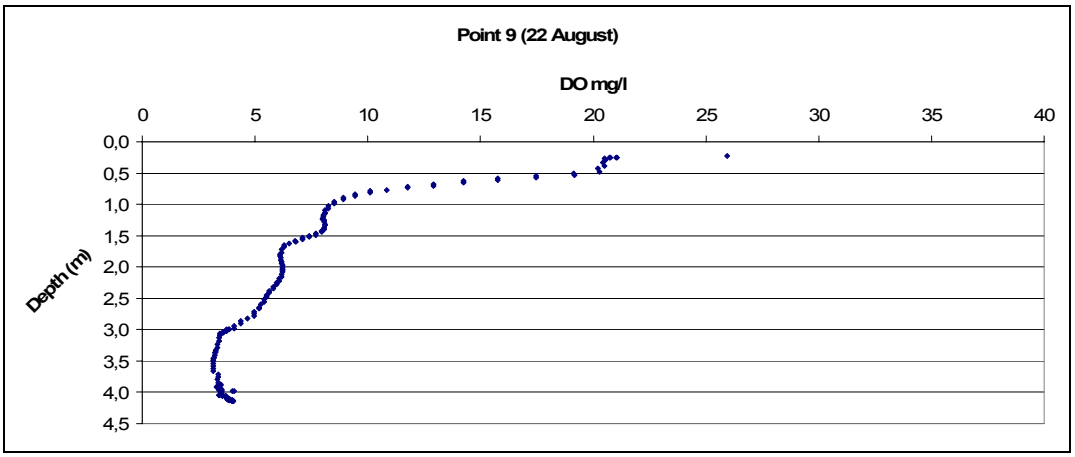


Figure 4.22.k

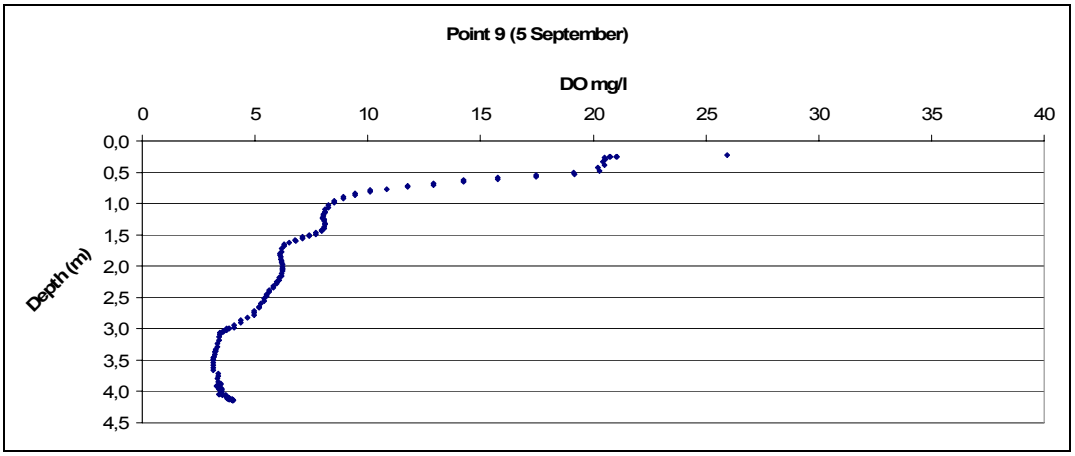


Figure 4.22.l

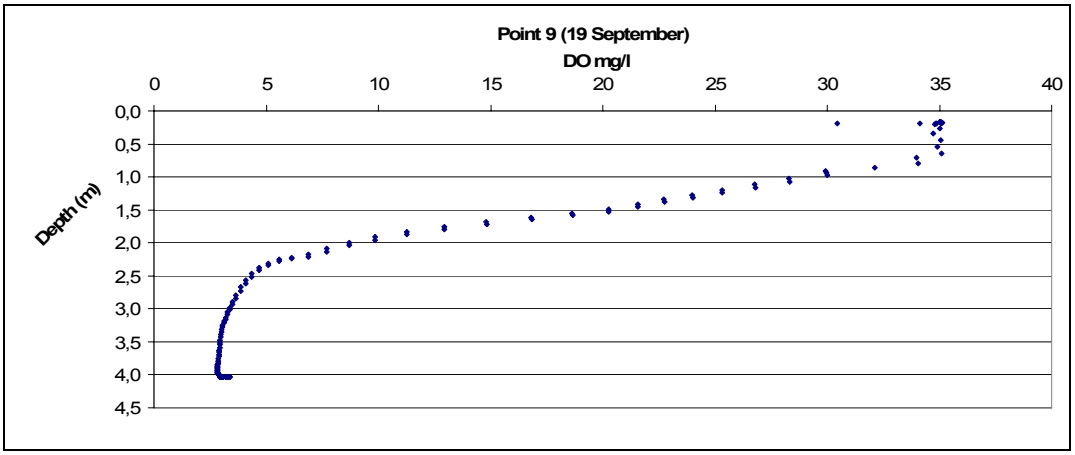


Figure 4.22.m

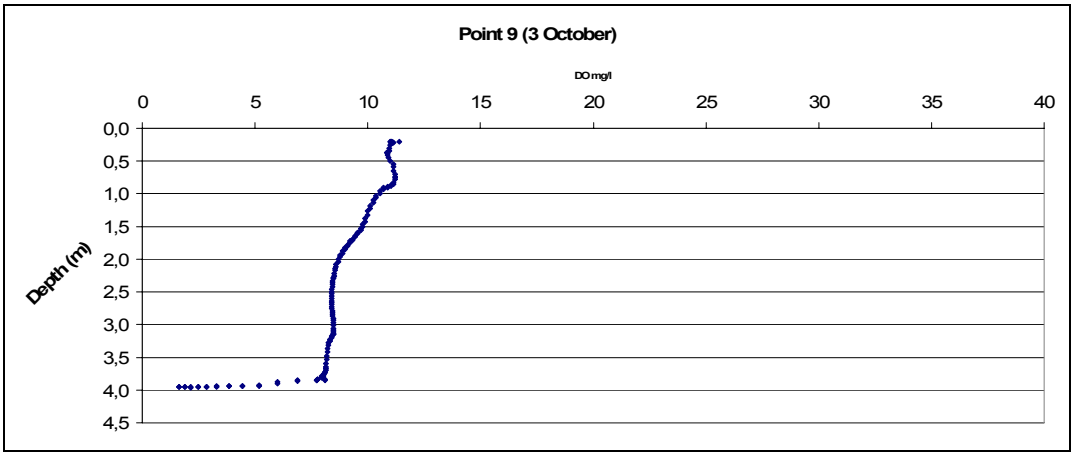


Figure 4.22.n

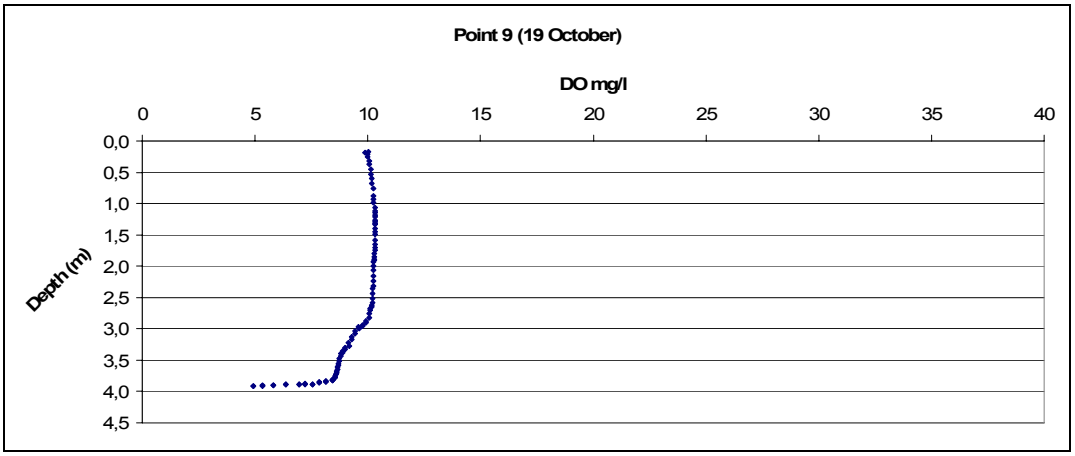


Figure 4.22.o

Figure 4.22: DO profiles with respect to depth for different sampling dates at station 9 starting from versus depth on different sampling dates starting from 26 March (a) to 19 October (o).

As depicted in Figure 4.22, in March and April, the DO profile with depth is relatively uniform which also indicates good mixing. However, by late April bottom DO levels drop to or less than 5 mg/l. By July, the bottom DO concentration is 0 mg/l and supersaturation builds up at the surface. This is due to temperature profiling starting at this time and algal

activity. The upper layer is aerated especially by the wind action and the algal activity. However, the bottom layers are DO deficient due to insufficient circulation and probable sediment oxygen demand. By summer months and September, the DO reaches to very high values, above saturation quantities. By this time algal blooms form at the surface and produce oxygen during the day. Therefore, pure oxygen is introduced into water. Since the transport of oxygen from the water layer to the atmosphere is small, DO levels as high as 150-200% of the saturation values are not uncommon (Thomann and Mueller, 1987). However, for such a high algal activity, drastic drops in DO at night can be expected as well, which is detrimental to aquatic life. By October, more uniform DO levels are observed. This is probably due to mixing of the lake following the fall turnover. Actually, uniform temperature profile for this time enhances mixing of bottom and top layers by wind action.

Figures 4.23, 4.24, and 4.25 show the average temperature, DO, and temperature, respectively. As seen in Figure 4.24, average DO concentration can reach to very high values with the algal activity, to saturation as high as 200%. As discussed in the previous paragraph, presence of algal blooms enhances this condition. As the sonde is put into water, it measures directly the photosynthetically. More importantly, due to excessive algal growth and photosynthesis, pH values are reaching to almost 10, which is detrimental for fish. Toxic ammonia production can be favored at such pH values. Ammonia is presents in fresh waters mainly as dissociated ion which is called ammonium ($NH_4^+$). $NH_4^+$ is harmless and taken up rapidly by phytoplankton and other aquatic plants (J.Horne, 1994). However, as pH and temperature increases, $NH_3$ rather than $NH_4^+$

is present in water. At a pH of 9 and above with temperature of about 25 $^{o}C$, the percentage of $NH_3$ is above 35% of total nitrogen (Trussell, 1972). Equation 1 (J.Horne, 1994) shows the relationship between ammonia and pH. As pH increases, hydroxyl ions increase which in turn shifts the equation to left producing more $NH_3$.

$$NH_3 + H_2O \leftrightarrow NH_4OH \leftrightarrow NH_4^+ + OH^- \qquad [1]$$

As given in Figure 4.25, pH is increased to above 9 by August. Therefore, the potential of $NH_3$ production build up by that time. By October, pH reaches up to almost 10. In field studies, death of fish was observed at this time.

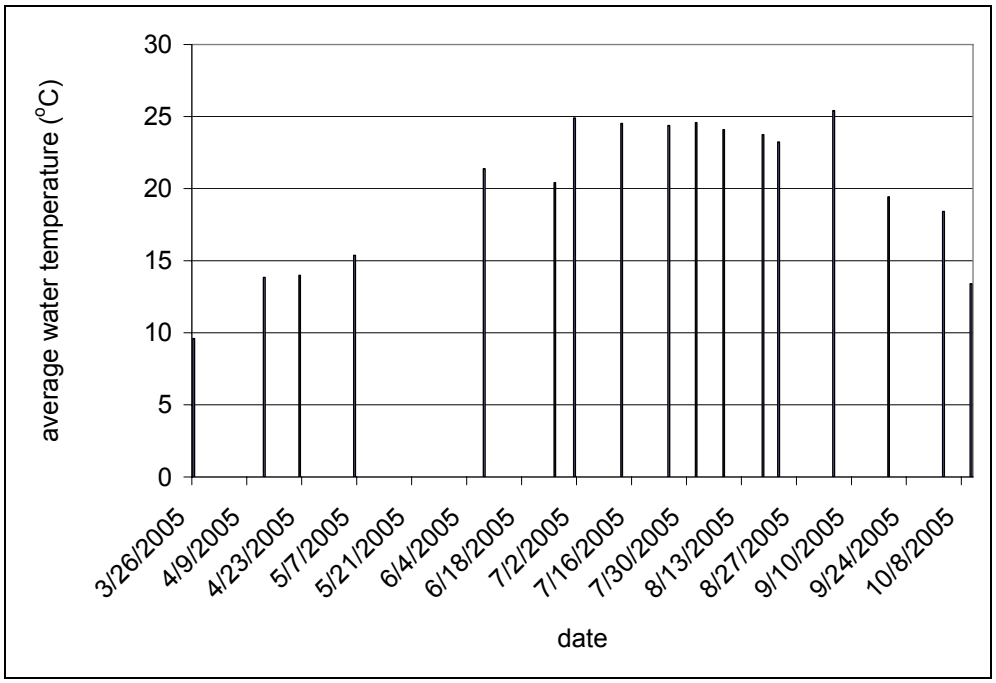


Figure 4.23: Monthly average water temperatures

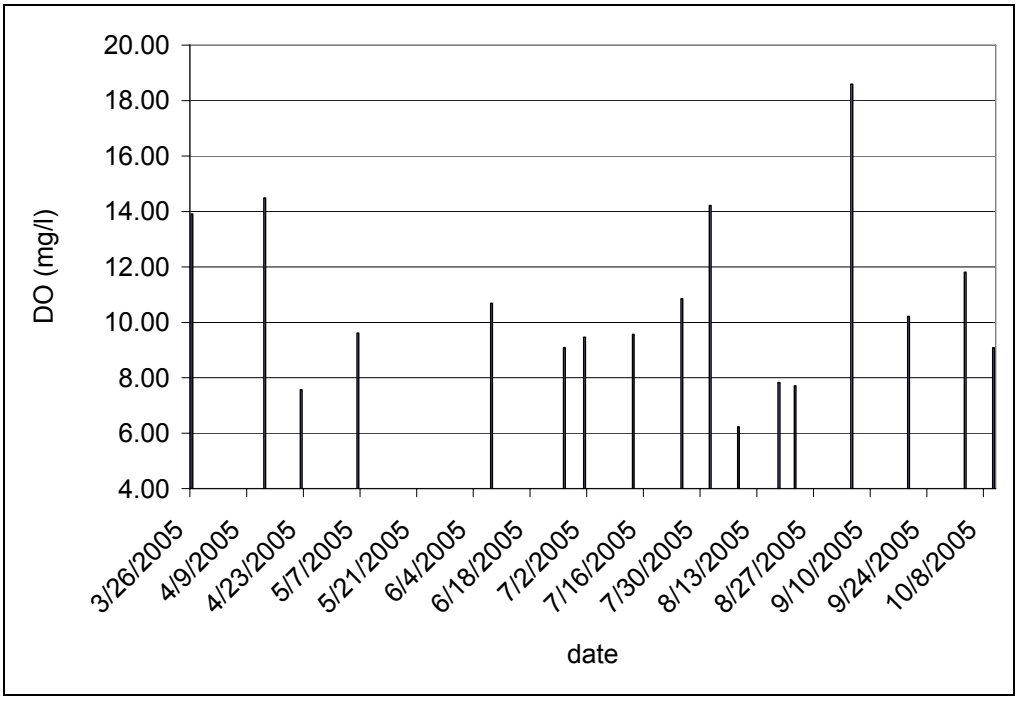


Figure 4.24: Monthly average DO

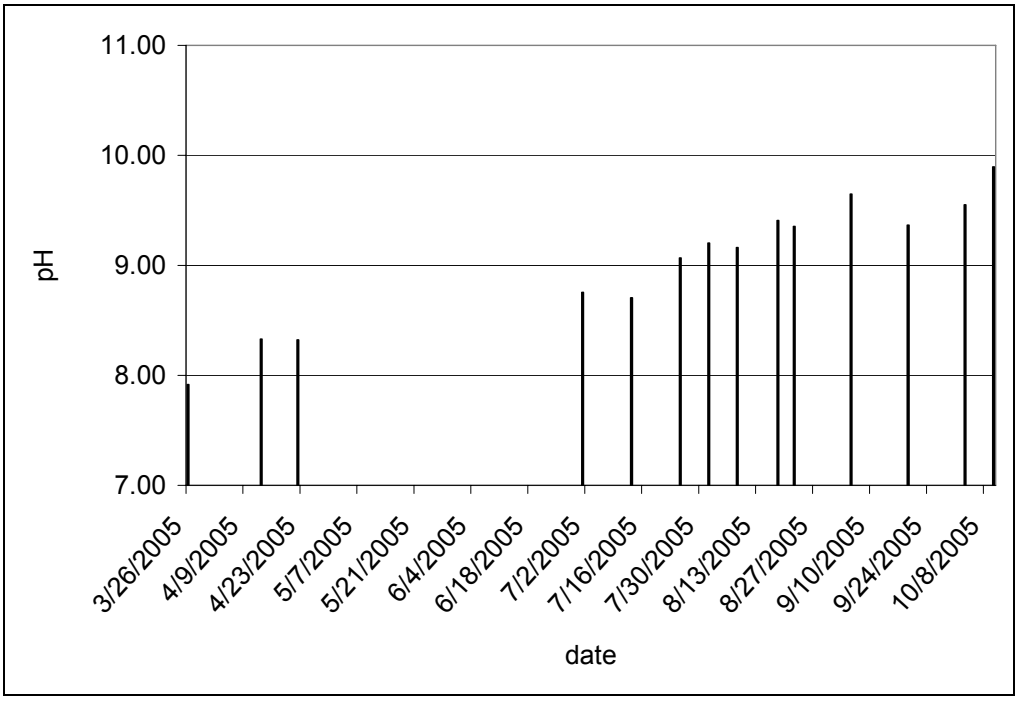


Figure 4.25: Average pH for all points on each day of measurement

### 4.3 Remotely Sensed data & Regression analysis

As mentioned before, two images were taken on 26th of June and 6th of August 2005, and regression analysis was employed for both. Both laboratory and probe data were used to derive the models to convert the pixel values in the images to Chl-a concentrations. For the image taken on 26th of June and 6th of August, the probe data of July 1st and August 8th, respectively, were utilized. For the model developed using the laboratory data, only the image taken on 26th of June is utilized. This is due to the fact that for the August 6th image, very few laboratory data were available. For this case, the laboratory data for June 18th were used.

The pixel values for each sampling point were taken from the images represented by the DNs belonging to three bands of the satellite; green (band 2), red (band 3), and near infrared (NIR) (band 4). These bands have been used in previous studies related with Chl-a. The peak reflectance values for Chl-a in water are observed in the green and NIR bands (Han, 1997). Red band is used to eliminate the effect of turbidity sources not related to Chl-a (Bartholomew, 2002). In the cases where the sampling points were in the border of a pixel, an averaging filter of 3x3 pixels was applied on the pixels around that point, and the average value was taken. Then those values were coupled with the ground truth data at the same locations and multi parametric regression analysis was performed to obtain regression models.

The information about the images taken on 26th of June and 6th of

August are listed in Tables 4.4 and 4.5, respectively. The images were radiometrically, sensor, and geometrically corrected, and mapped to a cartographic projection. The RMS of the geometric correction was ±23 m. Because this error is high, sampling points were located on the image visually since these locations were known. An algorithmic approach for geometric correction was not preferred due to possible bias in the handheld GPS receiver used in the study. In the best case, based on the characteristics of the GPS receiver used, at least 3 m error was expected in the coordinates of the sampling points, which is greater than the pixel size of the images. Therefore, manual point matching deemed acceptable.

Table 4.4: Information regarding the image captured on 26th of June

| Item | Value | Remarks |
|---|---|---|
| Collection Start | Date: 2005-06 26<br>Time: 08:49:50 | Date and time at which the image was collected. |
| Collection Stop | Date: 2005-06-26<br>Time: 08:50:03 | |
| Cloud Cover | -999.0 | There was no cloud cover. |
| Northwest Latitude | 39.84286258 | Upper left corner coordinates of the image |
| Northwest Longitude | 32.74574341 | |
| Southeast Latitude | 39.72376562 | Lower right corner coordinates of the image |
| Southeast Longitude | 32.86177978 | |

Table 4.5: Information regarding the image captured on 6th of August

| Item | Value | Remarks |
|---|---|---|
| Collection Start | Date:2005-08-06 Time:08:57:11 | Date and time at which the image was collected. |
| Collection Stop | Date:2005-08-06 Time:08:57:25 | |
| Cloud Cover | -999.0 | There was no cloud cover. |
| Northwest Latitude | 39.84252955 | Upper left corner coordinates of the image |
| Northwest Longitude | 32.77562449 | |
| Southeast Latitude | 39.77919954 | Lower right corner coordinates of the image |
| Southeast Longitude | 32.85074329 | |

In model development, the DNs for the three mentioned bands for different sampling point for the first and the second images were combined. The reason of this was to obtain a general equation applicable for the two images. A part of the data was used for the regression and the rest of the data for the validation of the model. The independent parameters were the green band, and the NIR band minus the red band. The reason the red band was subtracted from the NIR band is to eliminate the effect of turbidity sources not related to Chl-a (Bartholomew, 2002). Tables 4.6 and 4.7 show the input data (probe) for the regression model and validation. Similarly, Tables 4.8 and 4.9 summarize the data used for regression analysis and validation for the laboratory data.

Table 4.6: Input data used for regression analysis between the probe and remotely sensed data for the general model (14 points).

| Chl-a probe | Green | NIR-red |
|---|---|---|
| 86,50 | 286,00 | 21,00 |
| 117,30 | 304,00 | -7,00 |
| 186,70 | 320,00 | -11,00 |
| 126,80 | 273,00 | 5,00 |
| 286,60 | 302,00 | 22,00 |
| 227,60 | 287,00 | 31,00 |
| 143,50 | 272,00 | -1,00 |
| 30,00 | 293,00 | -72,00 |
| 45,00 | 292,00 | -53,00 |
| 36,00 | 248,00 | -44,00 |
| 50,00 | 255,00 | -44,00 |
| 55,00 | 260,00 | -33,00 |
| 30,00 | 273,00 | -64,00 |
| 40,00 | 290,00 | -55,00 |

Table 4.7: Data used for the validation of the general model

| Chl-a Probe µg/l | Green | NIR-Red |
|---|---|---|
| 404,20 | 280,00 | 37,00 |
| 286,00 | 292,00 | 40,00 |
| 328,20 | 273,00 | 30,00 |
| 555,00 | 291,00 | 46,00 |
| 295,00 | 280,00 | 36,00 |
| 567,60 | 288,00 | 35,00 |
| 31,00 | 286,00 | -67,00 |
| 20,00 | 322,00 | -66,00 |
| 24,00 | 301,00 | -69,00 |
| 60,00 | 288,00 | -42,00 |
| 50,00 | 292,00 | -67,00 |

Table 4.8: Input data used for regression analysis between the laboratory and remotely sensed data for the image taken on on 26th of June (5 points).

| Chl-a Lab µg/l | Green | NIR-Red |
|---|---|---|
| 49,728 | 293 | -59 |
| 14,208 | 249 | -27 |
| 40,256 | 297 | -67 |
| 23,68 | 265 | -40 |
| 37,888 | 304 | -74 |

Table 4.9: Data used for the validation of the modeled obtained from data in table 4.7.

| Chl-a Lab µg/l | Green | NIR-Red |
|---|---|---|
| 33,152 | 252 | -24 |
| 54,464 | 322 | -62 |
| 47,36 | 296 | -54 |
| 23,68 | 305 | -69 |
| 47,36 | 328 | -79 |

As a result for the multiple linear regression, the below models were developed. Equation 4.1 is based on the probe data and Equation 4.2 is based on the laboratory data from the first image only. Summary for the statistical analysis is given in Table 4.10.

Probe Data: Chl-a (μg/l) = 1.19*Green +1.77*(NIR-Red) -194 (4.1)

Lab Data: Chl-a (μg/l) = 2.88*Green +2.84*(NIR-Red) -625 (4.2)

Table 4.10: Result of regression analysis of remotely sensed data versus ground truth Chl-a data

| Combined Data | Probe data (general model) | Laboratory data (26th of June) |
|---|---|---|
| Observation points | 14 | 5 |
| $R^2$ | 0.88 | 0.99 |
| Standard error | 42.7 | 1.34 |
| Significance p | 0.0003 | 0.004 |

The results of regression analysis made between remotely sensed image and data obtained from laboratory for the image taken on 26th of June 2005 shows a very high correlation. The $R^2$ of 0.99 is considered as a high value compared to the similar studies in literature. The standard error value is around 1.34 μg/l. The average Chl-a concentration of the laboratory data for 18th of June is about 40 μg/l. Therefore, the standard error is around 3.4% of the observed mean value. This is an acceptable result when compared to similar studies. Bartholomew (2002) has reported a standard error of 30%. However, p value is also very low showing high significance of correlation. The model (Equation 4.2) is validated against validation data given in Table 4.9 (5 points). The plot of actual versus predicted values is depicted in Figure 4.26.

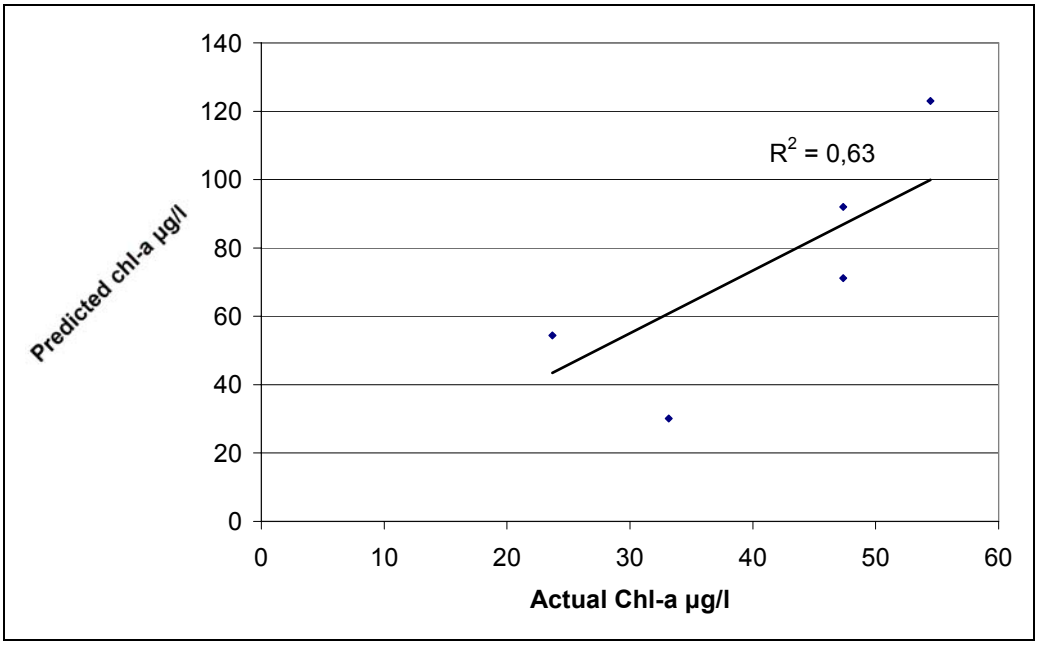


Figure 4.26: Actual versus predicted (using the model obtained with the laboratory data) Chl-a values for the image taken on 26th of June: validation.

The result of the validation showed and $R^2$ of 0.63 with a p value of 0.004. This value is lower than the $R^2$ (0.99) of the regression model given by Equation 4.2. This may be due to the number of data used in model development. Small number of data points used in model development may have resulted in high $R^2$ value (0.99) (Giardino & Pepe, 2001). In addition, the bias in the location of ground truth data may have resulted in different outcomes for the model building and validation steps. However, based on $R^2$ values presented in literature, an $R^2$ of 0.63 may still be accepted as acceptable.

The regression analysis for the general model (Equation 4.1) developed using the probe data resulted in an $R^2$ of 0.88, which is also a high value compared to the values stated for similar studies in literature.

The significance value is 0.0003, stating that the correlation between the dependent and independent variables are not by chance. The average Chl-a concentration for the set of data was about 170 µg/l, with a standard error of about 43 µg/l. This makes around 25% standard error, which is still on the acceptable side and lower than 30% of error reported by Bartholomew (2002). When the validation was performed using dataset in Table 4.6 (12 points) an $R^2$ of 0.67 was obtained (Figure 4.27) with a p value of 0.0003. This shows that general model can be applicable, statistically, for the two images studied. However, further analysis is made to make a statement as will be discussed.

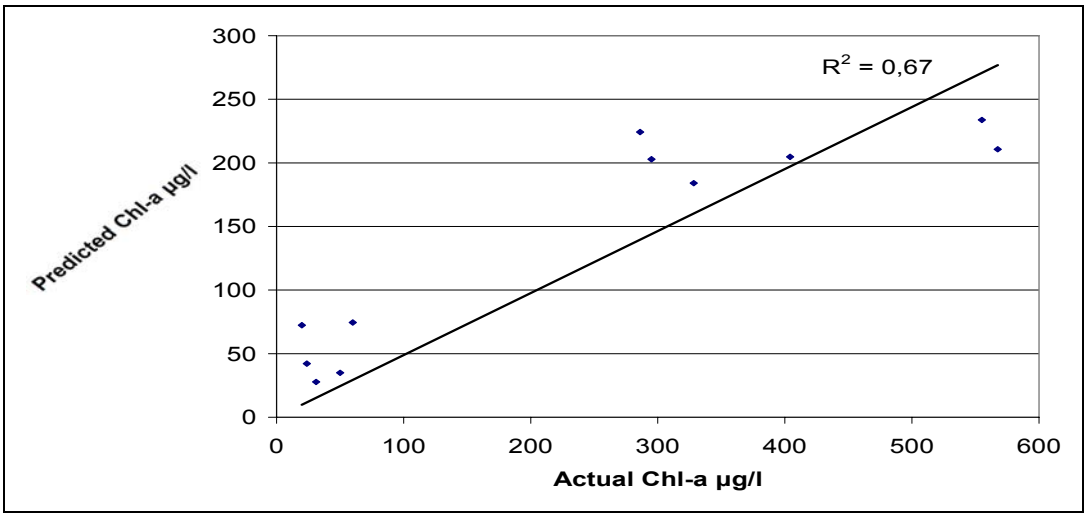


Figure 4.27: Actual versus predicted (using the model obtained with the general model obtained for the probe data) Chl-a values for both images.

The distribution of Chl-a concentrations obtained using the regression models obtained using the laboratory and probe data are given in Figures 4.28 and 4.29, respectively, for 26th of June. Figure 4.16 shows the distribution obtained using the general model (Equation 4.1) which utilized the probe data of July 1st and August 8th.

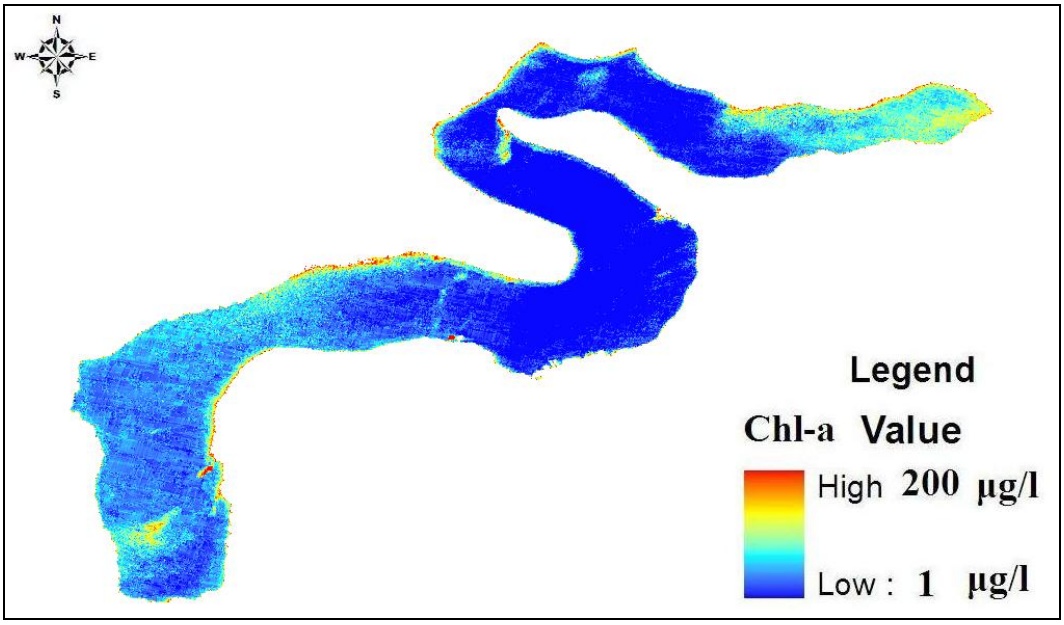


Figure 4.28: Remotely sensed Chl-a distribution on 26th of June for the model developed using the laboratory data.

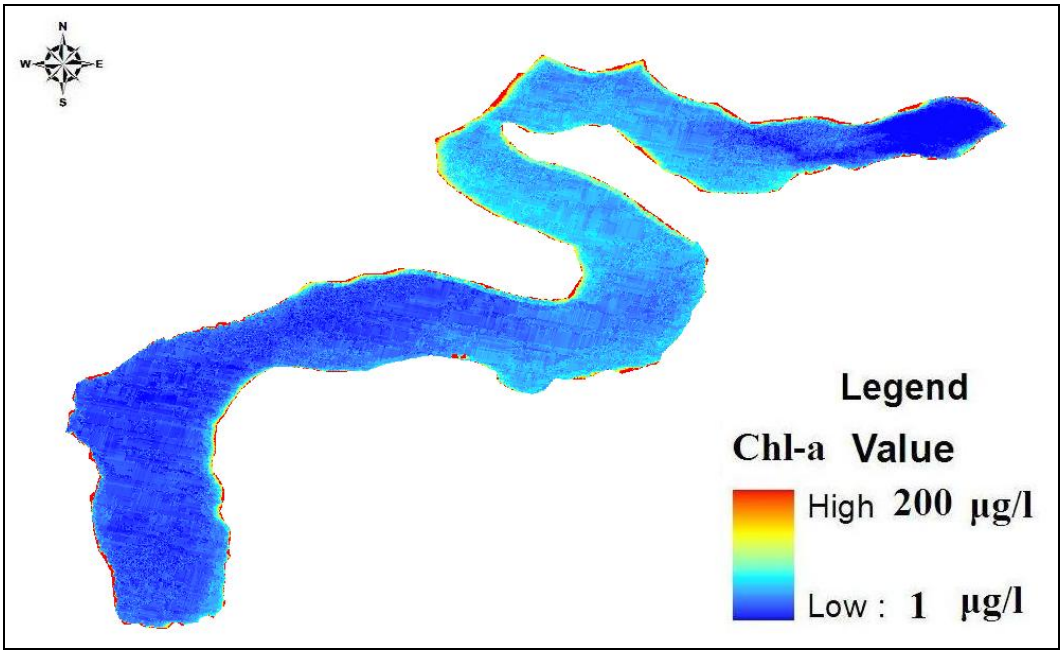


Figure 4.29: Remotely sensed Chl-a distribution on 26th of June for the general model developed using the probe data.

In Figures 4.28 and 4.29 different distributions were obtained. The concentration values are expected to be different since the values for the probe and laboratory data are of different magnitudes due to reasons discussed before. In addition, fewer data were used in model development for the laboratory data compared to probe data. However, the aim of comparison of the Chl-a distributions for different ground truth data origins is to check whether similar relative locations of high and low Chl-a concentrations could be obtained or not. In order to check the similarity of the Chl-a distributions, the lake area was divided into three sections (east, middle, and west) and average Chl-a values for these areas were calculated. For Figure 4.28, the average concentrations for the east, middle and west areas were 10, 46 and 23 µg/l respectively. For Figure 4.29, these values were 77, 7 and 37 µg/l, respectively. Therefore, in Figure

4.28, high concentration areas were in the east and west, rather than the middle section as in Figure 4.29. Therefore, although individually fair results were obtained for different models, the Chl-a distributions were not comparable. The mapping analysis was repeated for the second image captured on 6th of August (Figure 4.30) using the general model given by Equation 4.1.

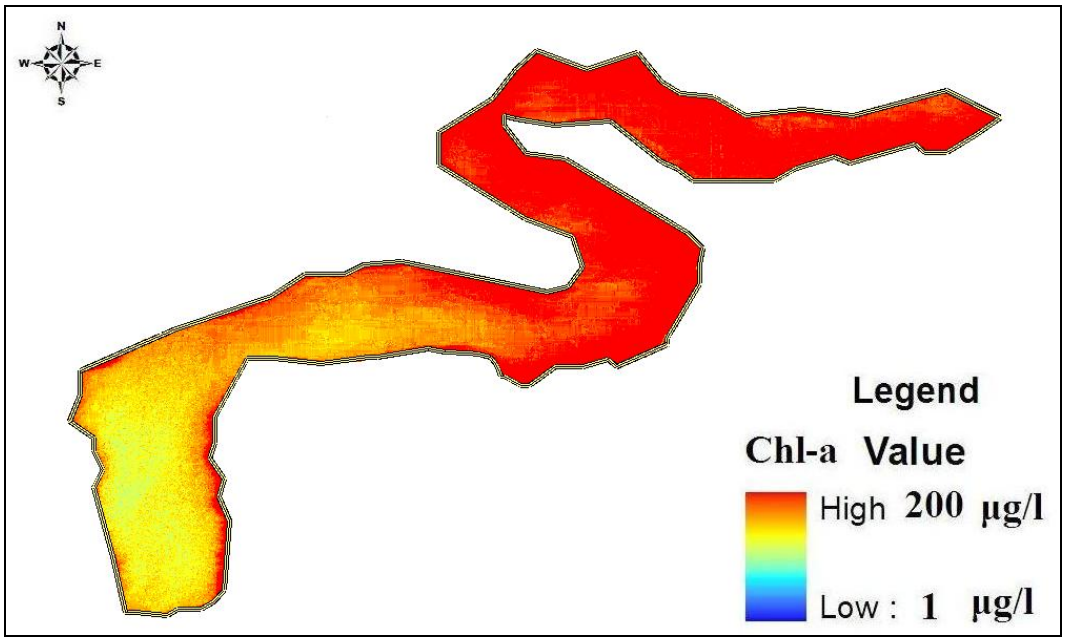


Figure 4.30: Remotely sensed Chl-a distribution on 6th of August for the general model developed using the probe data.

As mentioned earlier, the initial approach was to produce a general model that could be applied for images taken at different dates. However, this approach may not be applicable to eutrophic lakes. This may be due

to the change of algal species available with time which may change the reflectance characteristics of the water. For example, blue green algae may dominate the other forms when the nitrogen sources are scarce since they can apply nitrogen fixation. Therefore, regression analysis was also carried out separately for each image using the relevant probe data. In Tables 4.11 and 4.12, the datasets used for regression model development and model validation are introduced.

Table 4.11: Data set for regression analysis and model validation for image captured on 26th of June using the probe data of July 1st

| Regression Data | | |
|---|---|---|
| **Chl-a Probe µg/l** | **Green** | **NIR-Red** |
| 31,00 | 286,00 | -67,00 |
| 20,00 | 322,00 | -66,00 |
| 24,00 | 301,00 | -69,00 |
| 60,00 | 288,00 | -42,00 |
| 50,00 | 292,00 | -67,00 |
| 30,00 | 293,00 | -72,00 |
| **Validation Data** | | |
| 45,00 | 215,00 | -53,00 |
| 36,00 | 193,00 | -44,00 |
| 50,00 | 197,00 | -44,00 |
| 55,00 | 200,00 | -33,00 |
| 30,00 | 205,00 | -64,00 |
| 40,00 | 210,00 | -55,00 |

Table 4.12: Data set for regression analysis and model validation for image captured on 6th$^{h}$ of August using the probe data of August 8$^{th}$.

| Regression Data | | |
|---|---|---|
| **Chl-a (Probe)** | **Green** | **NIR-Red** |
| 86,50 | 286,00 | 21,00 |
| 117,30 | 304,00 | -7,00 |
| 186,70 | 320,00 | -11,00 |
| 126,80 | 273,00 | 5,00 |
| 286,60 | 302,00 | 22,00 |
| 227,60 | 287,00 | 31,00 |
| 143,50 | 272,00 | -1,00 |
| **Validation Data** | | |
| 203,60 | 268,00 | 34,00 |
| 404,20 | 280,00 | 37,00 |
| 286,00 | 292,00 | 40,00 |
| 328,20 | 273,00 | 30,00 |
| 555,00 | 291,00 | 46,00 |
| 295,00 | 280,00 | 36,00 |
| 567,60 | 288,00 | 35,00 |

The regression models derived individually for different images using the relevant probe data as reference are given in Equations 4.3 and 4.4:

$$26^{th} \text{ of June: Chl-a } (\mu g/l) = -0.55*\text{Green} +0.9*(\text{NIR-Red}) -256 \quad (4.3)$$

$$6^{th} \text{ of August: Chl-a}(\mu g/l) = 2.08*\text{Green} +2.43*(\text{NIR-Red}) -461 \quad (4.4)$$

The regression results for these models are presented in Table 4.13. As seen in the table, $R^2$ and p values were not as good as the general model that used the combination of data of different dates. Figures 4.31 and 4.32 show the validation results for the two images. The corresponding p values for the validation were similar to those given in Table 4.13. It is seen that the results were worse especially for 6$^{th}$ of August. This may be due to decreased number of data used in model development and validation.

Table 4.13: Result of regression analysis of remotely sensed data versus relevant ground truth Chl-a data (Probe) for each image.

| | 26th of June | 6th of August |
|---|---|---|
| Observation points | 6 | 7 |
| $R^2$ | 0.87 | 0.64 |
| Standard error | 9.9 | 66 |
| Significance P | 0.12 | 0.35 |

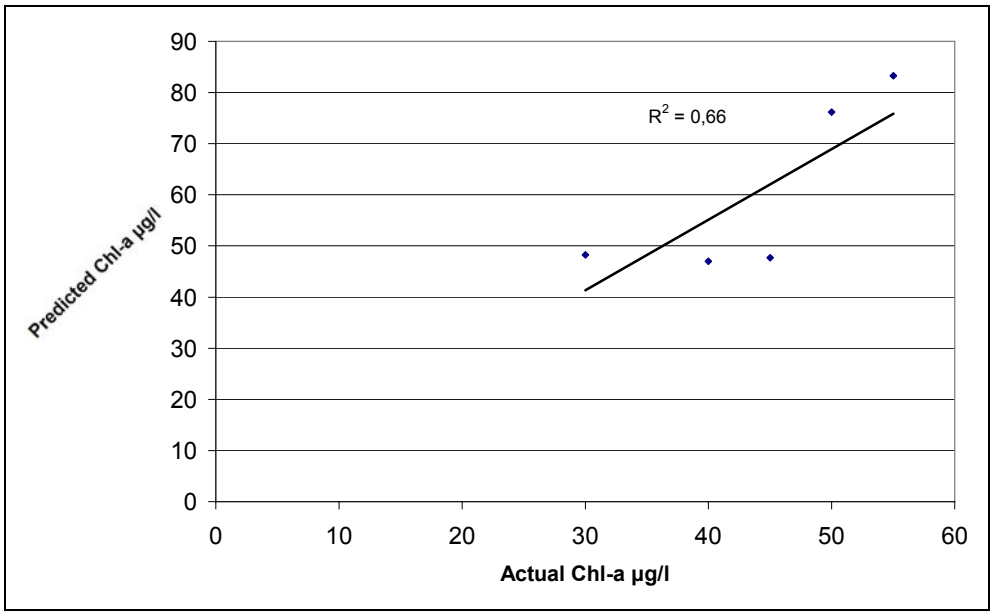


Figure 4.31: Actual versus predicted (using the model obtained with the Probe data) from image captured on 26th of June.

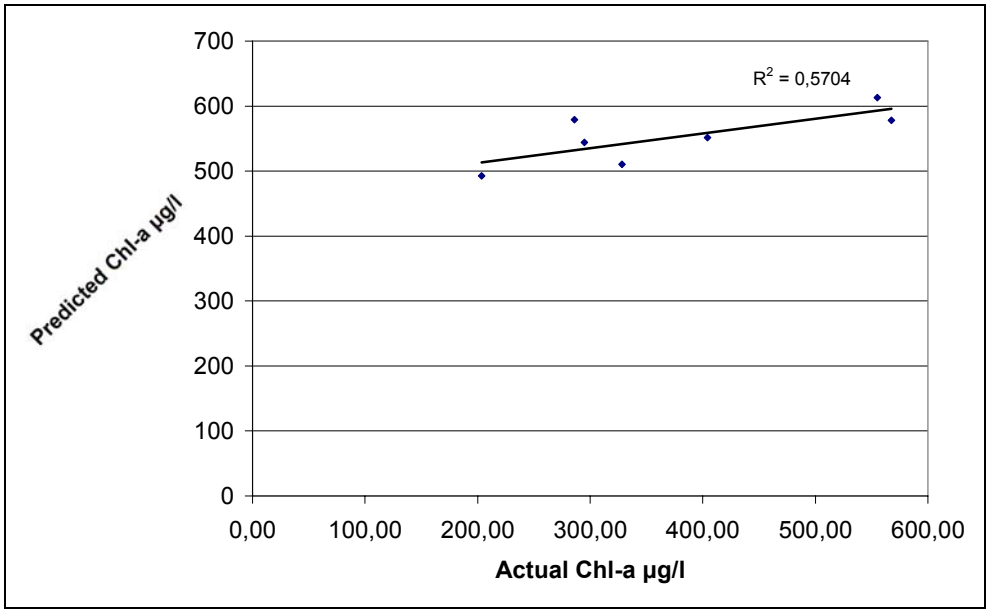


Figure 4.32: Actual versus predicted (using the model obtained with the Probe data) from image captured on 6th of August.

In Equation 4.3, it is seen that Chl-a concentrations are inversely proportional to the green band which may not be expected according to Figure 2.1. However, this may be as a result of domination of different algal species at different times. The annual average biomass percentages of different algal species reported by Beklioglu (2003) are listed in Table 4.14. Although the percentages may be different for different years, the discussion will be carried over the available data.

Table 4.14: Average annual biomass percentage of algal species in Eymir Lake (Beklioglu, 2003)

| **Algae** | **Annual Average Biomass %** |
|---|---|
| Diatoms (Golden Brown) | 2.5 |
| Green Algae | 76 |
| Dinoflagellates ( Red-Brown) | 2.5 |
| Cyanobacteria (blue-greens) | 3.6 |
| Cryptophyta (Various colors) | 15 |

Although the diatoms constitute only 2.5% of the algal biomass on the annual average, presence of diatoms may be observed in late spring in eutrophic lakes according to their good adaptation to temperature (Wetzel, 2001). As depicted in Figure 4.40, diatoms have a peak absorbance or a low reflectance in the green band region (520 to 600 nm). Therefore, dominance of diatoms may result in a negative coefficient for the green band in the regression model. The results of the regression models derived for each image alone were not better than the general model. As shown in table 4.13, for the 26$^{th}$ of June image, 6 points were used for regression and 6 for validation, the $R^2$ was 0.87, which is a high value with respect to literature. The standard error was about 10 μg/l which is about 25% of the average value (39 μg/l). The results of the August image were with lower $R^2$ of 0.64 and standard error of 66 μg/l which is about 24 % of the average concentration (272 μg/l). However, the significance p values of 0.12 and 0.35 for June and August images, respectively, are not acceptable (Bartholomew, 2002). This may be due to the number of points used and

bias in the exact location of the sampling points.

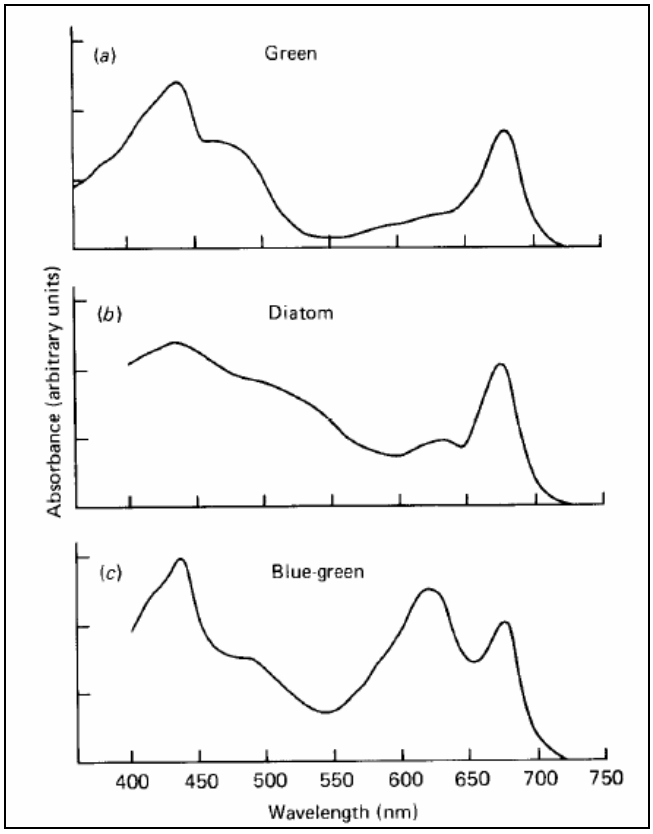


Figure 4.33: Absorbance distributions for different types of algae (Kirk, 1994).

For the June image, the average concentration of Chl-a in the lake obtained from regression model that used laboratory data (Equation 4.2), combined probe data (Equation 4.1) and probe data of 18$^{th}$ of June (Equation 4.3) were 52 μg/l, 54 μg/l, and 48 μg/l, respectively. While regarding the August image, the averages were 198 μg/l for the combined probe data and 187 μg/l for the probe data of August 8$^{th}$. Therefore, for

different models and different ground truth data origins, comparable average Chl-a values were obtained.

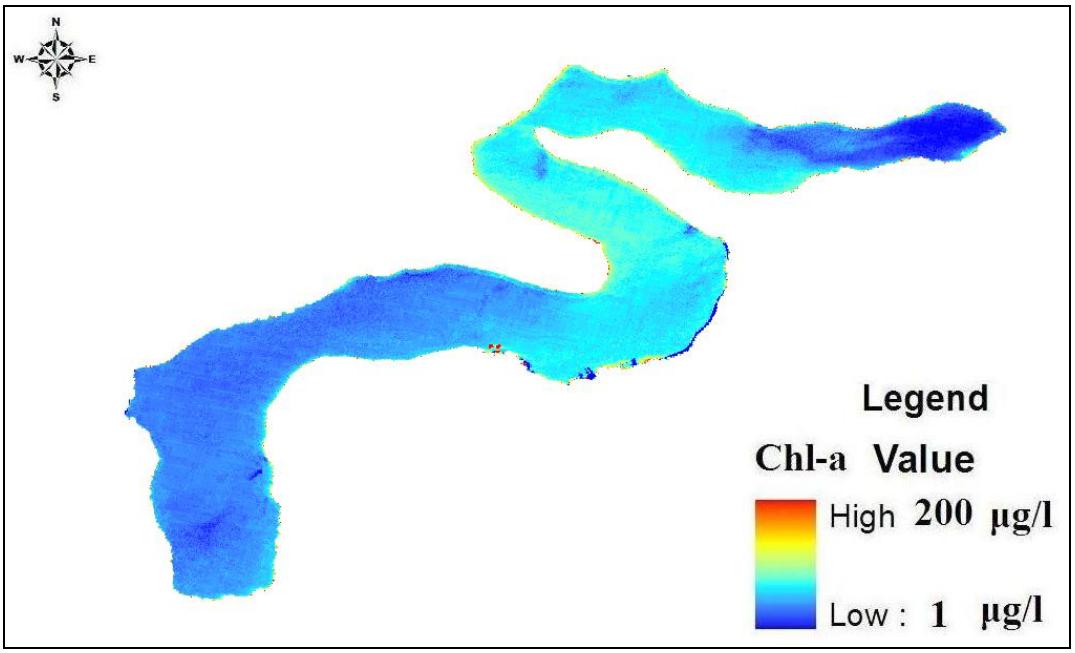


Figure 4.34: Remotely sensed Chl-a distribution on 26th of June for the model developed using the probe data of 18th of June.

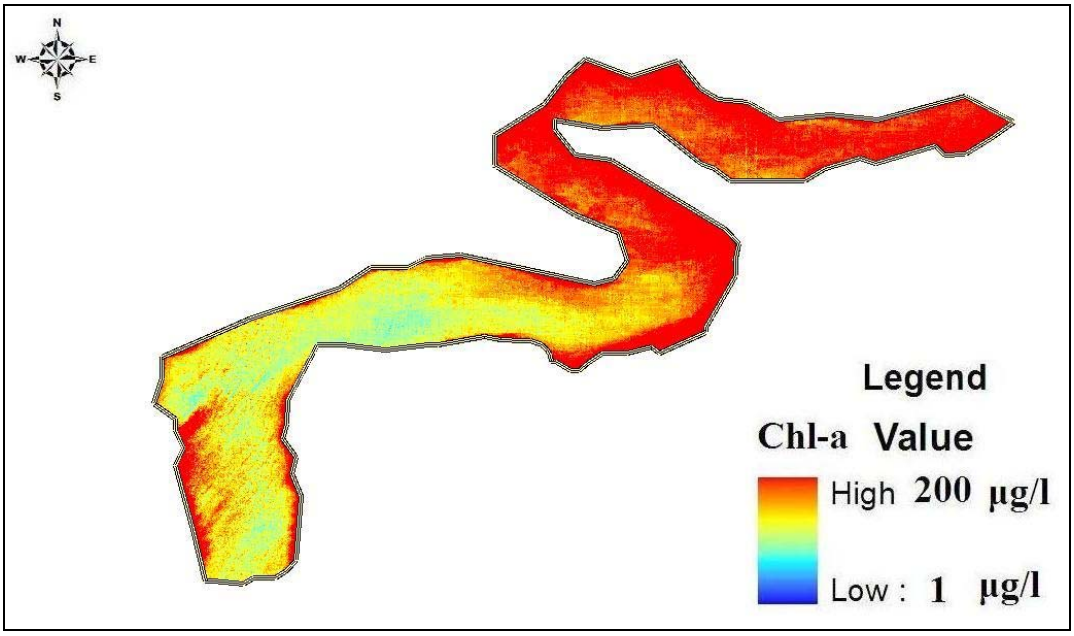


Figure 4.35: Remotely sensed Chl-a distribution on 6th of August for the model developed using the probe data (not combined).

It should also be noted, especially for the eutrophic lakes, presence of algal blooms may have a significant impact on the results. For example, if the surface of a lake is covered by blue-green algae, the reflectance of other species may be hindered. As given in Figure 4.34, different algal species may create a shift in the reflectance characteristics of the water body, which may require a different regression model. Therefore, for analysis of remotely sensed data and model development, it may be crucial to know the algal species present in the lake.

In Figure 4.35, the increased extend of higher Chl-a regions are clearly seen. Considering the previous image, it seems as if monitoring of these regions, the half that is closer to the exit, may be required to have a better understanding of the conditions of the lake. Although, locations

with higher and lower Chl-a concentrations can be identified, the exact concentration quantities can be in error due to the problems associated with probe readings.

In this study, obtained $R^2$ values ranged from 0.88 to 0.99; while the values in the literature[10] ranged from 0.5 to more than 0.9. The reasons of these variations, is that the performance of models can be dependent on several parameters. The conditions of data collection are important. If the time gap between the ground truth data collection and image acquiring increases, lower correlation can be expected (Zhang & Hu, 2006). Actually, for the second image the time gap was only 2 days and the best results were obtained for this case. If the data were collected on the same day, the results may have been better. This is especially important for dynamic systems where concentrations can change significantly or diurnally. Chl-a is an example for such constituents. In addition, other factors such as cloud can interfere with the performance, however, the images acquired for this study was free of this problem. Human error in laboratory and instrument error on-site also have some effects on the study. Number of samples used is also important (Zhang & Hu, 2006). However, time limitations, and site conditions may not always let us use a high number of ground truth data. However, determination of the exact locations of the ground truth data is crucial for a meaningful analysis. The optical properties of other constituents in the water may interfere in the reflectance (Ahn & Shanmugm, 2006). The effect of the reflectance from the bottom of the lake is higher in shallow places compared to deep places. Therefore, such a reflectance can introduce error into the results. In

[10] See Chapter 2: Background.

addition, the results may be sensitive to the error in the coordinates of the sampling points. Therefore, a sensitivity analysis may improve the results.

Despite some interference in model building, remote sensing is a promising technology and can be a very good method for the monitoring the lake. However, although it was not possible to obtain the ground truth data simultaneously as in the study by Giardino and Pepe, (2001) where the field data was taken within minutes or hours of image capturing, fair results were obtained. However, more analysis is required to have more conclusive outcomes. For high Chl-a concentrations greater than 20 μg/l, variations in reflectance largely depend on the concentrations of inorganic suspended matter in the water (Schalles, 1998). As shown in the analysis section for the laboratory results, there is a great correlation between the TSS and Chl-a, but the regression constant was not zero, this means that other constituents also affect the TSS. But this constant was near zero, which implies that most of the TSS in the lake is caused by Chl-a. As a conclusion, using remotely sensed data for the determination of Chl-a in hypereutrophic lakes like Eymir where inorganic suspended matter is low, is very reliable provided that the preciously discussed conditions to be satisfied.

Another regression analysis was performed to map the TSS concentrations in the lake using the image acquired on 26$^{th}$ of June. The input data are listed in Table 4.14. The regression model is given in Equation 4.5.

$$TSS\ (mg/l) = 0.39*Green-0.6*Red-0.17*NIR-39 \qquad (4.5)$$

The result of the analysis showed an $R^2$ value of 0.78. The standard error was 1.4 mg/l which is about 17% of the average TSS concentration (7.7 mg/l). The correlation was 0.021. The regression plot for the measured and predicted TSS values is presented in Figure 4.38.

Table 4.15: Input Data for the regression analysis between the laboratory TSS data and the image taken on 26th of June.

| TSS | Blue | Green | Red | NIR |
|---|---|---|---|---|
| 10 | 211 | 293 | 129 | 70 |
| 7 | 203 | 249 | 110 | 83 |
| 10 | 212 | 297 | 129 | 62 |
| 5 | 197 | 265 | 115 | 75 |
| 7 | 216 | 304 | 139 | 65 |
| 6 | 193 | 252 | 115 | 91 |
| 11 | 229 | 322 | 150 | 88 |
| 10 | 213 | 296 | 134 | 80 |
| 5 | 220 | 305 | 146 | 77 |
| 5 | 226 | 328 | 161 | 82 |

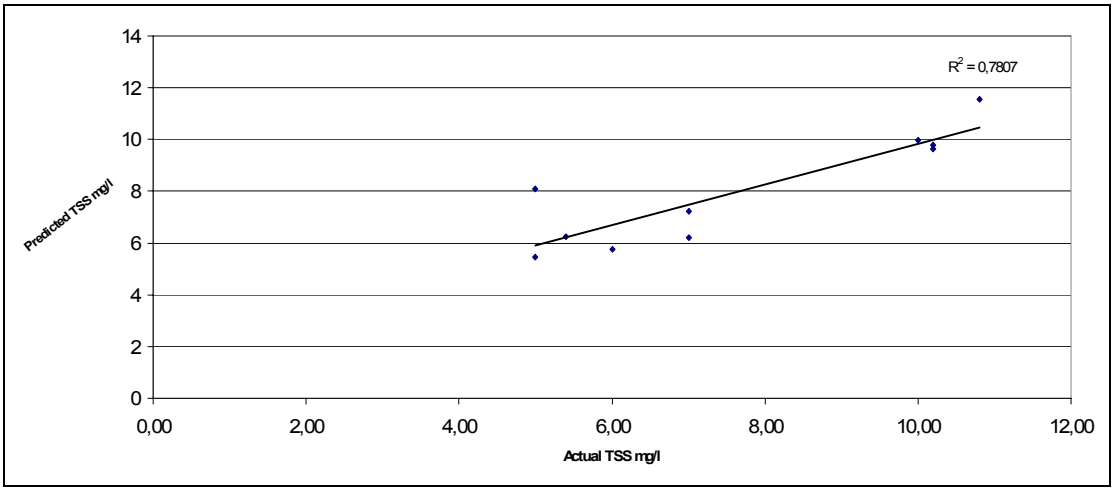


Figure 4.36: Actual versus predicted (using the model obtained with the probe data) TSS values for the image taken on 26th of June.

## 4.4 Progression of the water quality in Lake Eymir

A brief evaluation was also made for the general status of the lake with respect to the results obtained from past studies (Altinbilek, 1995; Beklioglu, 2002). In this comparison the parameters of trophic state determination were considered. Figure 4.37, the change of Chl-a with time is shown. As can be observed, a huge increase in the Chl-a concentration is seen in 2005 compared to years before. And as the Chl-a concentrations are one of the main indicator for the trophic state of the lake, the lake shifted from a eutrophic to hypereutrophic state by 2005 according to the OECD criteria. Therefore, biomanipulation and drought conditions which favored the algal growth had a significant impact on the Chl-a concentrations.

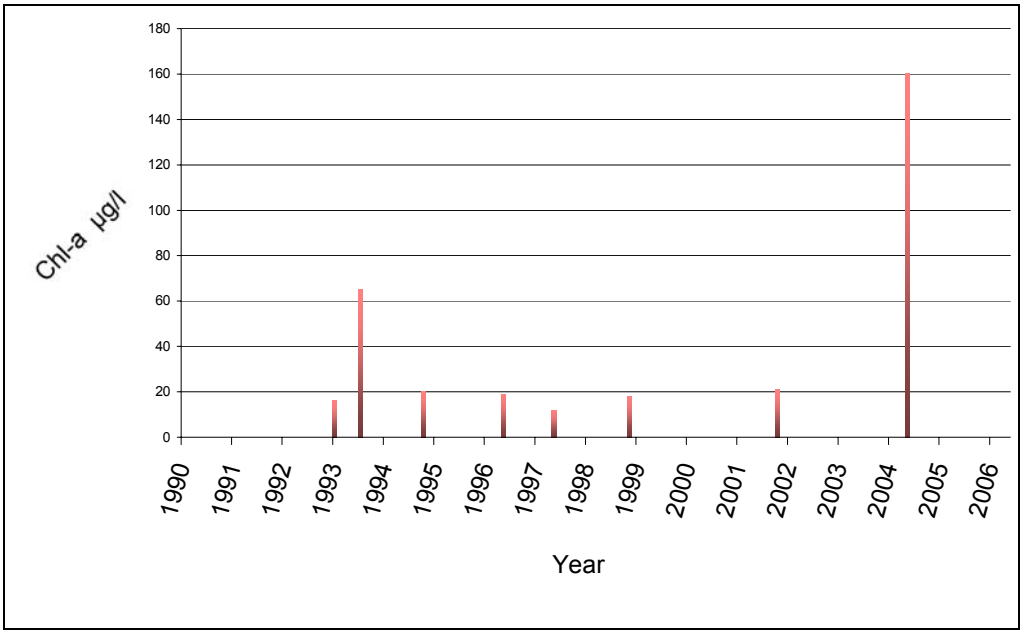


Figure 4.37: Change of Chl-a with time from 1993 to 2005.

When the change in nutrients was examined (Figure 4.38 & Figure 4.39), no significant improvement was observed. Regarding the total P, the Lake is still hypereutrophic as the concentration is greater than 0.1 mg/l (OECD). As the criteria of OECD states that lakes with $NO_3$ concentrations between 0.6 and 1.5 mg/l are considered as eutrophic, Lake Eymir is considered eutrophic with respect to this nutrient. But as the cause of high productivity in lakes is most frequently because of P availability (Wetzel, 2001), it will be more reliable to use it and the Chl-a concentrations in such evaluation (Wetzel, 2001). Additionally, when the sechi disc depth was examined, the values was around 0,5 m in 1995 (Altinbilek, 1995), and increased to around 1 meter in 1998 after the biomanipulation, but a severe decrease was observed in 2005 to around an average of 10 cm. This decrease can be related very much to the high production of algae in the lake. Generally, the lake water quality deteriorated more and more in the

last few years. The probable reason of this deterioration in the late years is the possible continuation of waste discharge from the Gölbasi municipality. In addition drought conditions and favored algal activity by biomanipulation together has resulted in worsening of the parameters related to trophic state.

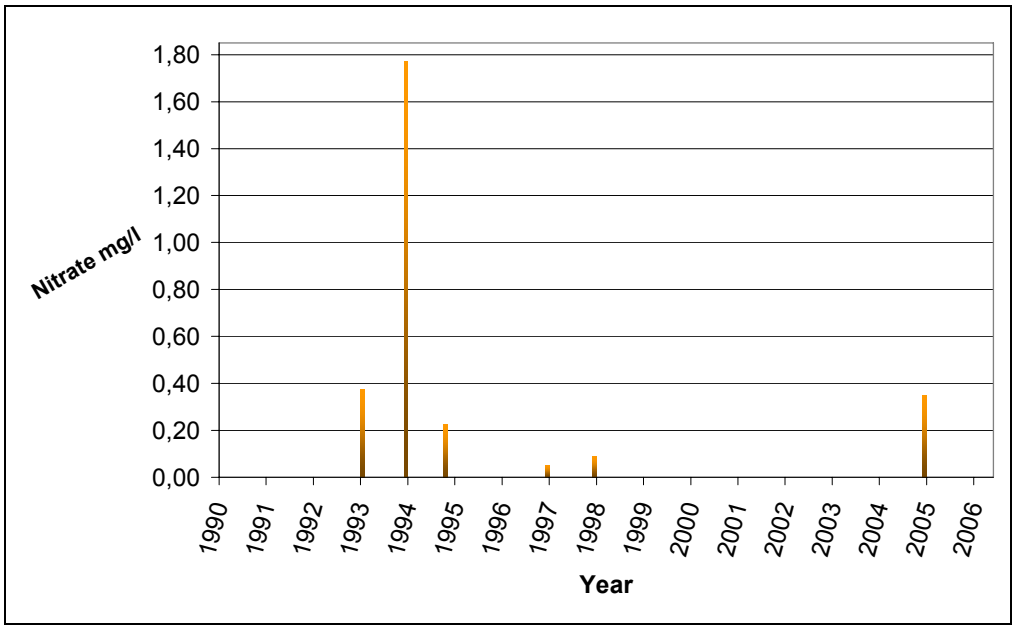


Figure 4.38: Change of Nitrate with time from 1993 to 2005.

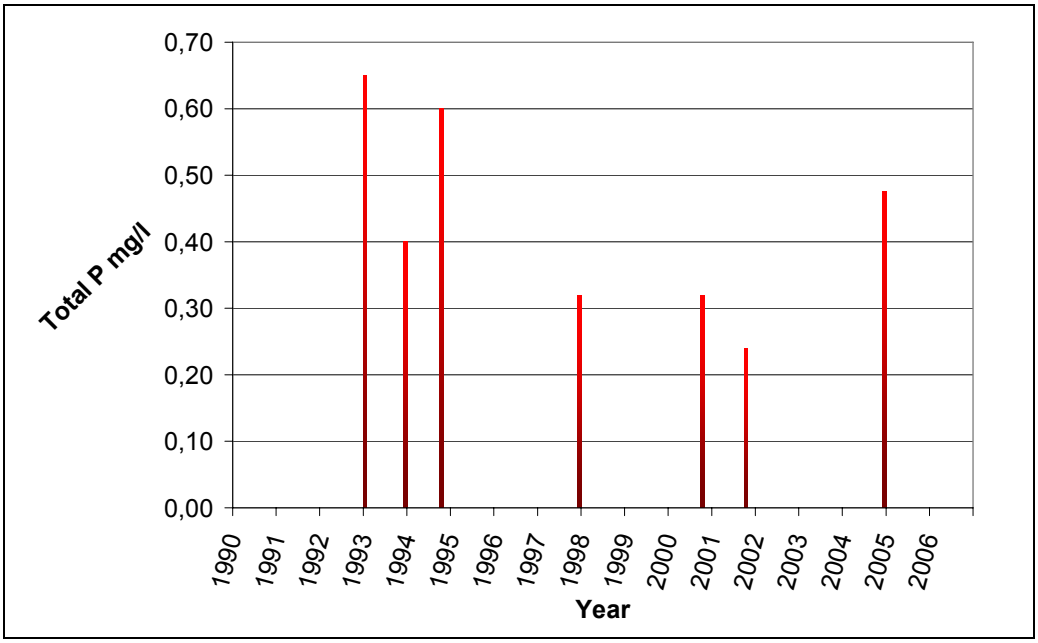


Figure 4.39: Change of Phosphate with time from 1993 to 2005

# *CONCLUSION*

In this study, chl-a was assessed in lake Eymir in many aspects. A regression analysis was made to find the relationship between remotely sensed image and ground truth data including both laboratory obtained and in-situ probe obtained data. Apart from that, mapping for Chl-a was composed using in-situ probe data for several dates in order to assess temporal and spatial distribution of Chl-a in the lake. Lastly, relationship of Chl-a with several parameters like TSS, temperature, and pH were assessed.

Regression analysis showed good correlation ($R^2$ of 0.88 to 0.99) between the ground truth data and the remotely sensed data. However, number of data and uncertainity in the exact locations of the sampling points may have prevented better results. Results also indicated that the accuracy of the ground truth data is important for successful model development. It was also suspected that the presence of different algal species may chance the reflectance characteristics of the lake. Use of remotely sensed data for the determination of Chl-a concentrations are promising. However, more work is needed.

The result of the mapping, showed big variations in the spatial distribution of algae in the lake. This variation may be the result of different availability of nutrients in different parts of the lake, depth of water, and wind effects. When Chl-a was assessed with respect to other parameters, it was found that Chl-a itself contributed highly to the turbidity in the lake. The increased Chl-a concentrations by late summer resulted in very high pH values which may be detrimental to aquatic life. DO profiles were greatly effected by the Chl-a. Chl-a values started from a very low barely detectable numbers in March and elevated with time reaching very high unacceptable values in September and October. This result with other results, like very high turbidity, very low secchi disc depth, show how much is the quality of lake is deteriorated and needs special attention and careful action. When the results were compared to the lake quality in earlier years, it was shown that the lake quality deteriorated with time.

Although the results of this study were affected by the number of sampling points (both spatial and temporal), human error in laboratory analysis, and with the errors originating from instruments used, the results of the remotely sensed data were promising. Remotely sensed data can be used as a very efficient tool in Lake Eymir for the determination of not only Chl-a but also other parameters such as turbidity and TSS depending on their optical characteristics. It will be cost beneficial to be used frequently to monitor the lake and help in better decision making and lake management. Although results using in-situ probe instrument to measure chlorophyll-a was fairly simultaneous, it needs more development to get more accurate results.

# *RECOMMENDATIONS FOR FUTURE WORK*

The remotely sensed data has shown to be a useful tool for Eymir Lake, the same method can be applied on other parameters like turbidity, SD, TSS and temperature. Equations for those parameters can be obtained also, and used anytime for the sake of assessment and monitoring. But some points are to be taken into consideration in order to get better and more precise results, the most important point is to try as much as possible to obtain ground truth data on the same date and time when the satellite image is taken, this will reflect more realistic results. The same thing can be considered for mapping to be used for other parameters. This is because mapping is a very useful visual tool of assessment. Additionally, other method for mapping the Chl-a can be tested like krigging, which is a more complicated interpolation method, and can give more accurate results. However, number of sampling points to aid in krigging would still be important for better results.

As a future recommendation, sediment samples should also be taken and analyzed for better assessment of the water quality. In addition, algal species present should be determined as well for better model building with remotely sensed data. Apart from that, the optical effect of the bottom of the lake must be evaluated and its contribution and effect on

the general optical properties of water can be assessed.

In order to acquire more realistic information regarding the optical properties of water, a handheld field spectrometer can be used in future studies. The advantage of this device is that, as the sample or measurement is being taken from a certain station, at the same moment measurements using this device can be done. By this way, problems with the lag time between satellite pass and sampling time, the atmospheric effect and the potential errors in station exact location positioning can be eliminated, and more realistic almost error free results can be obtained.

# *REFERENCES*

Alexander J.Horne, Charles R. Goldman. 1994 ***Limnology*** 2nd edition New York: McGraw-Hill.

Barrett, E.C., and Curtis L.F., 1992***, Introduction To Environmental Remote Sensing,*** Chapman and Hall, Inc., Singapore.

Buttner, M.Korandi, A.Gyomorei, Zs.Kote and Gy.Szabo (1987) ***Satellite Remote Sensing Of Inland Waters:Lake Balaton And Reservoir Kiskore***. Acta Astronomica Vol 15, No.6/7, pp.305-311.

Caiyun Zhang, Chuanmin Hu, Shaoling Shang, Frank E.Müller Karger, Yan Li, Minhan Dai, Bangqin Huang, Xiuren Ning, Huasheng Hong, 2006 ***Bridging Between Seawifs And Modis For Continuity Of Chlorophyll-A Concentration Assessments Off Southeastern China*** Remote Sensing of Environment 102(2006)250–263.

Catherine Ostlund, Peter Flink (2001) ***Mapping of The Water Quality Lake Erken, Sweden From Imaging Spectrometry And Landsat Thematic Mapper.*** The Science of the environment 268 (2001) 139-154.

C.D. Lloyd and P.M. Atkinson, 2004, ***Increased Accuracy Of Geostatistical Prediction Of Nitrogen Dioxide In The United Kingdom With Secondary Data,*** International Journal of Applied Earth Observation and Geoinformation, Volume 5, Issue 4,293-305.

Christopher Brönmark, Lars-Anders Hansson, ***The Biology of Lakes and Ponds,*** Biology of Habitats, New York: Oxford University Press, 1999.

Chuanmin Hu, Zhiqiang Chena, Tonya D.Clayton, Peter Swarzenski, John C.Brock, Frank E.Muller-Karger, 2004, ***Assessment Of Estuarine Water-Quality Indicators Using Modis Medium-Resolution Bands: Initial Results From Tampa Bay, Fl*** Remote Sensing of Environment 93(2004)423–441.

Claudia Giardino, Monica Pepe (2001) ***Detecting Chlorophyll, Secchi Disc Depth and Surface Temperature in Sub-Alpine Lake Using Landsat Imagery.*** The Science of the environment 268(2001)19-29.

DanLing Tang, Hiroshi Kawamura, ImSang Oh, Joe Baker, 2005 ***Satellite Evidence Of Harmful Algal Blooms And Related Oceanographic Features In The Bohai Sea During Autumn 1998*** Advances in Space Research 37(2006)681–689.

D.G.George (1997***). The Airborne Remote Sensing Of Phytoplankton Chlorophyll in the Lakes and Tarns of the English Lake District***. International Journal of Remote sensing, VOL. 18, No.9, 1961-1975.

Prof.Dr.Dogan Altinbilek (1995) ***Gölbaşi Mogan Eymir Gölleri İçin Su Kaynaklari Ve Çevre Yönetimi Plan Projesi.*** Ankara büyük belediye başkanlığı Ankara su ve kanalizasyon idaresi genel müdürlüğü.

Ele Vahtmäe, Tiit Kutser, Georg Martin, Jonne Kotta, 2006, ***Feasibility Of Hyperspectral Remote Sensing For Mapping Benthic Macroalgal Cover In Turbid Coastal Waters A Baltic Sea Case Study*** Remote Sensing of Environment 101(2006)342–351.

EPA, 2005, ***Technologies And Techniques For Early Warning Systems To Monitor And Evaluate Drinking Water Quality: A State-Of-The-Art Review***, Report no: EPA/600/r-05/156.

Frido Reinstorf, Maja Binder, Mario Schirmer, Jost Grimm-Strele and Wolfgang Walther, 2005, ***Comparative Assessment Of Regionalisation Methods Of Monitored Atmospheric Deposition Loads*** Atmospheric Environment, Volume 39, Issue 20, 3661-3674.

Han, Luoheng, 1997, ***Spectral Reflectance With Varying Suspended Sediment Concentrations In Clear And Algal-Laden Waters,*** Photogrammetric Engineering and Remote Sensing, Vol. 63, No.6, pp 701-705.

Harper, David M. 1992 ***Eutrophication of Freshwaters: Principles, Problems, and Restoration.*** 1st edition London; New York: Chapman & Hall, 1992.

Howard B.Glasgow, JoAnn M.Burkholdea, ***Real-Time Remote Monitoring Of Water Quality: A Review Of Current Applications, And Advancements In Sensor, Telemetry, And Computing Technologies*** Journalof Experimental Marine Biology and Ecology 300(2004)409–448.

Jianfeng Wu, Chunmiao Zheng and Calvin C. Chien, 2005, ***Cost-Effective Sampling Network Design For Contaminant Plume Monitoring Under General Hydrogeological Conditions,*** Journal of Contaminant Hydrology, Volume 77, Issues 1-2, 41-65.

Jingjie Zhanga, Sven Erik Jørgensen, Can Ozan Tan, Meryem Beklioglu, 2002, ***A structurally dynamic modelling—Lake Mogan, Turkey as a case study*** Ecological Modeling 164(2003)103–120.

Jingjie Zhanga, Sven Erik Jørgensen, Meryem Beklioglu, Ozlem Ince ***Hysteresis invegetation shift—Lake Mogaken prognoses*** Ecological Modelling 164(2003)227–238

John T. O. Kirk, ***Light and Photosynthesis in Aquatic Ecosystems***, 2nd Edition, Cambridge University Press, NewYork, 1994.

K.Hamilton, O.Davis,W.Joseph Rea, H.Pilorz and L.Carder (1993) ***Estimating Chlorophyll Content And Bathymetry Of Lake Tahoe Using Aviris Data.*** Remote sensing of the Environment: 44:217-230.

Liis Sipelgas, Urmas Raudsepp, Tarmo Kouts, 2006, ***Operational Monitoring Of Suspended Matter Distribution Using Modis Images And***

***Numerical Modeling*** Advances in Space Research (2006).

Lima, B. De Vivo, D. Cicchella, M. Cortini and S. Albanese, 2003, ***Multifractal Idw Interpolation And Fractal Filtering Method In Environmental Studies: An Application On Regional Stream Sediments Of (Italy), Campania Region,*** Applied Geochemistry, Volume 18, Issue 12, 1853-1865.

Lubos Matejıcek, Pavel Engst, Zbynek Janour, 2006 ***A Gis-Based Approach To Spatio-Temporal Analysis Of Environmental Pollution In Urban Areas: A Case Study Of Prague's Environment Extended By Lidar Data*** Ecological modeling (2006).

Nelson, S.A.C., P.A. Soranno, K.S. Cheruvelil, S. Batzli and D. Skole. 2003. ***Regional Assessment Of Lake Water Clarity Using Satellite Remote Sensing***. Journal of Limnology 62(Suppl. 1): 27-32.

Papista, E., Acs, E., and Boddi, B., 2002***. Chlorophyll-A Determination With Ethanol– A Critical Test,*** Hydrobiologia, 485, 191-198.

Paul Bartholomew, 2002, ***Mapping And Modeling Chlorophyll-A Concentrations In The Lake Manassas Reservoir Using Landsat Thematic Mapper Satellite Imagery.*** Thesis submitted to the Faculty of Virginia Polytechnic Institute and State University in partial fulfillment for the degree of Master of Science in Civil Engineering.

Paul V.Zimba, Anatoly Gitelson 2006, ***Remote Estimation Of Chlorophyll Concentration In Hyper-Eutrophic Aquatic Systems: Model Tuning And Accuracy Optimization.*** Aquaculture256(2006)272–286

Petert Wolter, Carol A.Johnston, Gerald J.Niemi, ***Mapping Submergent Aquatic Vegetation In The US Great Lakes Using QuickBird Satellite Data***, International Journal of Remote Sensing Vol.26, No.23, 10 December 2005, 5255–5274.

P.E O'Sullivan, C.S.Reynolds, ***The Lakes Handbook Volume I,*** Blackwell Publishing, 2004.

P. Shevyrnogov and A. F. Sid'ko, 1998***, Ground Truth Methods As A Part Of Space Mapping Of Inland Water Phytopigment Dynamics Adv.*** Space Res. Vol. 22, No. 5, pp. 705-708.

Richard H.French, Julianne J.Miller, Charles Dettling, James R.Car ***Use Of Remotely Sensed Data To Estimate The Flow Of Water To A Playa Lake*** Journal of Hydrology 325(2006)67–81

Robert G.Wetzel, ***Limnology, Lake and River Ecosystems,*** Third Edition, Elsevier Academic Press, 2001.

Sabine Thiemann and Hermann Kaufmann (2000) ***Determination Of Chlorophyll Content And Trophic State Of Lakes Using Field Spectrometer And Irs-1c Satellite Data In The Mecklenburg Lake District, Germany.*** Remote sensing of the environment 73:227-235.

Tan C.O., Beklioglu, M., 2005, ***Catastrophic-Like Shifts In Shallow Turkish Lakes: A Modeling Approach***, Ecological Modelling, 183 (4): 425-434.

Thomann, R.V., and Mueller, J.A**.,** ***Principles of surface water quality modeling and control***, Harper Collins Publishers Inc., NewYork, 1987.

T.P. Robinson and G. Metternicht, 2006, ***Testing The Performance Of Spatial Interpolation Techniques For Mapping Soil Properties,*** Computers and Electronics in Agriculture, Volume 50, Issue, 97-108.

Vollenweider, R.A. and J.J. Kerekes. 1980. ***Synthesis Report, Cooperative Programme On Monitoring Of Inland Waters (Eutrophication Control).*** Report prepared on behalf of Technical Bureau, Water Management Sector Group, Organization for Economic Cooperation and Development (OECD), Paris.

Winfried Lampert, Ulrich Sommer; translated by James F. Haney 1997 ***Limnoecology: The Ecology Of Lakes And*** Streams New York: Oxford University Press.

Wetzel R.G., 1975 ***Limnology***, W.B. Saunders Co., London.

Yu-Hwan Ahn, Palanisamy Shanmugam, ***Detecting the Red Tide Algal Blooms from Satellite Ocean Color Observations in Optically Complex Northeast-Asia Coastal Waters*** Remote Sensing of Environment (2006).